AD NUMBER
AD841794
LIMITATION CHANGES
TO: **Approved for public release; distribution is unlimited.**
FROM: **Distribution authorized to DoD only; Administrative/Operational Use; JUL 1968. Other requests shall be referred to U.S. Army Aviation Materiel Laboratories Fort Eustis, Virginia.**
AUTHORITY
USAAMTDL ltr, 29 Jan 1976

AD 841794

AD

USAAVLABS TECHNICAL REPORT 68-51

AN EVALUATION OF ARMORED AIRCREW CRASH SURVIVAL SEATS

By

Clifford I. Gatlin

James W. Turnbow

July 1968

U. S. ARMY AVIATION MATERIEL LABORATORIES
FORT EUSTIS, VIRGINIA

CONTRACT DAAJ02-68-C-0027
DYNAMIC SCIENCE
DIVISION OF MARSHALL INDUSTRIES
PHOENIX, ARIZONA

Disclaimers

Dispostion Instructions

DEPARTMENT OF THE ARMY
U. S. ARMY AVIATION MATERIEL LABORATORIES
FORT EUSTIS, VIRGINIA 23604

This report was prepared by the Dynamic Science AvSER Facility under the terms of Contract DAAJ02-68-C-0027. The object of this contractual effort was to test dynamically and to evaluate an armored seat design incorporating a new energy-absorption concept.

Test results indicate that the seat design and load attenuating devices are technically feasible, but additional design effort is required to optimize the structural and functional capabilities of the seating system.

The conclusions and recommendations presented in this report are concurred in by this Command.

Task 1F121401A15003
Contract DAAJ02-68-C-0027
USAAVLABS Technical Report 68-51
July 1968

AN EVALUATION OF ARMORED AIRCREW CRASH SURVIVAL SEATS

AvSer 68-4

by

Clifford I. Gatlin
James W. Turnbow

Prepared by

Dynamic Science (The "AvSer" Facility)
Division of Marshall Industries
Phoenix, Arizona

for

U. S. ARMY AVIATION MATERIEL LABORATORIES
FORT EUSTIS, VIRGINIA

SUMMARY

The Aviation Safety Engineering and Research (AvSER) Facility of Dynamic Science has extensively tested experimental armored crew seats. This report presents an evaluation of an armored seat design incorporating a new energy absorption concept. The seat was designed by Hayes International Corporation and was provided to AvSER by the U. S. Army Aviation Materiel Laboratories, Fort Eustis, Virginia (USAAVLABS).

The structure of the test seat is unique in that it is made up of two triangular frames interconnected by cross members at each apex and by diagonal braces in the plane of the aft members. Energy absorption in all axes is accomplished by bending steel rods around rollers in a controlled manner. The armor is not integral to the seat; thus, the seat can be used either with or without armor.

The tests indicate that additional design effort is warranted to make the seat function more properly within the design limitations.

PRECEDING PAGE BLANK-NOT FILMED

TABLE OF CONTENTS

	Page
SUMMARY	iii
LIST OF ILLUSTRATIONS	vi
LIST OF TABLES	xiii
INTRODUCTION	1
DESCRIPTION OF TEST ITEM	2
TEST PROCEDURES AND CONDITIONS	8
UH-1A Crash Test	8
Static Tests	9
Dynamic Tests	13
Test Instrumentation	18
TEST RESULTS	21
General	21
Drop Tower Tests	21
Horizontal Accelerator Tests	31
EVALUATION OF TEST RESULTS	39
Vertical Tests	39
Horizontal Test	45
Lateral Test	45
Triaxial Test	46

TABLE OF CONTENTS (CONT'D)

	Page
CONCLUSIONS	47
RECOMMENDATIONS	48
APPENDIX, TIME HISTORIES	49
DISTRIBUTION	110

LIST OF ILLUSTRATIONS

Figure		Page
1	Aircrew Crash Survival Seat (Without Armor)	3
2	Aircrew Crash Survival Seat (With Armor)	6
3	Front View - Hayes Armored Aircrew Survival Seat . .	7
4	Rear View - Hayes Armored Aircrew Survival Seat . .	7
5	Side View - Hayes Armored Aircrew Survival Seat . .	7
6	Pretest View - Armored Crash Survival Seat Installed in UH-1A Helicopter	8
7	Postcrash Side View of Armored Survival Seat	10
8	Postcrash Front View of Armored Survival Seat . . .	10
9	Support Tube Joint Installed in Testing Machine . . .	11
10	Test Setup for Longitudinal Static Test	11
11	Failure of Front Cross Tube During Longitudinal Static Test	12
12	Failed Energy Absorber Rod on Hayes-Buil' Seat . . .	13
13	Anthropomorphic Dummy with Modified Pelvis and Chest Armor	15
14	Drop Tower Facility	15
15	Drop Tower and Short Horizontal Sled Test Facility . .	17
16	Pretest Side View - Test 1.	23
17	Pretest Rear View - Test 1	23
18	Pretest View of Energy Absorber Device - Test 1 . . .	24

LIST OF ILLUSTRATIONS (CONT'D)

Figure		Page
19	Posttest Side View - Test 2	25
20	Energy Absorbers After Test 2	25
21	Pretest Side View - Test 3.	27
22	Pretest View of Energy Absorber Device - Test 3	27
23	Posttest View of Seat - Test 3.	28
24	Posttest View of Energy Absorbers - Test 3	28
25	Pretest View of Seat - Test 4	29
26	Pretest View of Energy Absorber Device - Test 4	29
27	Posttest View of Seat - Test 4	30
28	Posttest View of Energy Absorber - Test 4	30
29	Pretest View of Seat - Test 5	32
30	Posttest View of Seat - Test 6	32
31	Posttest View of Left Energy Absorber - Test 6	33
32	Posttest View of Right Energy Absorber - Test 6	33
33	Pretest Side View - Test 7	35
34	Pretest Rear View - Test 7	35
35	Posttest View of Seat - Test 8A	36
36	Pretest Side View - Test 9	36
37	Pretest Rear View - Test 9	37
38	Posttest Side View - Test 9	38

LIST OF ILLUSTRATIONS (CONT'D)

Figure		Page
39	Posttest Rear View - Test 9	38
40	Free-Body Diagram of the Seat Support Structure	40
41	Friction Load in the Seat Pan Guide - Test 2	41
42	Free-Body Diagram of the Seat Pan	44
43	Composite Acceleration Data Overlay - Test 6	46
44	Acceleration-Time History - Test 2	49
45	Acceleration-Time Histories - Test 2	50
46	Acceleration-Time Histories - Test 2	51
47	Acceleration-Time History - Test 2	52
48	Stroke-Time History - Test 2	53
49	Force-Time History - Test 2	54
50	Force-Time History - Test 2	55
51	Force-Time History - Test 2	56
52	Force-Time Histories - Test 2	57
53	Acceleration-Time History - Test 3	58
54	Acceleration-Time Histories - Test 3	59
55	Acceleration-Time Histories - Test 3	60
56	Acceleration-Time History - Test 3	61
57	Acceleration-Time History - Test 3	62
58	Stroke-Time History - Test 3	63

LIST OF ILLUSTRATIONS (CONT'D)

Figure		Page
59	Force-Time History - Test 3	64
60	Force-Time Histories - Test 3	65
61	Force-Time Histories - Test 3	66
62	Acceleration-Time History - Test 4	67
63	Acceleration-Time History - Test 4	68
64	Acceleration-Time History - Test 4	69
65	Acceleration-Time Histories - Test 4	70
66	Stroke-Time History - Test 4	71
67	Force-Time History - Test 4	72
68	Force-Time Histories - Test 4	73
69	Force-Time Histories - Test 4	74
70	Acceleration-Time Histories - Test 6	75
71	Acceleration/Force-Time Histories - Test 6	76
72	Force-Time Histories - Test 6	77
73	Acceleration/Stroke-Time Histories - Test 6	78
74	Force-Time History - Test 6	79
75	Force-Time History - Test 6	80
76	Force-Time History - Test 6	81
77	Force-Time History - Test 6	82
78	Force-Time Histories - Test 6	83

LIST OF ILLUSTRATIONS (CONT'D)

Figure		Page
79	Acceleration-Time Histories - Test 8	84
80	Acceleration-Time History - Test 8	85
81	Force-Time Histories - Test 8	86
82	Force-Time Histories - Test 8	87
83	Force-Time Histories - Test 8	88
84	Acceleration-Time Histories - Test 8A	89
85	Acceleration-Time History - Test 8A	90
86	Acceleration-Time History - Test 8A	91
87	Acceleration-Time History - Test 8A	92
88	Force-Time Histories - Test 8A	93
89	Force-Time History - Test 8A	94
90	Force-Time History - Test 8A	95
91	Force-Time Histories - Test 8A	96
92	Acceleration-Time History - Test 9	97
93	Acceleration-Time Histories - Test 9	98
94	Acceleration-Time History - Test 9	99
95	Acceleration-Time Histories - Test 9	100
96	Acceleration-Time History - Test 9	101
97	Acceleration-Time Histories - Test 9	102
98	Force/Stroke-Time Histories - Test 9	103

LIST OF ILLUSTRATIONS (CONT'D)

Figure		Page
79	Acceleration-Time Histories - Test 8	84
80	Acceleration-Time History - Test 8	85
81	Force-Time Histories - Test 8	86
82	Force-Time Histories - Test 8	87
83	Force-Time Histories - Test 8	88
84	Acceleration-Time Histories - Test 8A	89
85	Acceleration-Time History - Test 8A	90
86	Acceleration-Time History - Test 8A	91
87	Acceleration-Time History - Test 8A	92
88	Force-Time Histories - Test 8A	93
89	Force-Time History - Test 8A	94
90	Force-Time History - Test 8A	95
91	Force-Time Histories - Test 8A	96
92	Acceleration-Time History - Test 9	97
93	Acceleration-Time Histories - Test 9	98
94	Acceleration-Time History - Test 9	99
95	Acceleration-Time Histories - Test 9	100
96	Acceleration-Time History - Test 9	101
97	Acceleration-Time Histories - Test 9	102
98	Force/Stroke-Time Histories - Test 9	103

LIST OF ILLUSTRATIONS (CONT'D)

Figure		Page
99	Force-Time Histories - Test 9	104
100	Force-Time History - Test 9	105
101	Force-Time History - Test 9	106
102	Force-Time History - Test 9	107
103	Force-Time History - Test 9	108
104	Force-Time Histories - Test 9	109

LIST OF TABLES

Table		Page
I	Summary of Seat Weight	4
II	Summary of Attenuators - Preliminary Sizing	5
III	Test Conditions	16
IV	Instrumentation Location	19
V	Summary of Recorded Data	22

PRECEDING PAGE BLANK-NOT FILMED

INTRODUCTION

In February 1963, the U. S. Army Aviation Materiel Laboratories published a report entitled "Crew Seat Design Criteria for Army Aircraft" (TRECOM Technical Report 63-4), based on work performed by Aviation Safety Engineering and Research (AvSER), a Division of the Flight Safety Foundation, Inc., under Contract DA 44-177-AMC-888(T). Using the criteria presented in the report, the U. S. Army contracted with four aircraft manufacturers for the design and fabrication of two experimental crew seats. The resulting eight seats were sent to AvSER, and a dynamic test program was conducted under Contract DA 44-177-AMC-191(T).

The results of this test program were published in July 1965 in a report entitled "Survivability Seat Design Dynamic Test Program" (USAAVLABS Technical Report 65-43). The report presented the results of dynamic tests on the four different concepts of experimental armored crew seats. Included in the design of each seat were provisions for limiting the vertical acceleration of the passenger. The limitation was provided by energy absorbers which allowed the seat pan to displace downward when the vertical load reached a preset value. The results of this test series disclosed several problem areas associated with energy absorber design.

The Hayes International Corporation then received a contract from the U. S. Army to evaluate the four experimental seat designs and to develop a new design which would incorporate the information gained from the evaluation. AvSER was selected to conduct a series of drop tests on two of the experimental seats being evaluated by Hayes.

Using the data gathered during the AvSER test series, Hayes International designed and fabricated two examples of an experimental armored seat, incorporating energy absorption in all three principal axes. Four additional examples of this seat were fabricated by USAAVLABS, using drawings and specifications furnished by Hayes International.

The two seats built by Hayes International and three of the seats built by USAAVLABS were sent to AvSER, and a test program was conducted under Contract DAAJ02-68-C-0027. The objective of this program was to collect data for use in the evaluation of the structural integrity of the seat structure and its energy absorption capabilities under dynamic crash conditions.

This report presents the results of this test program.

DESCRIPTION OF TEST ITEM

The seat design consists of a tubular steel structure supporting a seat bucket fabricated of aluminum alloy sheet. The basic layout of the seat is shown in Figure 1. The support structure is made up of two triangular frames interconnected by cross members at each apex and by diagonal braces in the plane of the aft members. It was necessary to place the entire support structure aft of the seat bucket to provide sufficient clearance for both lateral and vertical movement during the energy absorbing stroke. The seat bucket is supported on two cross members between the forward support tubes. Fittings at the ends of the cross members allow the seat to slide on the forward support tubes for the energy absorbing stroke. The seat slides on the cross members for the lateral energy absorbing stroke. A vertical adjustment of 5 inches is accomplished by a linear electrical actuator, which moves the bucket on tracks attached to the support cross member.

The seat bucket is designed to withstand the loads from the restraint harness and to transmit these loads to the support structure. The restraint harness consists of a lap belt, a lap belt tiedown strap, and a shoulder harness, all terminating at a single point; the operation of a rotary buckle at this point releases all the straps simultaneously. To reduce the total length of the shoulder straps and, therefore, the total elongation of the system, the inertia reel is mounted on the top of the seat back. With the inertia reel located so close to the occupant, a dual strap reel is required for proper operation. The seat bottom and back are slightly curved, and very thin comfort cushions are provided.

The complete seat, including the support structure, is adjusted fore and aft by movement along two floor-mounted tracks. Adjustment is positioned and locked by engaging the pins on the seat into holes in each of the tracks. For an energy absorbing stroke in the forward direction, the seat moves on rollers. A forward roller on each side engages the floor tracks. An aft roller on each side engages a separate track that is locked to the floor tracks by the positioning pins.

Energy absorption in all axes is accomplished by bending steel rods around rollers in a controlled manner. Stroke distances of 7 to 12 inches are provided in the vertical direction (depending on the adjusted height of the seat bucket), 2 inches in either direction laterally, and 5.6 inches in the forward direction.

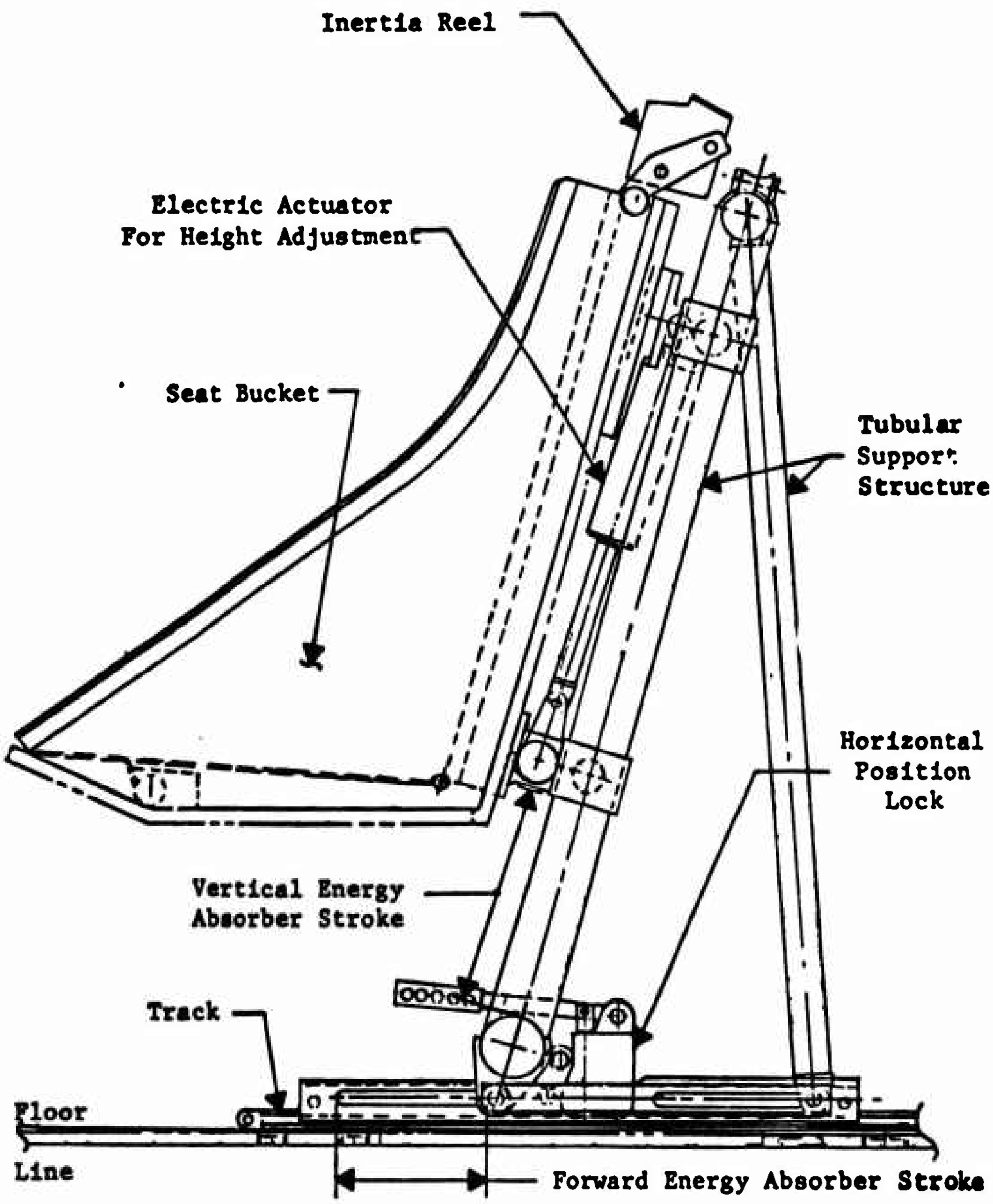

Figure 1. Aircraft Crash Survival Seat (Without Armor).

A composite armor system, designed and developed by Hayes International Corporation, is used for ballistic protection. A shell fabricated of flat panels surrounds the seat bucket to provide protection for the torso of a 95th-percentile occupant. This shell is attached at the same points used to attach the seat bucket to the support and moves with the bucket during adjustment or the energy absorber stroke. The armor is not used as structure; therefore, the seat can be used either with or without armor.

The composite armor was not used in the test program; it was simulated by panels of 3/16-inch steel plate backed by 1/2-inch plywood. This simulated armor gave the same total weight and weight distribution as the actual armor.

A summary of seat weights is given in Table I. Table II lists the energy absorber sizings.

Figure 2 is a sketch of the armor installation. Figures 3 through 5 show the seat with the armor installed.

TABLE I. SUMMARY OF SEAT WEIGHT

Seat Component	Weight (lb)
Seat Bucket (Includes inertia reel, restraint harness, cushions, vertical actuator switch)	39.85
Vertical Actuator	4.87
Vertical Slide Assembly (Includes lateral energy absorption device)	15.50
Support Frame (Includes vertical and longitudinal energy absorption devices)	37.00
Total Seat Weight	97.22
Armor	
Mounted to Bucket	95.00
Chest Armor	14.00
Total Armor	109.00
Total Seat Weight with Armor	206.22

TABLE II. SUMMARY OF ATTENUATORS - PRELIMINARY SIZING

	Desired Attenuation Force			
	With Armor		Without Armor	
	200-lb Occupant	135-lb Occupant	200-lb Occupant	135-lb Occupant
Vertical (lb)	4960	4355	3360	2630
Inertia (G)*	17	17	17	17
Lateral Upper (lb)	1400	1493	1276	1345
Lateral Lower (lb)	1537	1547	1473	1472
Inertia (G)*	11.15	13.6	16.0	21.6
Forward (lb)	8505	8505	6160	6160
Inertia (G)*	22.5	25.9	22.5	29.1

Preliminary Attenuator Sizing With 4130 Steel Rods, 150 Ksi Ultimate

Vertical (lb)	(8 Units) (5000)	(7 Units) (4375)	(5 Units) (3125)	(4 Units) (2500)

Total of 8 Units with 625-lb rating: Single Spindle, Rod Dia = 5/32 in., Spindle Dia = .493 in.

Lateral Upper - 2 Units with 700-lb rating: Single Spindle, Rod Dia = 3/16 in., Spindle Dia = .823 in.

Lateral Lower - 2 Units with 750-lb rating: Single Spindle, Rod Dia = 3/16 in., Spindle Dia = .750 in.

Forward (Armor) - 4 Units with 2125-lb rating: Double Spindle Rod Dia = 7/32 in., Spindle Dia = .845 in.

Forward (No Armor) - 4 Units with 1540-lb rating: Double Spindle, Rod Dia = 3/16 in., Spindle Dia = .725 in.

*It was anticipated that these inertia loads would be slightly lower during this test series, since the seat and occupant weights were in excess of the design weights as follows: (1) the seat was 10 pounds heavier than the estimated weight used in the attenuator design, (2) the dummy used was 17 pounds heavier than the 200-pound dummy used in the design, and (3) the 14-pound chest armor was not considered in the attenuator design.

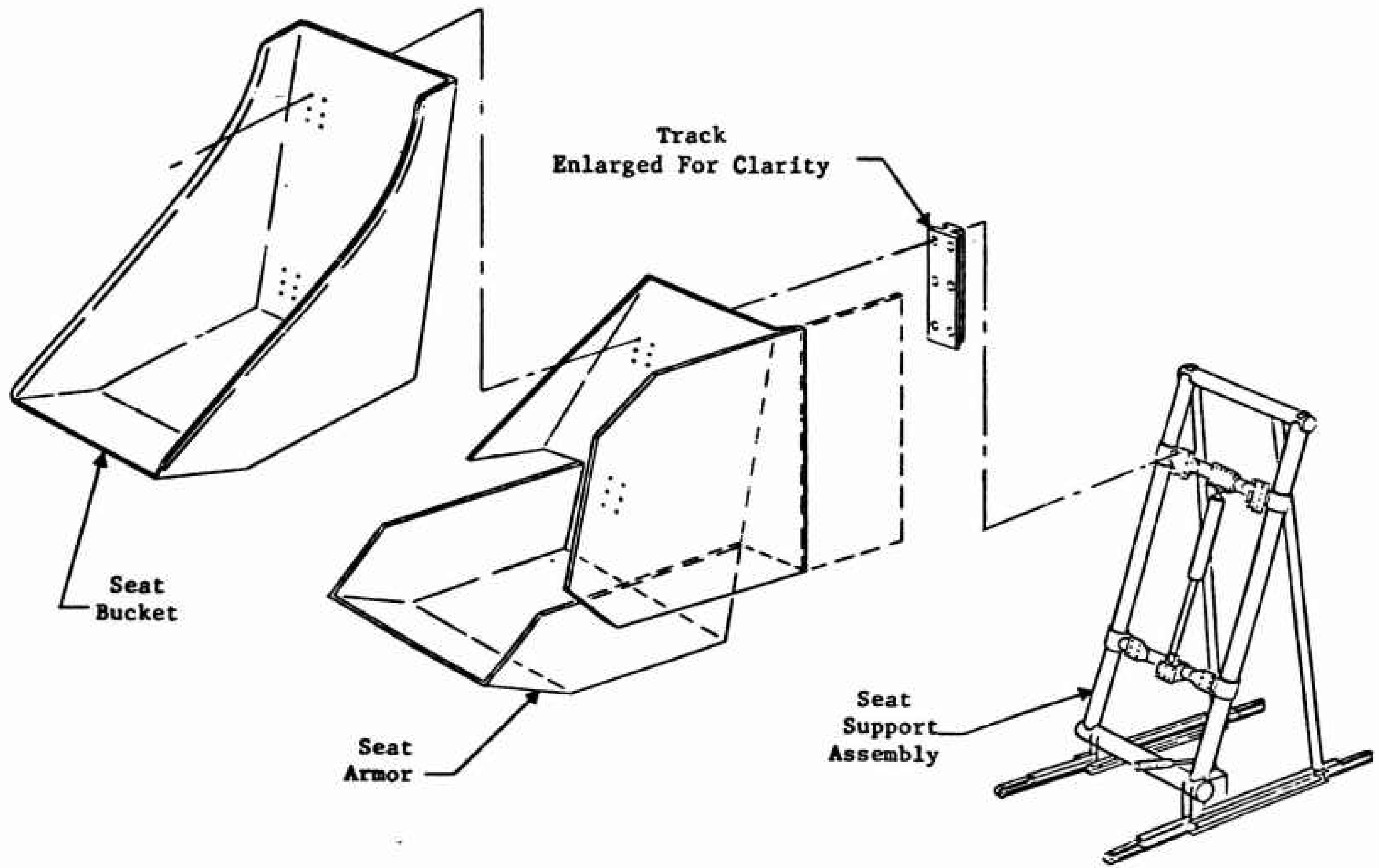

Figure 2. Aircrew Crash Survival Seat (With Armor)

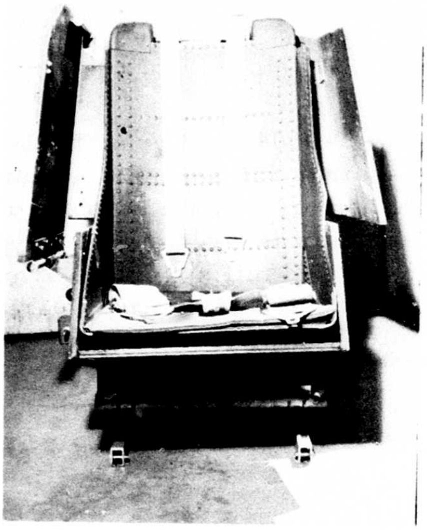

Figure 3. Front View - Hayes Armored Aircrew Survival Seat.

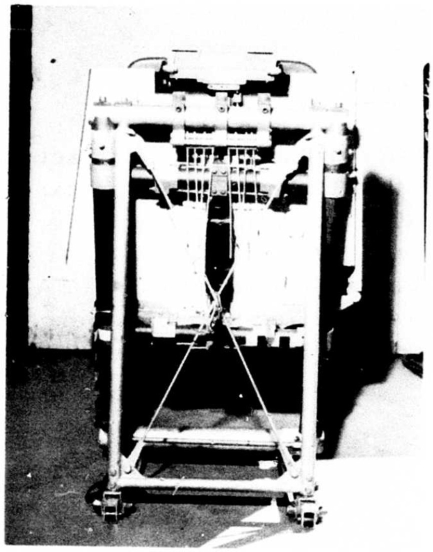

Figure 4. Rear View - Hayes Armored Aircrew Survival Seat.

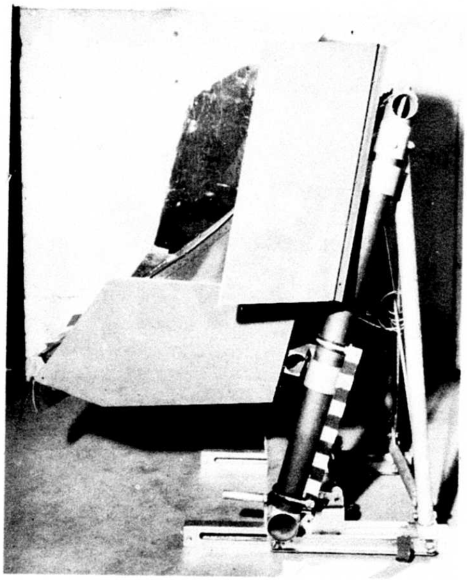

Figure 5. Side View - Hayes Armored Aircrew Survival Seat.

UH-1A CRASH TEST

In accordance with Contract DAAJ02-67-C-0004, and prior to the start of this test program, an example of this armored seat was mounted in the cargo compartment of a UH-1A helicopter, and the helicopter was crash tested by drone control to evaluate a crash-resistant fuel system. The seat, fabricated by USAAVLABS, carried full simulated armor and was occupied by a 95th-percentile anthropomorphic dummy wearing chest armor. Figure 6 shows the seat mounted in the aircraft prior to the test.

Figure 6. Pretest View - Armored Crash Survival Seat Installed in UH-1A Helicopter.

The aircraft was crashed in a 10-degree nosedown attitude, impacting at an angle of 15.5 degrees at vertical and horizontal velocities of 23 and 81 feet per second, respectively. This crash test was considered marginally survivable due to loss of occupiable area caused by structural collapse of the fuselage.

Postcrash inspection of the seat showed that the forward support tubes had failed at their junction with the forward cross tube, as shown in Figures 7 and 8. None of the energy absorbers had stroked, indicating that failure had occurred below their design load.

The shoulder harness had also released during the crash. This was due to inadvertent operation of the separate shoulder harness release built into the release buckle. This release was included to allow the occupant to release the shoulder harness without disturbing the lap belt. However, this release is designed to function by pushing <u>outward</u> on a small tab (Point A, Figure 8). Since total tab movement required for release is only 1/8 inch, it is relatively easy for the occupant's body to activate this tab under high loading.

Instrumentation had been installed to measure seat-pan accelerations; however, a malfunction in the recording system resulted in the loss of this data.

STATIC TESTS

In view of the apparent weakness noted in the seat during the crash test, several static tests were conducted prior to subjecting the seat to dynamic tests.

In the first of these static tests, a sample forward support tube/lower cross tube joint was fabricated using parts from the failed seat. This joint was fabricated according to Hayes International Corporation Drawing No. 201-00003. The completed joint was mounted in a Dillon Testing Machine, and a compressive load of 10,000 pounds was applied. Figure 9 shows the joint just prior to testing. The only failure noted was that of the seat roller, which failed at 10,000 pounds.

Following this test, a seat fabricated by USAAVLABS was installed on the static test jig for a longitudinal static test. The AvSER static loading dummy was placed in the seat and held in place by the standard restraint system. Figure 10 shows this test setup just prior to testing.

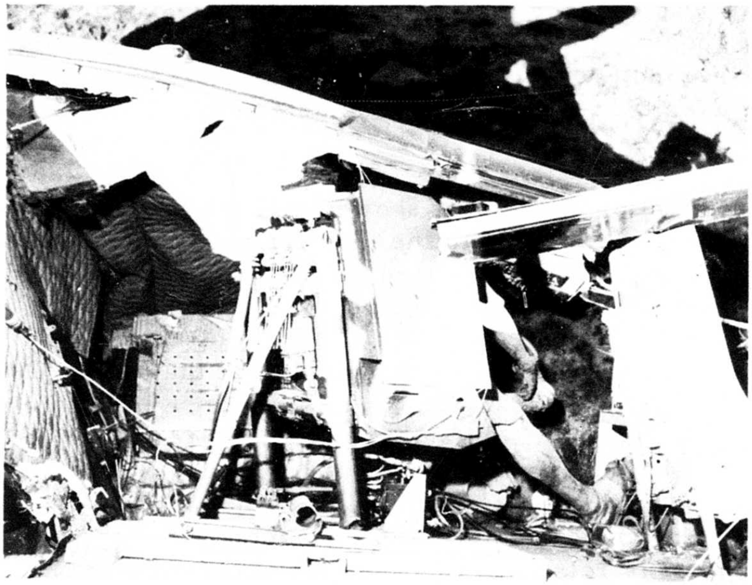

Figure 7. Postcrash Side View of Armored Survival Seat. Note Failure of Forward Support Tubes.

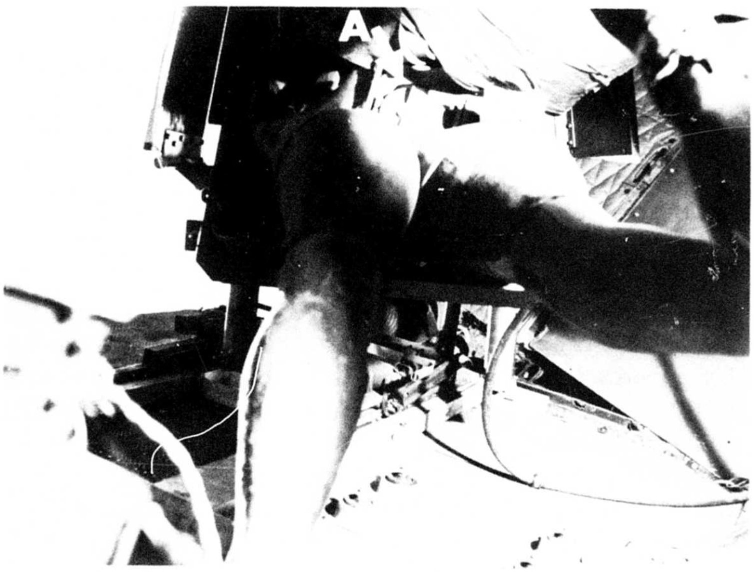

Figure 8. Postcrash Front View of Armored Survival Seat.

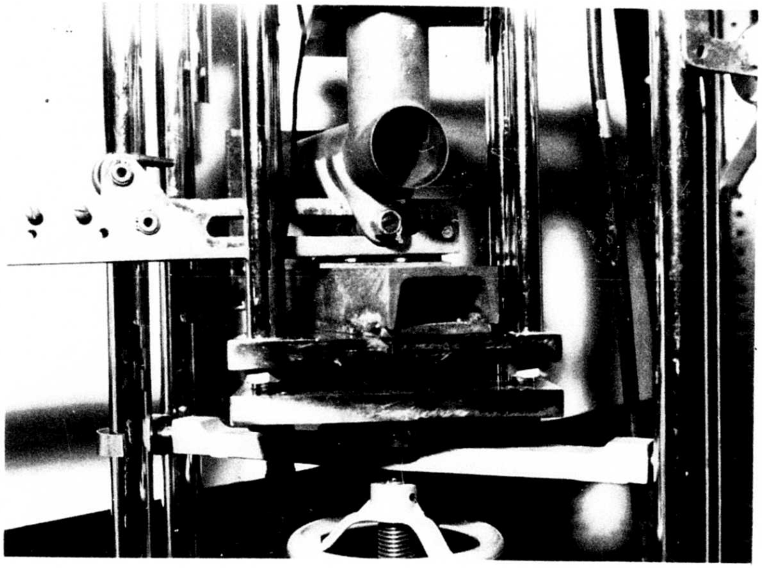

Figure 9. Support Tube Joint Installed in Testing Machine.

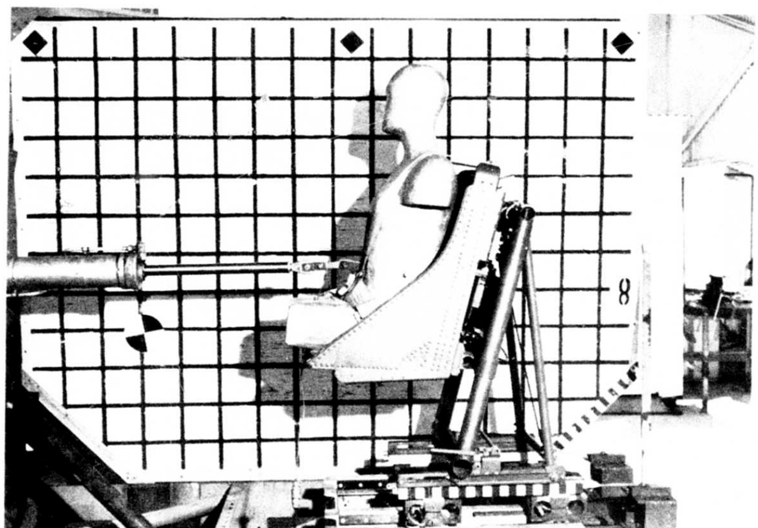

Figure 10. Test Setup for Longitudinal Static Test.

Load was applied by a hydraulic cylinder and measured by a 10,000-pound-capacity strain gauge linked to a strain indicator.

The load was increased to 7,800 pounds, at which point the front cross tubes buckled at their junction with the forward support tubes. The longitudinal energy absorbers did not stroke. Figure 11 shows the failed cross tube.

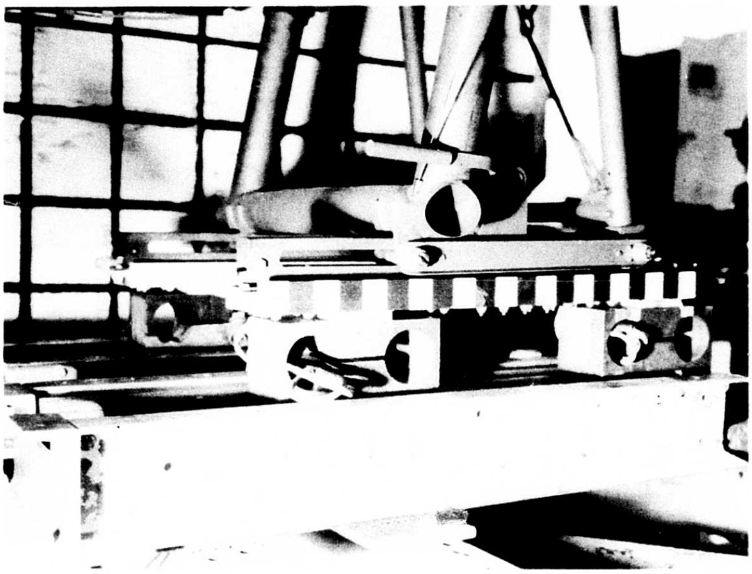

Figure 11. Failure of Front Cross Tube During Longitudinal Static Test.

Following this test, a second longitudinal static test was conducted using a seat manufactured by Hayes International Corporation. To avoid the possibility of stressing the restraint harness beyond its design limits, the seat bucket was removed and the load was applied through a frame fabricated to fit in place of the seat bucket. In the initial test of this seat, the left inboard energy absorber rod failed at the weld joining the rod to its threaded fastener end. This failure occurred when a load of 4,600 pounds was applied to the seat frame. Figure 12 shows this failure.

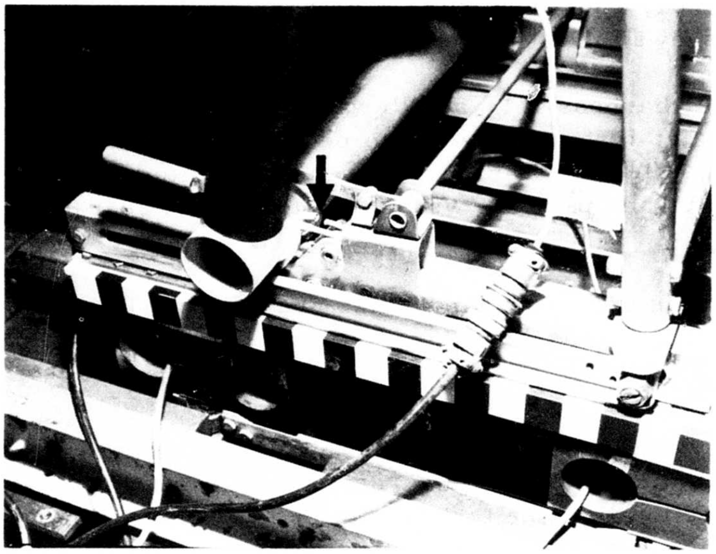

Figure 12. Failed Energy Absorber Rod
on Hayes-Built Seat.

This rod was replaced and the test was repeated. At a load of 9,000 pounds, the energy absorbers began to stroke. No failures of the seat frame occurred. From the results of these three static tests, it was concluded that the USAAVLABS-built seats were weak at the juncture of the forward support tubes with the front cross tubes. This weakness was due to either improper heat-treating of the parts or improper welding techniques.

Because of this obvious weakness in the USAAVLABS-built seats, only Hayes-built seats were used in the dynamic tests.

DYNAMIC TESTS

General

During all dynamic tests, the test seat was occupied by an Alderson F-95 anthropomorphic dummy fitted with a modified pelvis that more nearly reproduces the pelvic contours of a seated man. Accelerometers were installed in the pelvis and head.

Since this armor kit does not include chest armor, the dummy was fitted with the armor, chest protector, and carrier (FSN 8470-926-1575). Figure 13 shows the fully equipped dummy prior to testing.

The shoulder harness release tab was removed from the release buckle of all restraint systems in seats to be tested. Mounts for the accelerometer and deflection transducers were fabricated and installed on the seats. Scales and pointers were installed on the seat to measure deflection.

Test conditions for all dynamic tests are given in Table III.

Drop Tower Tests

The drop tower facility, shown in Figure 14, was used to produce the vertical input accelerations for Tests 1 through 4. The drop tower cage was modified to allow the test seat to be mounted in it. The seat was installed in the cage, and the cage was raised to the proper height to give the required input velocity. Upon release, the cage fell freely, impacting a stack of paper honeycomb that was graduated in a cross-sectional area to produce the desired input acceleration pulse.

Calibration tests were conducted to determine the proper honeycomb stack design for each of the four vertical tests.

Three high-speed cameras were positioned around the drop tower to provide overall side and rear views of the test seat as well as a close-up of the vertical energy absorbers in action.

The seat was mounted in the drop cage, and Tests 1 and 2 were conducted. The armor was then removed from the seat and dummy, the energy absorbers were adjusted to compensate for the reduced weight, and Test 3 was conducted.

To provide a 135-pound occupant for Test 4, the arms and legs were removed from the dummy and the torso was used as the occupant. This torso weighed 132 pounds including instrumentation and was, in fact, more nearly representative of a 160-pound occupant, since the weight was concentrated in the seat pan. The energy absorbers were again adjusted to allow for the reduced weight, and Test 4 was conducted.

The same seat was used for all four of the drop tower tests.

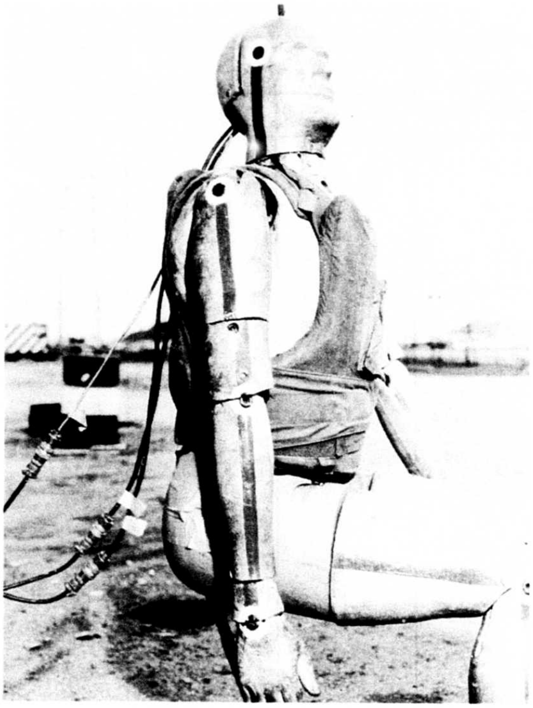

Figure 13. Anthropomorphic Dummy With Modified Pelvis and Chest Armor.

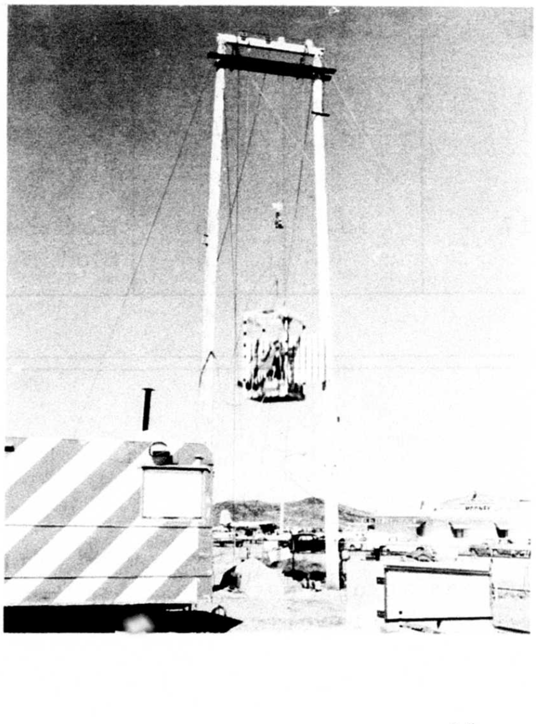

Figure 14. Drop Tower Facility.

TABLE III. TEST CONDITIONS						
Test No.	Orientation	Armor	Occupant Weight (lb)*	Pulse Data		Test Facility
				Peak G	Velocity	
1	Vertical	Seat & Chest	217	7.5	13	Drop Tower
2	Vertical	Seat & Chest	217	40	32	Drop Tower
3	Vertical	None	217	40	32	Drop Tower
4	Vertical	None	135	40	32	Drop Tower
5	Longitudinal	Seat & Chest	217	11	23	Horizontal Sled
6	Longitudinal	Seat & Chest	217	30	40	Horizontal Sled
7	Lateral	Seat & Chest	217	4	8	Horizontal Sled
8	Lateral	Seat & Chest	217	14	17	Horizontal Sled
9	45^{o} pitch 15^{o} yaw	Seat & Chest	217	30	38	Horizontal Sled

*Includes Instrumentation

Horizontal Accelerator Tests

The horizontal accelerator facility shown in Figure 15 was used to produce the longitudinal, lateral, and triaxial input acceleration pulses for Tests 5 through 9. In this device, the drop tower was fitted with a 5000-pound weight connected by a cable and a series of pulleys to a sled

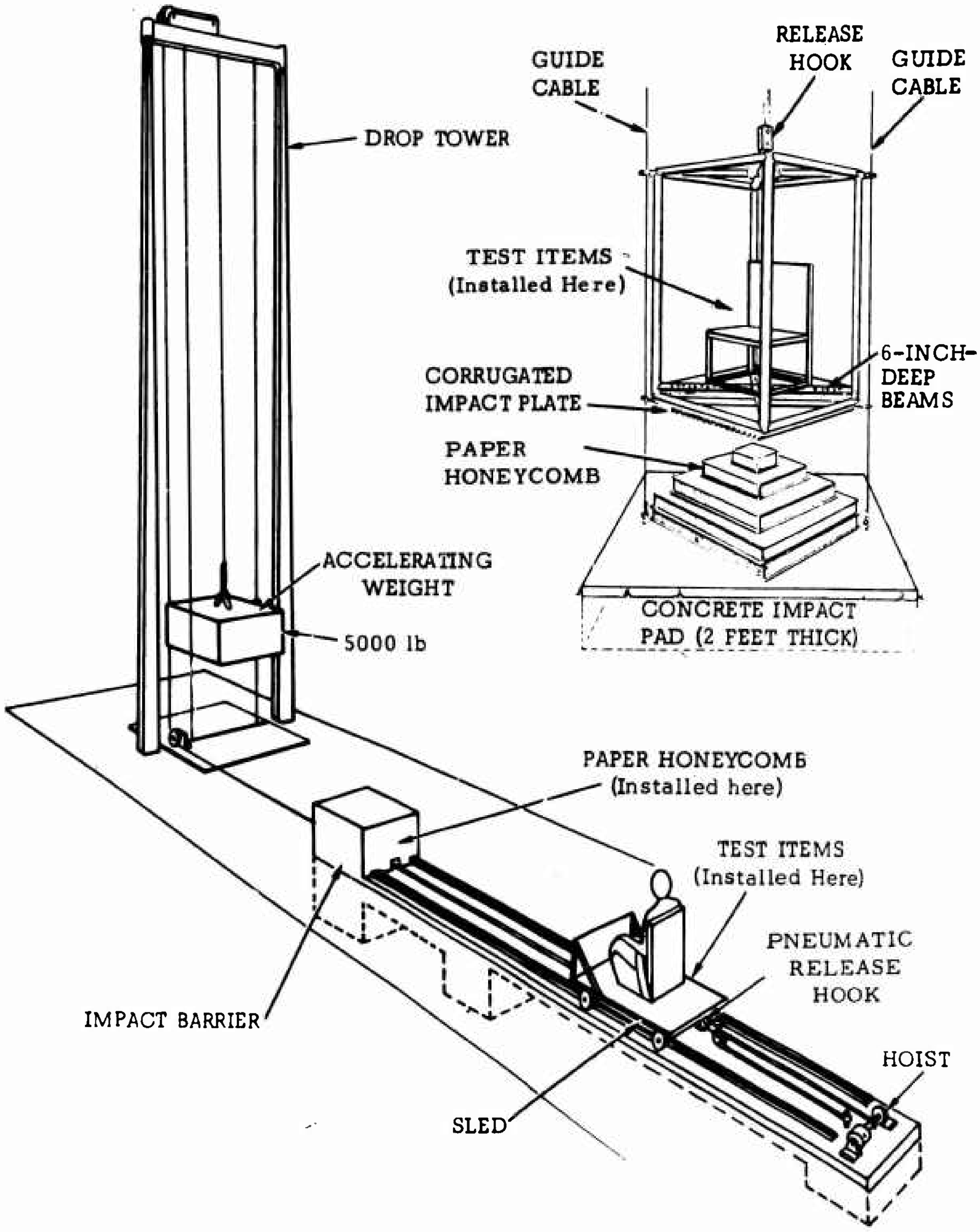

Figure 15. Drop Tower and Short Horizontal Sled Test Facility.

mounted on the horizontal track. In operation, the sled was drawn back along the track, raising the weight in the tower to the prescribed height. When released, the sled was accelerated to the specified velocity by the falling weight. The falling weight was stopped by a pile of sand, allowing the sled to run free and to impact a graduated stack of paper honeycomb mounted on the face of the impact barrier, creating the acceleration pulse on the sled.

Calibration tests were performed to determine the proper honeycomb stack design and drop height for each of the five horizontal tests.

Three high-speed cameras were positioned to provide overall views of the seat as well as close-up views of the energy absorbers in each test.

A new seat was oriented longitudinally on the accelerator sled, and Tests 5 and 6 were conducted. The seat was then oriented laterally, and Tests 7 and 8 were conducted. The lateral energy absorbers did not stroke during Test 8. In an effort to induce stroking, Test 8A was conducted, during which the seat was subjected to a modification of the pulse used in Test 5. No stroking occurred during this test. The seat previously used in the vertical tests was then oriented on the sled for the triaxial test, and Test 9 was conducted.

TEST INSTRUMENTATION

Transducers

The accelerometers used in this test program were Statham Instruments, Models A5 and A6. These instruments provided a frequency response in excess of 200 cycles per second. The force transducers used were calibrated strain links fabricated by AvSER. Deflection transducers which were also fabricated by AvSER, consisted of a rotary potentiometer fitted with a rack and pinion drive. In operation, the rack was affixed to the item whose deflection was to be measured while the potentiometer, with its pinion drive, was affixed at a stationary location. The rack was then drawn out by the motion of the item in question, turning the pinion to drive the potentiometer.

Table IV shows the instrumentation locations.

TABLE IV. INSTRUMENTATION LOCATION		
Measurement	Orientation	Instrument
Input Acceleration		
Drop Tower	Vertical	A-5
Horizontal Accelerator	Longitudinal	A-5
Seat Pan Acceleration	Longitudinal	A-5
	Lateral	A-5
	Vertical	A-5
Occupant Pelvic Acceleration	Longitudinal	A-5
	Lateral	A-5
	Vertical	A-5
Lap Belt Load	Right	AvSER
	Left	AvSER
Shoulder Harness Load		AvSER
Seat Leg Reactions		
Right Front	Vertical	AvSER
Left Front	Vertical	AvSER
Right Rear	Vertical	AvSER
	Horizontal	AvSER
Left Rear	Vertical	AvSER
	Horizontal	AvSER
Energy Absorber Load	Vertical	AvSER
Energy Absorber Deflection	Vertical	AvSER
	Horizontal	AvSER
	Lateral	AvSER
Occupant Head Acceleration	Longitudinal	A-6
	Lateral	A-6
	Vertical	A-6

Electronic Data Recording System

The measurements listed in Table IV were recorded on a magnetic tape recording system. This recording system utilized a constant bandwidth FM/FM multiplex modulation technique in which the analog signal from the transducer was converted by a subcarrier oscillator into a frequency deviation proportional to the input signal amplitude. Seven of these subcarrier oscillator outputs were combined in a mixer amplifier, and the resulting composite signal was recorded on one track of a 14-track tape recorder.

Electronic Data Processing System

The data recorded on the magnetic tape recording system were recovered by utilizing a compatible data processing system. In this system, a playback tape recorder removed the composite signal from each track of the test tape and processed it through a series of FM discriminators, which separated the composite signal into various subcarrier frequency deviations. These frequency deviations were then converted to an analog signal, which was recorded directly on an oscillograph plotter. The resulting oscillograph record was then processed and was available as a scaled analog plot of the recorded parameter.

Photo Instrumentation

Three Photosonic Model 16-1B high-speed cameras operating at 500 frames per second and one Traid 200 high-speed camera operating at 200 frames per second were used to record the dynamic response of the seat and dummy during each test run. One Photosonic camera was mounted to photograph the front of the seat/dummy installation, while the remaining two Photosonic cameras were installed to provide overall and close-up coverage of the appropriate energy absorbers. The Traid 200 camera was used only to record the full-load tests for documentary purposes and was installed to give a three-quarter front view of the test setup.

TEST RESULTS

GENERAL

The test series was conducted in the planned sequence except for the insertion of Test 8A between Tests 8 and 9. This test was added in an effort to cause the lateral energy absorbers to stroke. No seat damage was noted in any of the tests.

The data recording system functioned properly during all tests with the single exception of the left seat belt load in Tests 8A and 9. This transducer came in contact with the seat pan during these tests and was damaged, resulting in invalid data.

A summary of maximum data readings for each full-load test is presented in Table V. Only those channels of data considered to be significant for each full-load test are presented. Time histories of these data are presented in the Appendix.

All accelerometer and load directions are given with respect to the occupant of a forward-facing seat.

DROP TOWER TESTS

Test 1

This was a half-load test of the seat in the vertical orientation. Figures 16 through 18 show, respectively, pretest side and rear views of the seat and a close-up of the vertical energy absorber device.

No seat damage or stroking of the energy absorber occurred during the test.

Test 2

This test was a full-load vertical test of a fully armored seat, using the same test setup as Test 1.

The test pulse had a peak acceleration of 41G and produced a velocity change of 35.6 feet per second. During the test, the vertical energy absorber deflected 5.96 inches under a load of 4,800 pounds. This

TABLE V. SUMMARY OF RECORDED DATA

ITEM	UNIT	TEST NUMBER 2	3	4	6	8	8A	9
Drop Cage Vertical	G	41.0	40.0	41.2	-	-	-	-
Sled Longitudinal	G	-	-	-	21.0	18.4	20.8	36.6
Seat Longitudinal	G	14.0	17.8	20.0	32.0	-	-	24.8
Seat Vertical	G	24.8	28.5	36.7	-	-	-	30.0
Seat Lateral	G	-	-	-	-	11.1	33.5	19.0
Pelvic Longitudinal	G	24.5	32.4	-	48.6	-	-	15.3
Pelvic Vertical	G	27.4	24.6	30.5	-	-	-	30.3
Pelvic Lateral	G	-	-	-	-	19.2	65.0	10.0
Head Longitudinal	G	42.0	34.7	-	40.0	-	-	40.8
Head Vertical	G	-	25.6	32.9	-	-	-	33.0
Head Lateral	G	-	-	-	-	27.2	41.6	6.5
E/A Load Vertical	Lb	4800	3000	3120	-	-	-	5800
E/A Stroke Vertical	In	5.96	6.63	6.87	-	-	-	2.72
E/A Stroke Longitudinal	In	-	-	-	2.18	-	-	0
E/A Stroke Lateral	In	-	-	-	-	0	-	0
Lap Belt Right	Lb	-	-	-	2220	1000	1780	960
Lap Belt Left	Lb	-	-	-	1640	600	-	-
Shoulder Harness	Lb	-	-	-	1850	800	3000	1270
R/F Seat Leg Vertical	Lb	5000	3350	4050	8850	1840	2640	10,500
L/F Seat Leg Vertical	Lb	4300	2800	3560	6100	2050	2970	7860
R/R Seat Leg Vertical	Lb	1100	2550	1360	7500	4800	8120	5850
L/R Seat Leg Vertical	Lb	1900	2350	2060	5850	4850	8120	6270
R/R Seat Load Longitudinal	Lb	-	-	-	3980	-	-	2380
L/R Seat Load Longitudinal	Lb	-	-	-	6740	-	-	3240

Tests 1, 5 and 7 - No damage to seat or stroking of energy absorber developed at half loads.

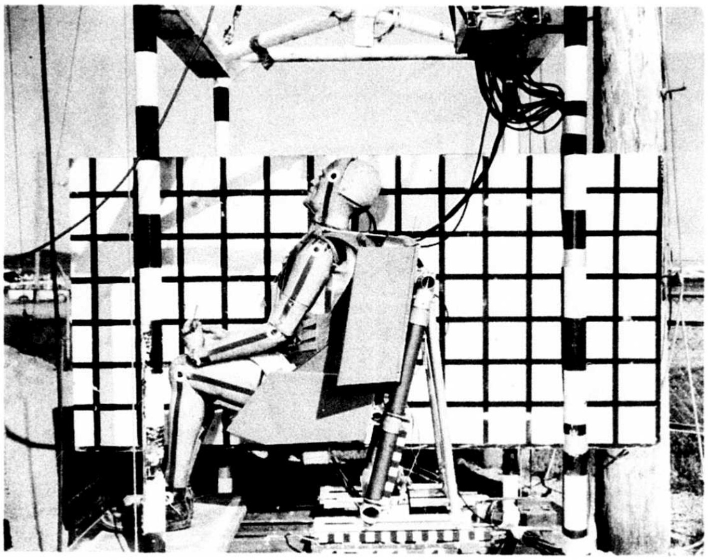

Figure 16. Pretest Side View - Test 1.

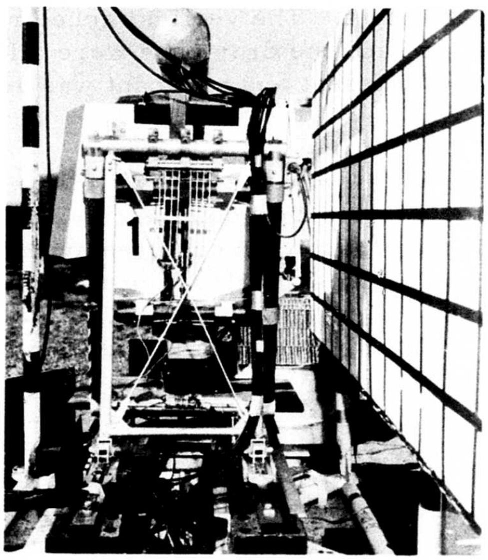

Figure 17. Pretest Rear View - Test 1.

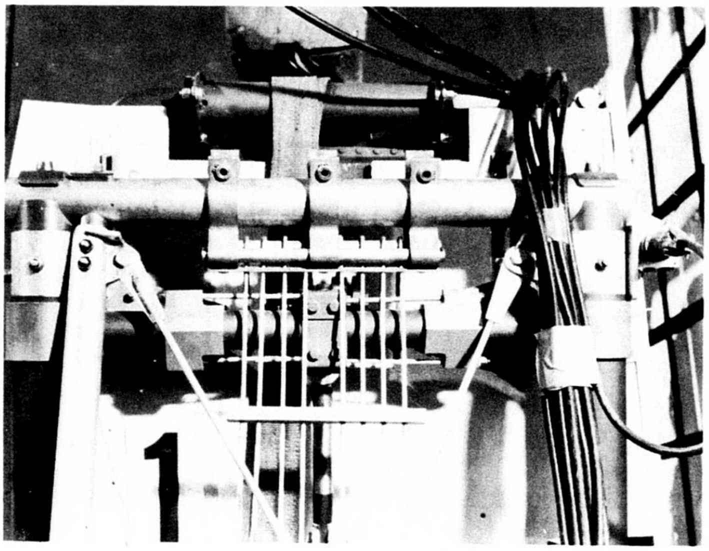

Figure 18. Pretest View of Energy Absorber Device - Test 1.

deflection limited the vertical acceleration of the occupant's pelvis to a peak of 27.4G from a 41G input. The vertical accelerations of the seat pan, the occupant's pelvis, and the drop cage were all in phase, so that the full combined mass of the seat and occupant was acting to load the energy absorbers.

Because the seat pan moves forward as well as downward during stroking, a significant positive longitudinal acceleration is introduced into the occupant's pelvis, producing a compressive contact between the seat back and the occupant. This acceleration reached a peak of 24.5G in this test and indicated a velocity change of 17.8 feet per second. Dynamic overshoot of 2.45 to .1 was present between the seat pan and pelvic acceleration.

Figures 19 and 20 show posttest views of the seat and energy absorbers. All eight energy absorber rods were used, in accordance with the requirements given in Table II for an armored seat with a 200-pound occupant.

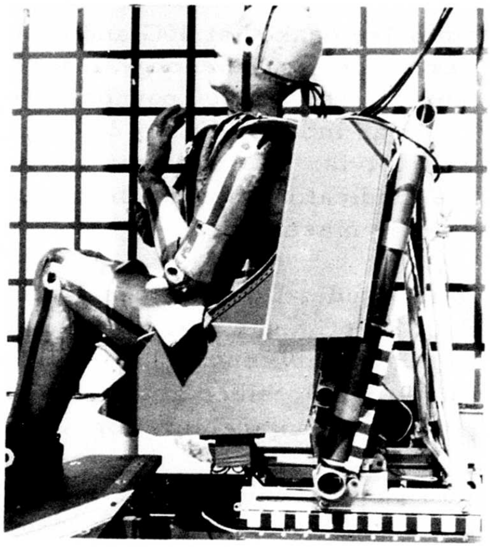

Figure 19. Posttest Side View - Test 2.

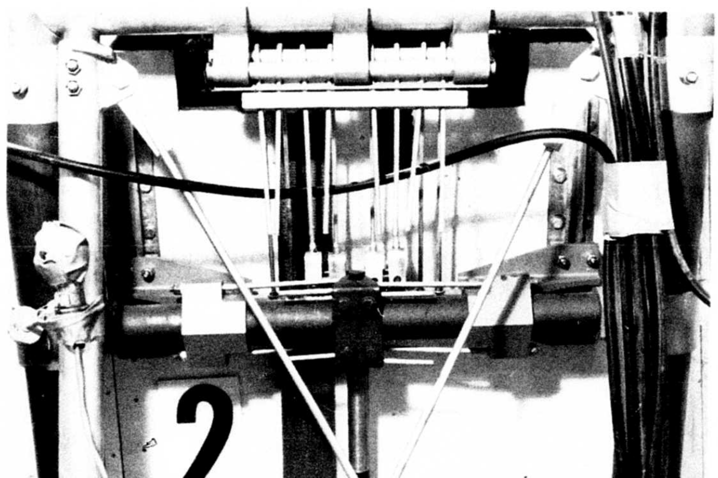

Figure 20. Energy Absorbers After Test 2.

Test 3

This was a full-load vertical test of an unarmored seat. Figures 21 and 22 show pretest views of the seat and energy absorbers.

The input acceleration pulse peaked at 40G and produced a velocity change of 40. 7 feet per second. The energy absorbers stroked 6. 6 inches at a load of approximately 3, 000 pounds. Vertical accelerations were reduced from the peak input of 40G to 28. 5G at the seat pan and 24. 6G in the occupant's pelvis. The seat pan and occupant pelvic accelerations were in phase, indicating that the seat pan and dummy were acting virtually as a single mass.

A significant positive longitudinal pelvic acceleration was also present in this test, with a peak of 32. 6G and a velocity change of 21. 2 feet per second. Dynamic overshoot between the longitudinal accelerations of the pelvis and the seat was 4. 5 to 1, since at the time of the peak pelvis acceleration of 32. 6G, the seat pan acceleration was 7. 3G.

Figures 23 and 24 show posttest views of the seat and energy absorbers. Five energy absorber rods were used, in accordance with the requirements in Table II for an unarmored seat with a 200-pound occupant.

Test 4

This was a full-load test of an unarmored seat with a 135-pound occupant. Figures 25 and 26 show pretest views of the seat and energy absorbers.

The input acceleration pulse peaked at 41. 2G and produced a velocity change of 39. 8 feet per second. The energy absorbers stroked 6. 87 inches and reduced accelerations from the 41G input to 30. 5G at the occupant's pelvis. Figures 27 and 28 show posttest views of the seat and energy absorbers. Four energy absorber rods were used, in accordance with the requirements in Table II for an unarmored seat with a 135-pound occupant.

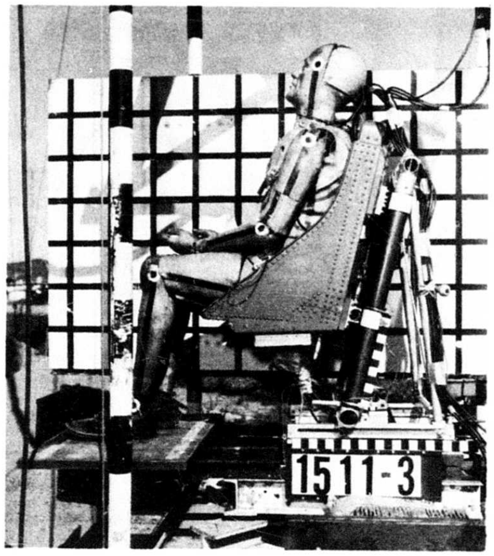

Figure 21. Pretest Side View - Test 3.

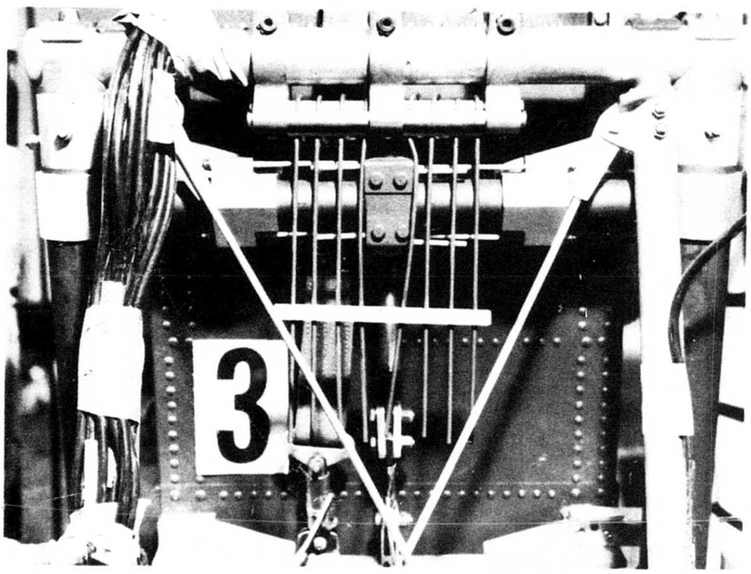

Figure 22. Pretest View of Energy Absorber Device - Test 3.

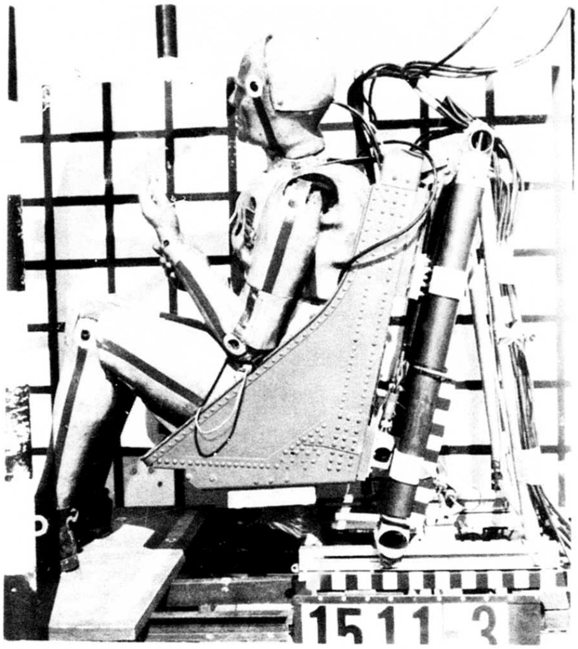

Figure 23. Posttest View of
Seat - Test 3.

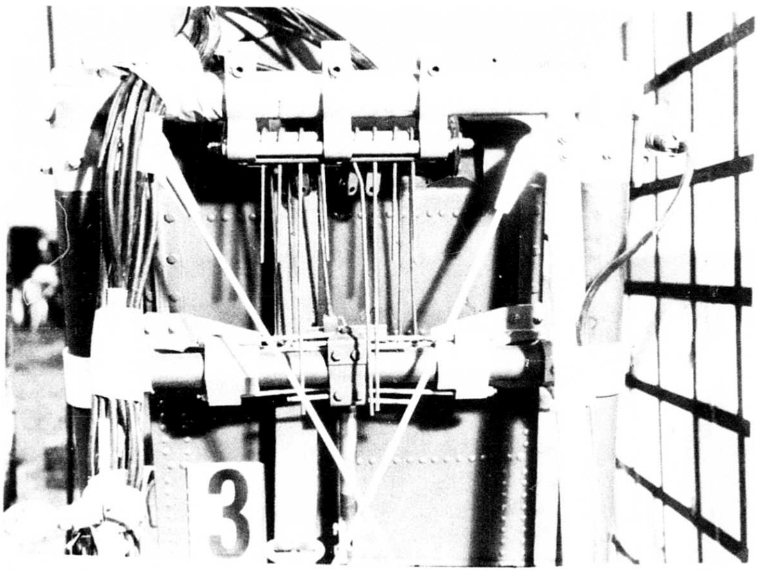

Figure 24. Posttest View of Energy
Absorbers - Test 3.

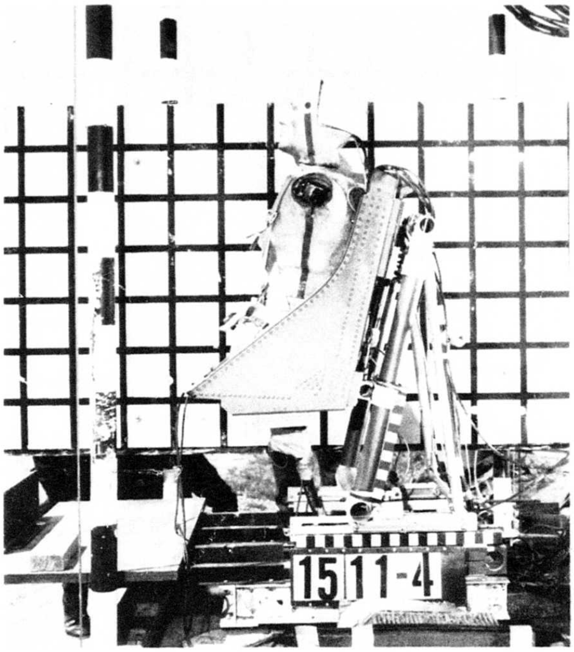

Figure 25. Pretest View of Seat - Test 4.

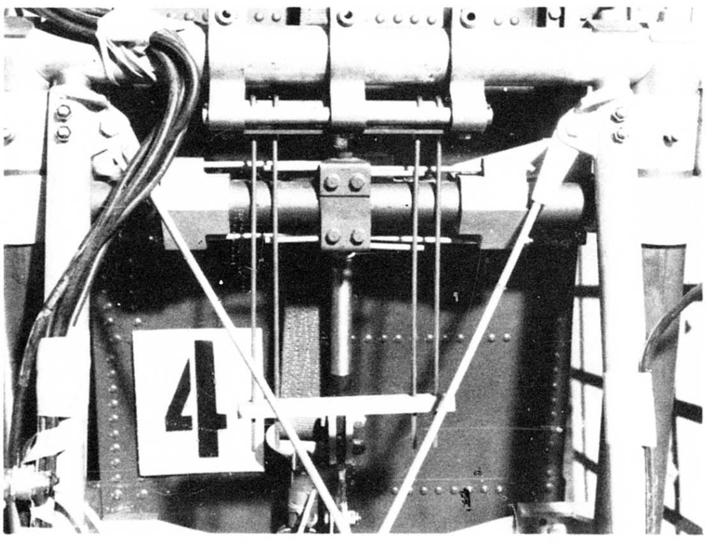

Figure 26. Pretest View of Energy Absorber Device - Test 4.

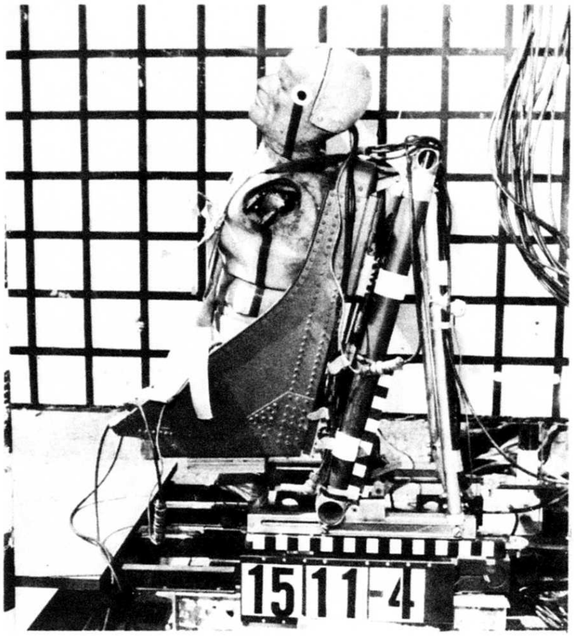

Figure 27. Posttest View of Seat - Test 4.

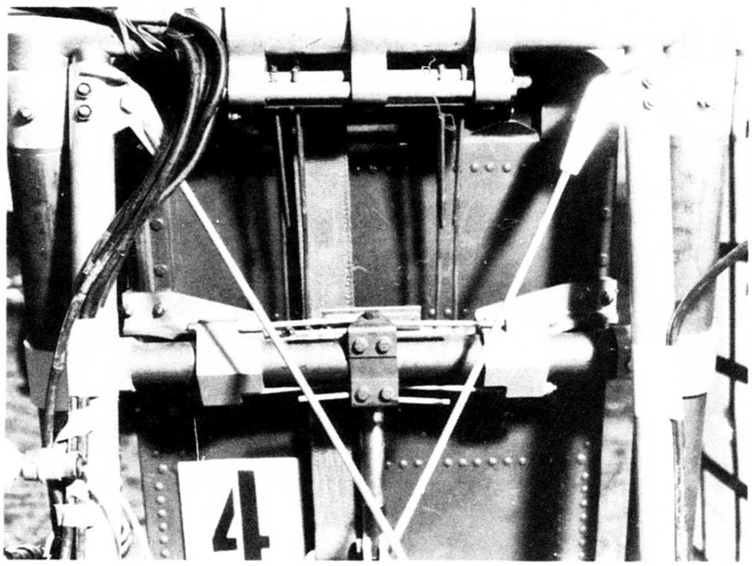

Figure 28. Posttest View of Energy Absorbers - Test 4.

HORIZONTAL ACCELERATOR TESTS

Test 5

This was a half-load longitudinal test of an armored seat. Figure 29 shows a pretest view of the seat. No failures of the seat or stroking of the energy absorbers was noted during the test.

Test 6

This was a full-load longitudinal test of an armored seat, using the same setup as Test 5.

Premature crushing of one of the safety pads resulted in a pulse with a peak of 21G and a velocity change of 43.2 feet per second. Figure 30 shows a posttest view of the seat.

The energy absorbers stroked 2.18 inches. The left outboard energy absorber rod failed at the weld joining the threaded attachment end to the rod. Examination of the high-speed film and electronic data indicated that this failure occurred early in the loading cycle. This failure probably limited deflection by allowing the left side of the seat to move ahead of the right side, thus binding the seat on the slides. High-speed film coverage shows the left side moving ahead of the right side and substantial twisting of the seat frame. Further evidence of this binding is the fact that the left front and right rear seat rollers failed. Figures 31 and 32 show posttest views of the left and right energy absorbers, respectively.

Considerable overshoot was evidenced in both the seat pan and the pelvic accelerations. This was due to the fact that the elasticity of the dummy and the restraint system prevented the seat and dummy from acting as a single mass. The seat pan acceleration showed two distinct peaks, each of about 30G. The pelvic acceleration showed a peak of 48G, followed by a second peak of 24G. The energy absorber stroked immediately following the 48G peak of the pelvic acceleration. The maximum lap belt load occurred simultaneously with this peak.

Analysis of the high-speed film coverage of this test showed little jackknifing or submarining of the dummy. There was considerable flailing of the extremities.

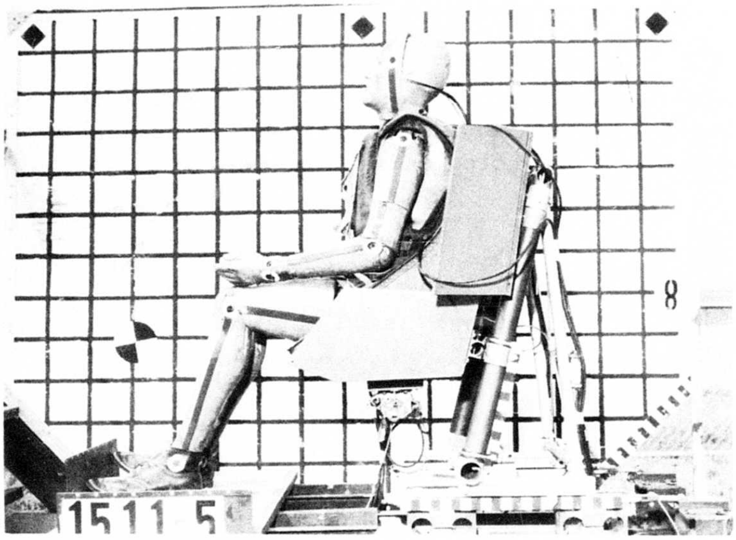

Figure 29. Pretest View of Seat - Test 5.

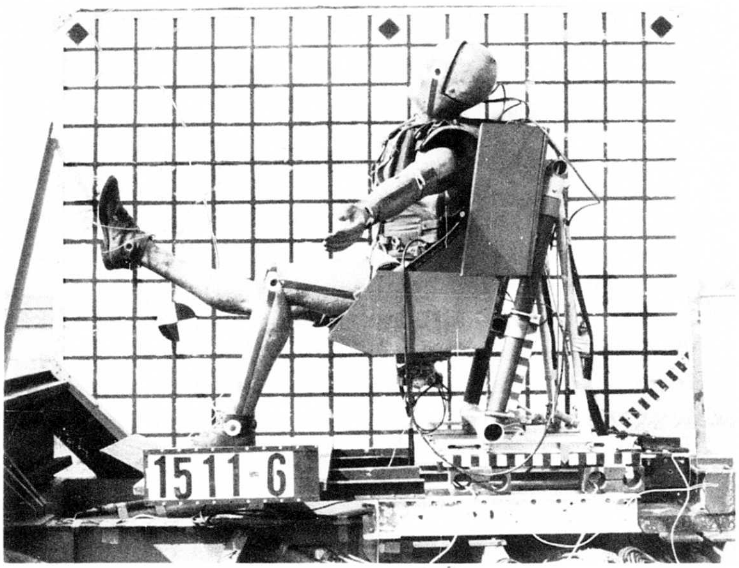

Figure 30. Posttest View of Seat - Test 6.

Figure 31. Posttest View of Left Energy Absorber - Test 6.

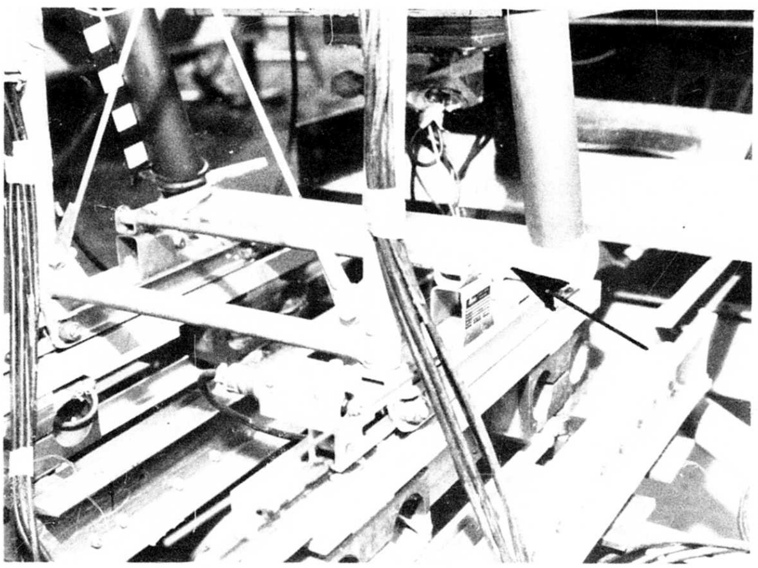

Figure 32. Posttest View of Right Energy Absorber - Test 6.

Test 7

This was a half-load lateral test of a fully armored seat. Figures 33 and 34 show pretest side and rear views of the seat. No seat damage or stroking of the energy absorbers was noted.

Test 8

This was a full-load lateral test of a fully armored seat, using the same setup as Test 7. The acceleration pulse applied had a peak of 8.4G and produced a velocity change of 18.5 feet per second. No seat damage or stroking of the energy absorbers occurred in this test. The seat-pan and occupant pelvic accelerations showed peak values of 11.1G and 19.2G, respectively. These peaks did not occur at the same time; thus, the full combined loads of the seat pan and the occupant were not applied simultaneously to the energy absorbers. Since no stroking of the energy absorbers or seat damage occurred during the test, no posttest photographs were made.

Test 8A

In an effort to produce stroking in the lateral energy absorbers, a second full-load test was conducted utilizing a more severe input pulse. This pulse, which was a modification of the pulse used in Test 5, showed a peak acceleration of 20.8G and produced a velocity change of 30.1 feet per second.

No seat damage or stroking of the energy absorbers occurred in this test, although the seat-pan and occupant pelvic accelerations peaked at 33.5G and 65G, respectively.

The high-speed film coverage showed considerable flailing of the occupant's extremities.

Figure 35 shows a view of the rear of the seat after this test.

Test 9

This, the final test in the series, was a full-load triaxial test of a fully armored seat. Figures 36 and 37 show pretest side and rear views of the seat. The actual test pulse showed a peak of 36.6G with a velocity change

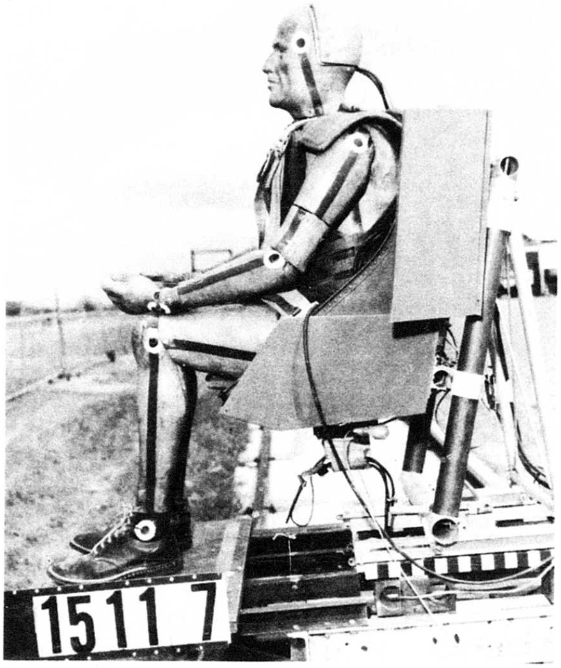

Figure 33. Pretest Side View - Test 7.

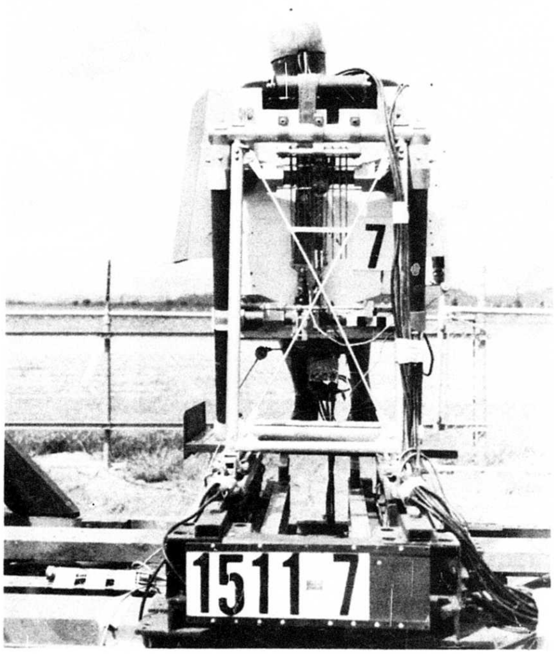

Figure 34. Pretest Rear View - Test 7.

Figure 35. Posttest View of Seat - Test 8A.

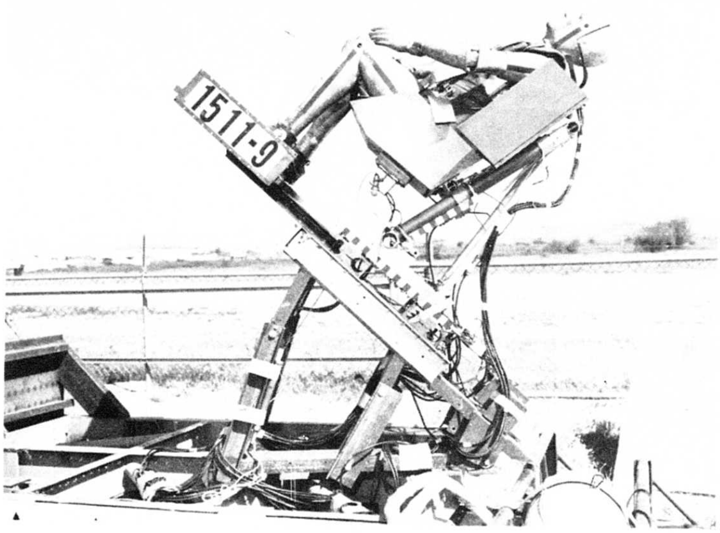

Figure 36. Pretest Side View - Test 9.

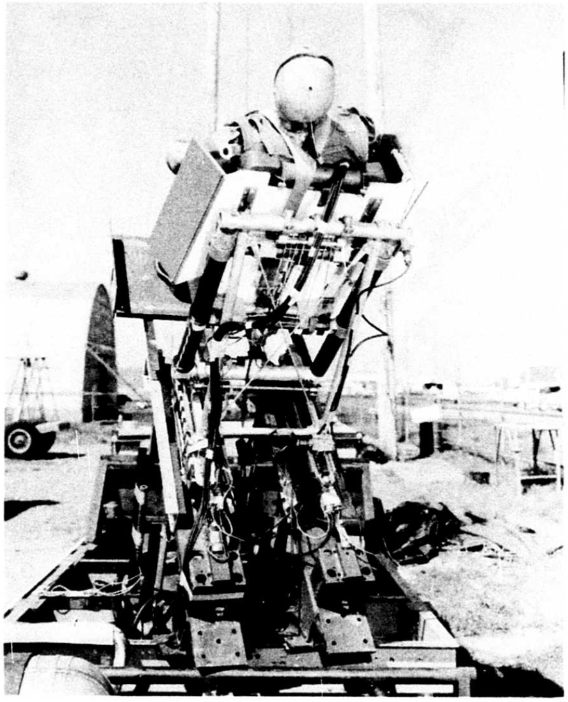

Figure 37. Pretest Rear View - Test 9.

of 46.2 feet per second. No seat damage occurred. The vertical energy absorber stroked 2.72 inches, while the longitudinal and lateral energy absorbers did not stroke. The high seat-pan and occupant pelvic accelerations in the vertical axis reflect the limited energy absorber travel. These vertical accelerations were approximately in phase with the vertical input pulse, particularly during the early part of the pulse.

The reversal in the longitudinal seat-pan acceleration was probably caused by the release of a rear tiedown bolt on the seat mount. At the peak of the input pulse this bolt came free, allowing the seat mount to flex upward and forward.

Figures 38 and 39 show posttest side and rear views of the seat.

Figure 38. Posttest Side View - Test 9.

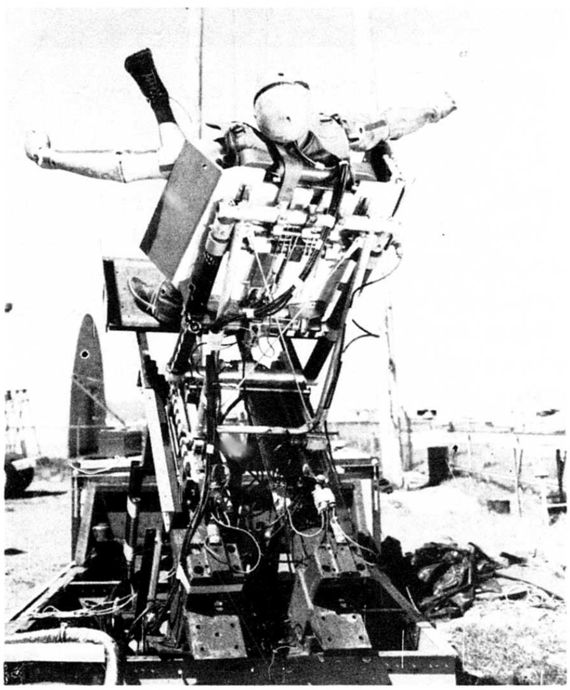

Figure 39. Posttest Rear View - Test 9.

EVALUATION OF TEST RESULTS

VERTICAL TESTS

The performance of the bending rod energy absorber design during the dynamic loading conditions was very close to the static design specifications. For example, in the full-load vertical test (Test 2) of the armored seat, the design load for actuation of the energy absorber was 5,000 pounds. The average load recorded in the energy absorber during the stroke in this test was 4,700 pounds.

The occupant pelvic acceleration that should have resulted from this energy absorber load is 16G. However, a peak of 27G in the occupant's pelvis and 25G on the movable portion of the seat pan were recorded at the same time after impact as the 4,700-pound energy absorber load. This can only mean that an additional force was applied to the seat pan other than that applied through the energy absorber. Investigation of the possible sources of this additional force revealed that large friction forces (F_r) may exist between the front tubes of the seat support structure and the seat pan guides, as shown in Figure 40.

Figure 40 shows the eight typical forces that may be applied to the seat support structure in a vertical impact. These include the total seat reaction loads on the floor (R_S, R_1 and R_2), the seat inertia load (F_I), the seat-pan guide loads (P_1, P_2), the guide frictional load (F_r), and the energy absorber load P_E. The load R_S is effectively zero for pure vertical drops along the "x" axis. Summing the forces along the longitudinal axis of the front support tube in Figure 40 gives

$$F_r = R_1 \text{ Cos } 16^\circ + R_2 \text{ Cos } 21^\circ - F_I \text{ Cos } 16^\circ - P_E \tag{1}$$

Equation (1) has been solved for F_r for Test 2 and is plotted as a function of time in Figure 41.

The friction load increased to approximately 4,200 pounds at 0.037 second and then dropped to 2,000 pounds as maximum stroking rate occurred at 0.05 second. The friction force reduced to zero at 0.08 second, at which time the absorber stroke was completed and rebound started. Approximately 1 inch of rebound occurred, during which the friction force was reversed with respect to the direction shown in Figure 40. The friction force thus remained in opposite direction to the relative motion of the two mating parts.

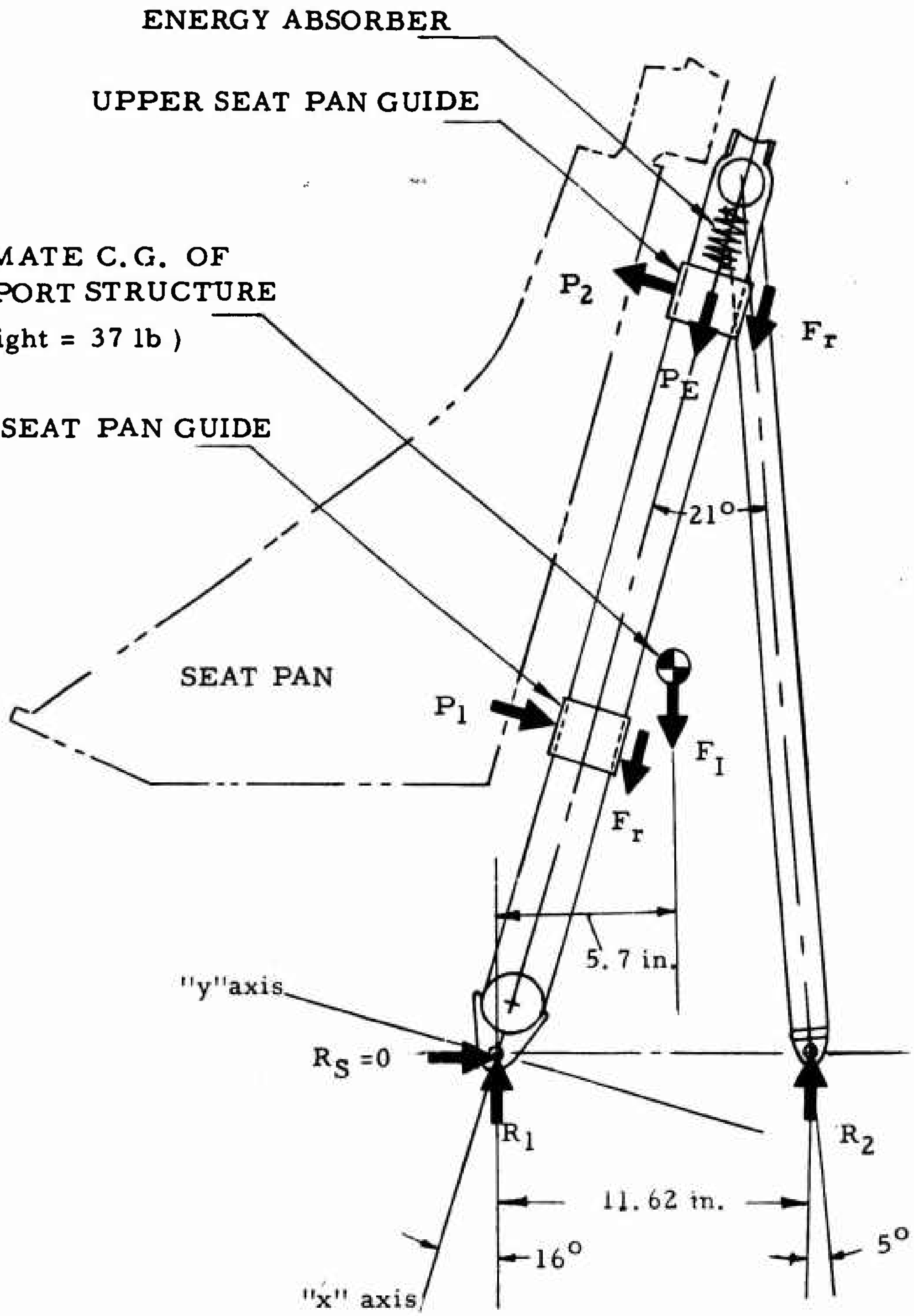

Figure 40. Free-Body Diagram of the Seat Support Structure.

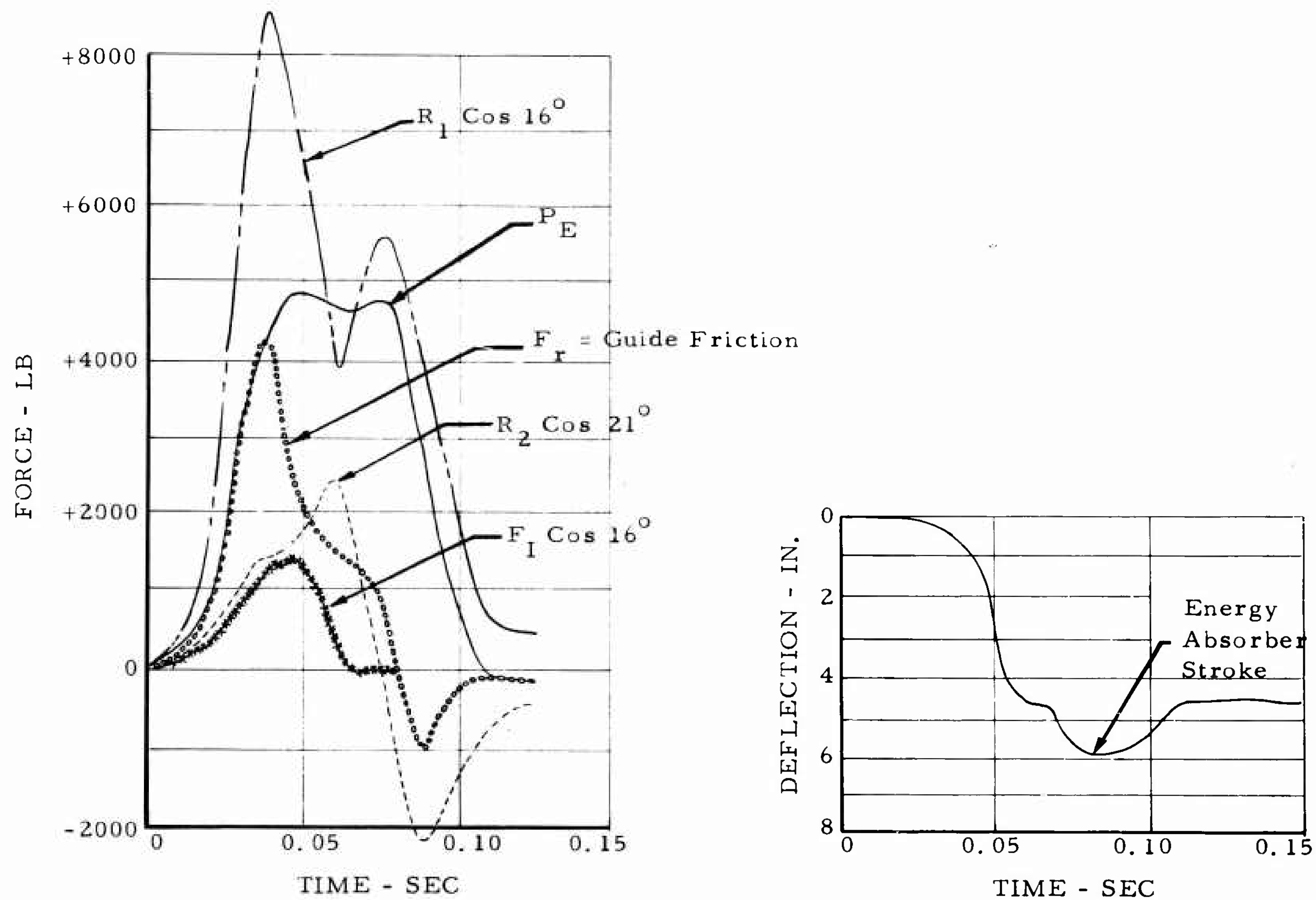

Figure 41. Friction Load in the Seat Pan Guide - Test 2.

Whether the 4,200-pound friction force calculated in the analysis of Test 2 is due to binding or due to the usual dry friction given by

$$F_r = \mu N \qquad (2)$$

where F_r = A force parallel to the surface in contact

N = A force normal to the surface in contact

μ = Coefficient of static friction

cannot be fully resolved. However, if it is assumed that the seat pan (155 pounds) is decelerating at the peak value of 25G and that the effective body mass (173 pounds) and the body armor (14 pounds) are decelerating at the maximum pelvic rate of 27G, then the seat inertia and occupant inertia loads P_{SI} and P_{OI} in Figure 42 are 3,880 and 5,050 pounds, respectively.

Then, summation of moments in Figure 42 gives

$$P_2 (14.25) - P_{SI} (4.84) \cos 16^{\circ} - P_{OI} (16.25) \cos 16^{\circ} + P_{SI} (8.95) \sin 16^{\circ} + P_{OI} (6.85) \sin 16^{\circ} = 0$$

$$P_2 = \frac{\left[P_{SI} (4.84) + P_{OI} (16.25)\right] \cos 16^{\circ}}{14.25} - \frac{\left[P_{SI} (8.95) + P_{OI} (6.85)\right] \sin 16^{\circ}}{14.25}$$

$$P_2 = \frac{\left[(3880)(4.84) + (5050)(16.25)\right] .96126}{14.25} - \frac{\left[(3880)(8.95) + (5050)(6.85)\right] .27564}{14.25}$$

$$P_2 = 5461 \text{ lb}$$

$$P_1 (14.25) - P_{SI} (4.84) \text{ Cos } 16^\circ + P_{OI} (16.25) \text{ Cos } 16^\circ$$

$$- P_{SI} (5.30) \text{ Sin } 16^\circ + P_{OI} (7.40) \text{ Sin } 16^\circ = 0$$

$$P_1 = \frac{\left[P_{SI} (4.84) + P_{OI} (16.25)\right] \text{Cos } 16^\circ + \left[P_{SI} (5.30) + P_{OI} (7.40)\right] \text{Sin } 16^\circ}{14.25}$$

$$P_1 = \frac{\left[(3880)(4.84) + (5050)(16.25)\right] .96126}{14.25}$$

$$+ \frac{\left[(3880)(5.30) + (5050)(7.40)\right] .27564}{14.25}$$

$$P_1 = 7923 \text{ lb}$$

The total normal load on the guide system would then be

$$N = \left|P_1\right| + \left|P_2\right| = 13,384 \text{ lb} \qquad (3)$$

and the required coefficient of friction to realize the calculated 4,200-pound frictional load would be

$$\mu = \frac{F_r}{N} = \frac{4200}{13384} = 0.31 \qquad (4)$$

This does not appear to be an excessively high coefficient, particularly if dust or other foreign material is present. In fact, the measured coefficient on one of the four seats was found to be 0.45 with 145 pounds of normal load applied and 0.30 with 310 pounds of normal load applied. It may thus be considered reasonable that dry friction is present in this seat design since the calculated 4,200-pound frictional load results.

It should be noted that the peak friction force (4,200 pounds) is almost equal to the peak energy absorber load (4,700 pounds). As a result, the load being applied to the seat pan is almost double that of the desired load. Obviously, a suitable means must be found to eliminate this variable friction force. One solution would be the use of linear bearings or rollers in the guide system. In fact, one of the four original seat designs referred to in the Introduction of this report used a roller guide system. Caution must be exercised on the part of the seat designers to

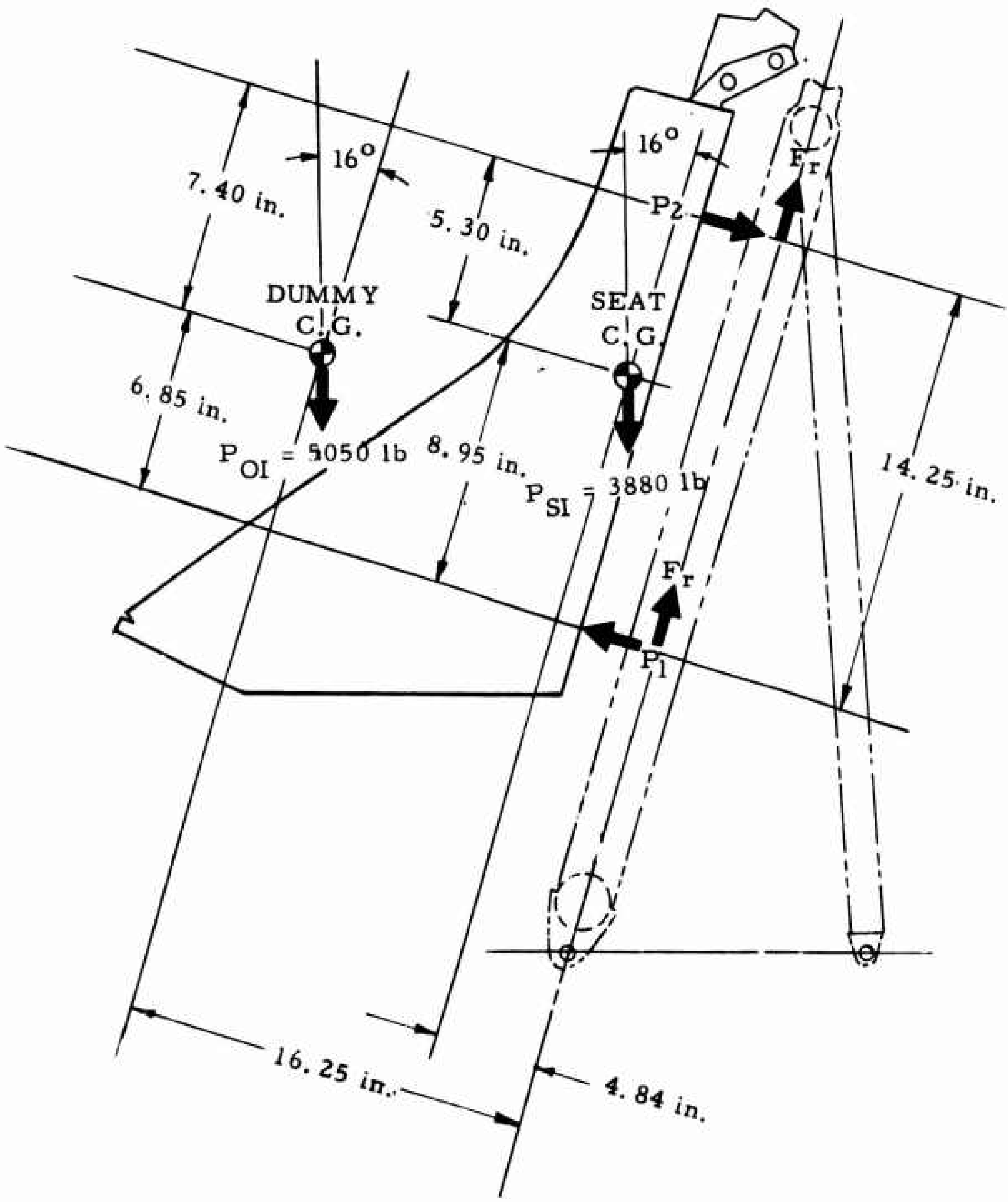

Figure 42. Free-Body Diagram of the Seat Pan.

make certain that the movable part of the energy absorbing seat system not only is free of friction but strokes smoothly without variable resistance. This must occur when the seat is subjected to all anticipated loads, even though distortion of the seat pan guide system occurs. Such distortion occurs in the form of bending of the guide rails and torsion and shearing deformations due to lateral loads and floor buckling. Close-fitting seat-pan guide systems (as in the Hayes seat tested in this project) should be expected to bind and/or experience excessive frictional forces when subjected to these loading conditions.

HORIZONTAL TEST

The performance of the bending rod energy absorber design during the dynamic loading condition cannot be completely evaluated, as one of the four rods failed during the stroke. As a result of this failure, the left side of the seat moved ahead of the right side and caused the seat track to bind. This energy absorber failure at the weld between the rod and the seat attachment was also observed in the static test of the seat. It is apparent that either the design of the rod must be changed or better welding procedures combined with good quality control must be assured before this design is tested further.

A detailed examination of the acceleration and force data recorded during the test indicates that the energy absorber might not have functioned as designed in this test, even if the energy-absorber had not failed. The forward deflection of the occupant, although small in comparison to tests of other seats, was sufficient to allow the dummy inertia force to lag the seat inertia force by 0.02 second, as shown in Figure 43. This resulted in a high pelvic acceleration of 48G peak at 0.07 second. This acceleration level is at the upper limit of human tolerance; even more important, the high rate of onset of 2500G per second is considered to be excessive from a human tolerance standpoint. Methods of insuring that the seat and occupant inertia forces act more in phase with each other must be investigated before proper operation of the longitudinal energy absorber can be expected.

LATERAL TEST

The lateral energy absorber did not function in either of the two full-load tests conducted. The level of the first test (Test 8) was chosen to produce the full design loads. After examination of the seat for structural failures, another test (Test 8A) was conducted at a level twice that of the

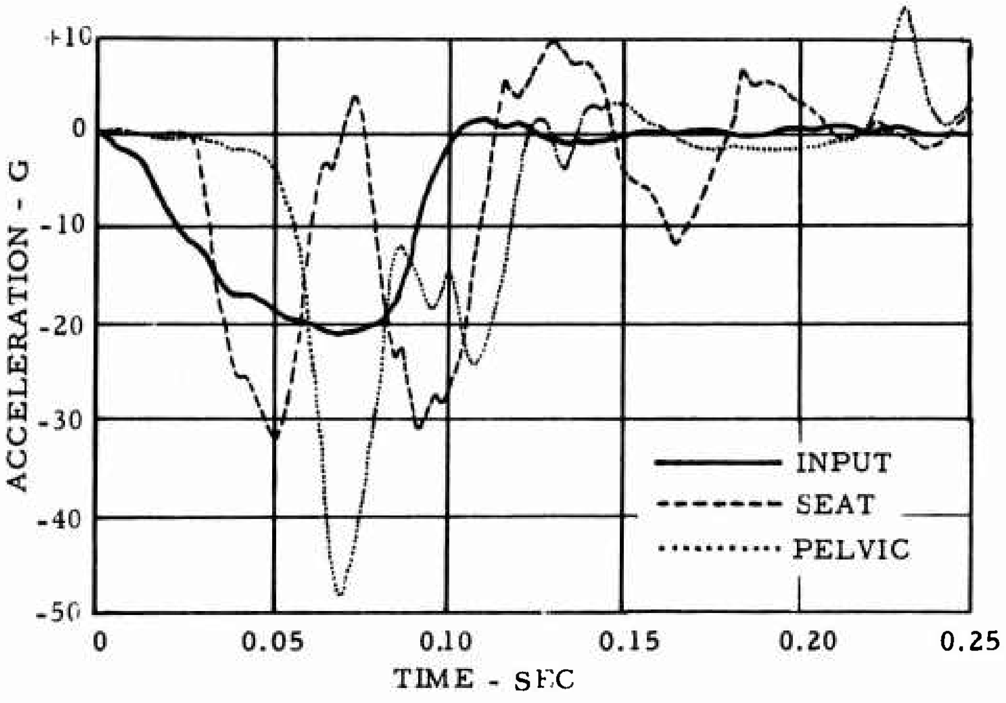

Figure 43. Composite Acceleration Data Overlay - Test 6.

design load, and the seat was again examined for structural failures. There were no structural failures noted; however, violent motions of the dummy were observed during the test. Examination of the accelerometer and force data revealed that the occupant inertia force lagged the seat inertia force by 0.02 second in both tests. Dynamic overshoot in the pelvic area resulted in peak acceleration of 18G in Test 8 and 63G in Test 8A. These forces, combined with the violent action of the dummy observed from the high-speed film, indicate that considerable redesign for the lateral load condition is required before satisfactory test results can be obtained.

TRIAXIAL TEST

The results of this test confirm the results of the previous tests. Only the vertical energy absorber functioned, since only in this axis did the seat pan and occupant accelerations remain in phase. Even so, the dummy vertical pelvic acceleration was above the design levels, as were these pelvic accelerations in all other axes. All pelvic accelerations were within the recognized limits of human tolerance.

CONCLUSIONS

Based on the data gathered during this test series, it is concluded that:

1. The vertical energy absorber system functions at approximately the design load; however, it does not limit the seat and pelvic accelerations to the design limits. Excessive frictional loads in the seat pan guide system seem to be responsible.

2. The longitudinal energy absorber system does not limit the seat and pelvic accelerations to the design limits because the seat and occupant do not load the absorber as a single mass.

3. The lateral energy absorber system does not limit the seat and pelvic accelerations to the design limits because the seat and occupant do not load the absorber as a single mass.

4. The weldment that joins the longitudinal energy absorber rods to the threaded attachment fittings fails at loads below that required to stroke the rod.

5. Pelvic accelerations experienced by the occupant during all tests were within the limits of human tolerance with respect to duration.

6. Pelvic accelerations experienced by the occupant during Test 6 and Test 8A could have been injurious to a human due to the high onset rate combined with the high peak values.

7. The seat design results in a sturdy seat, capable of remaining intact under very high loads.

8. The merits of the single-point gather (rotary buckle) for the lap belts and shoulder harness are negated by the tendency of the buckle to release when the tab is pushed outward by a seat occupant under stress.

RECOMMENDATIONS

Based on the foregoing conclusions, it is recommended that:

1. The vertical seat pan slide be modified to minimize friction loads.

2. The longitudinal energy absorber system be redesigned, taking into account the fact that the seat and occupant do not act as a single mass, and additional tests be conducted.

3. The seat be tested under static loading in the lateral direction to determine the load required to stroke the energy absorber. The lateral energy absorber system should then be redesigned on the basis of the results of this test and further dynamic tests should be conducted.

4. The welded joint be eliminated from the longitudinal energy absorber rods, or better manufacturing controls be established to prevent failure.

5. Consideration be given to reducing the ratio of effective seat weight to effective occupant weight to as far below one-to-one as possible without sacrificing strength, particularly in the longitudinal and lateral axes.

6. The shoulder harness release tab be removed from all restraint harness buckles of this type.

APPENDIX
TIME HISTORIES

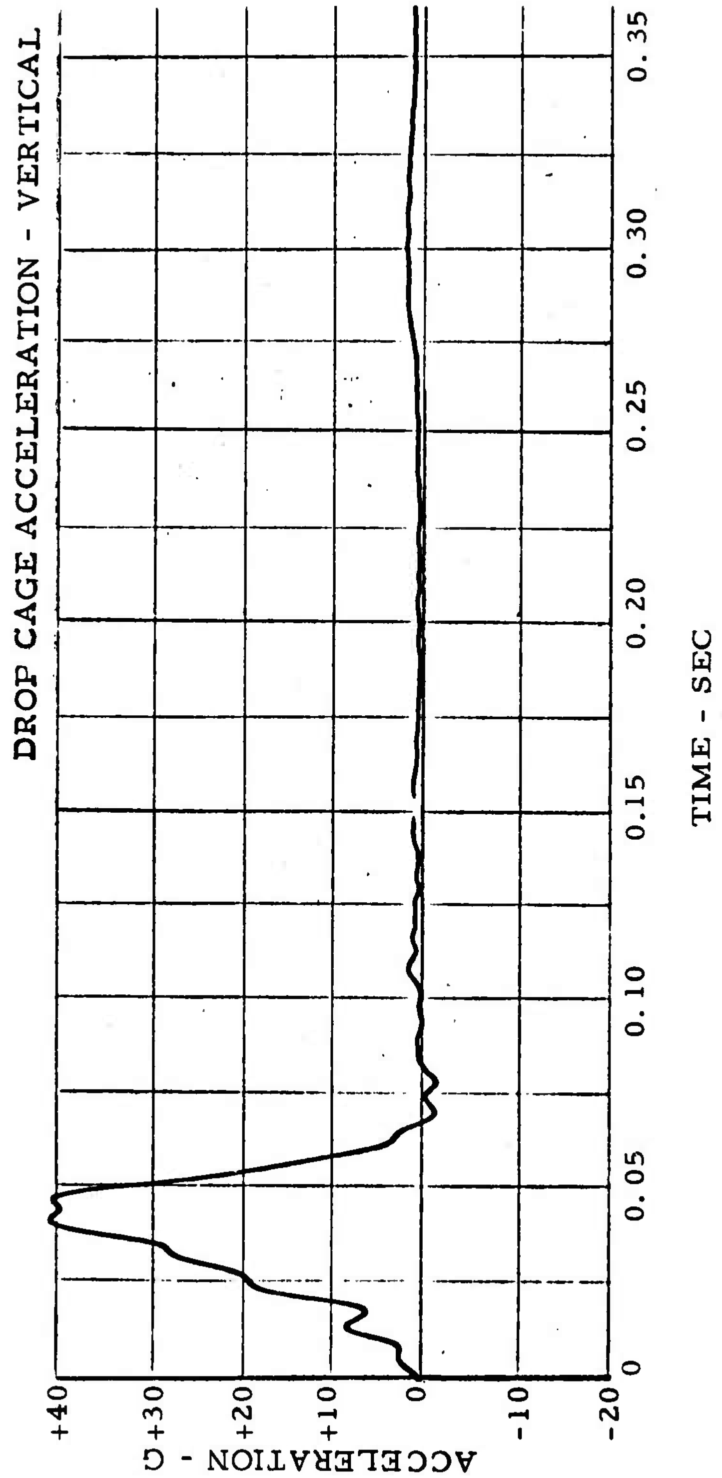

Figure 44. Acceleration-Time History - Test 2.

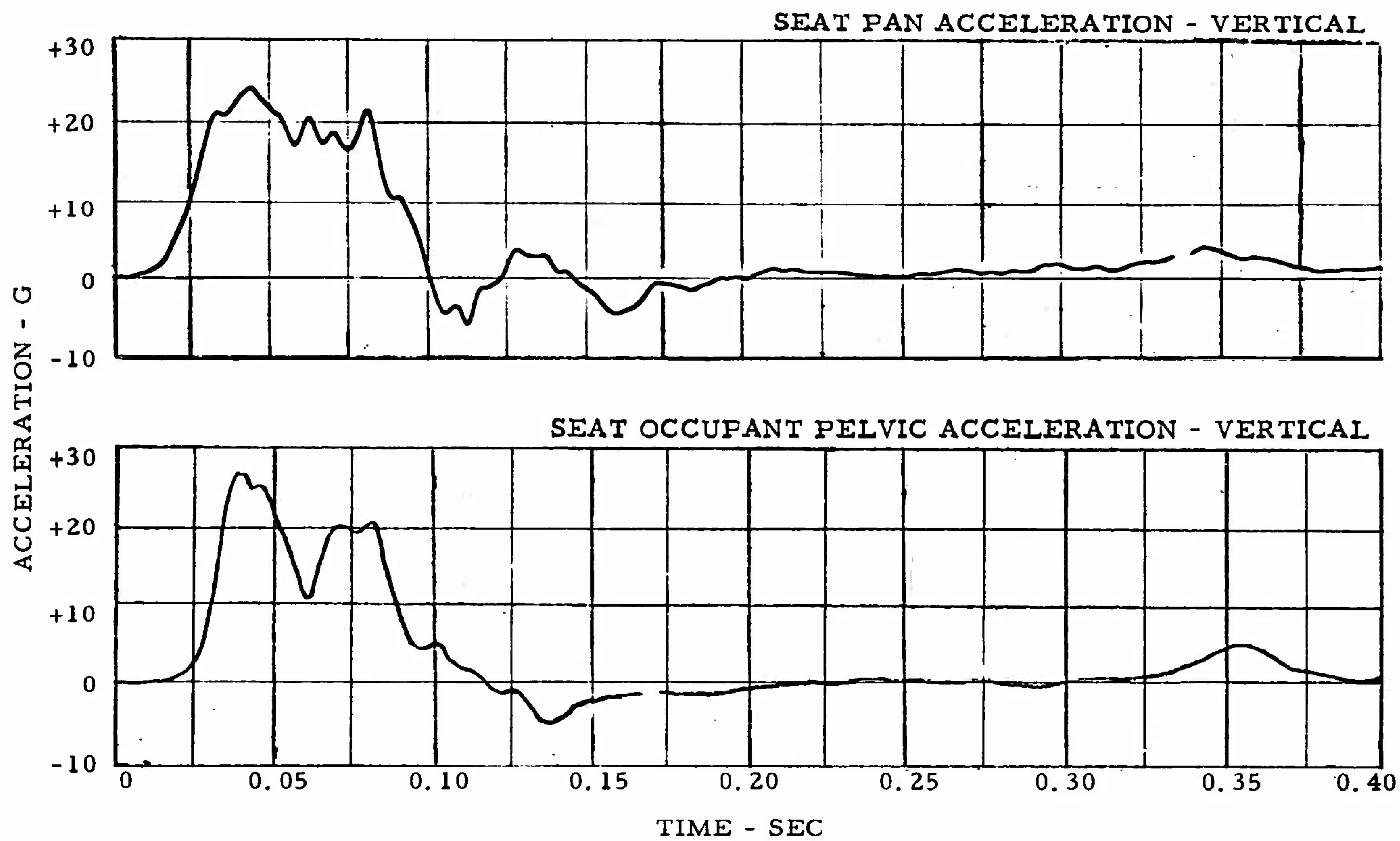

Figure 45. Acceleration-Time Histories - Test 2.

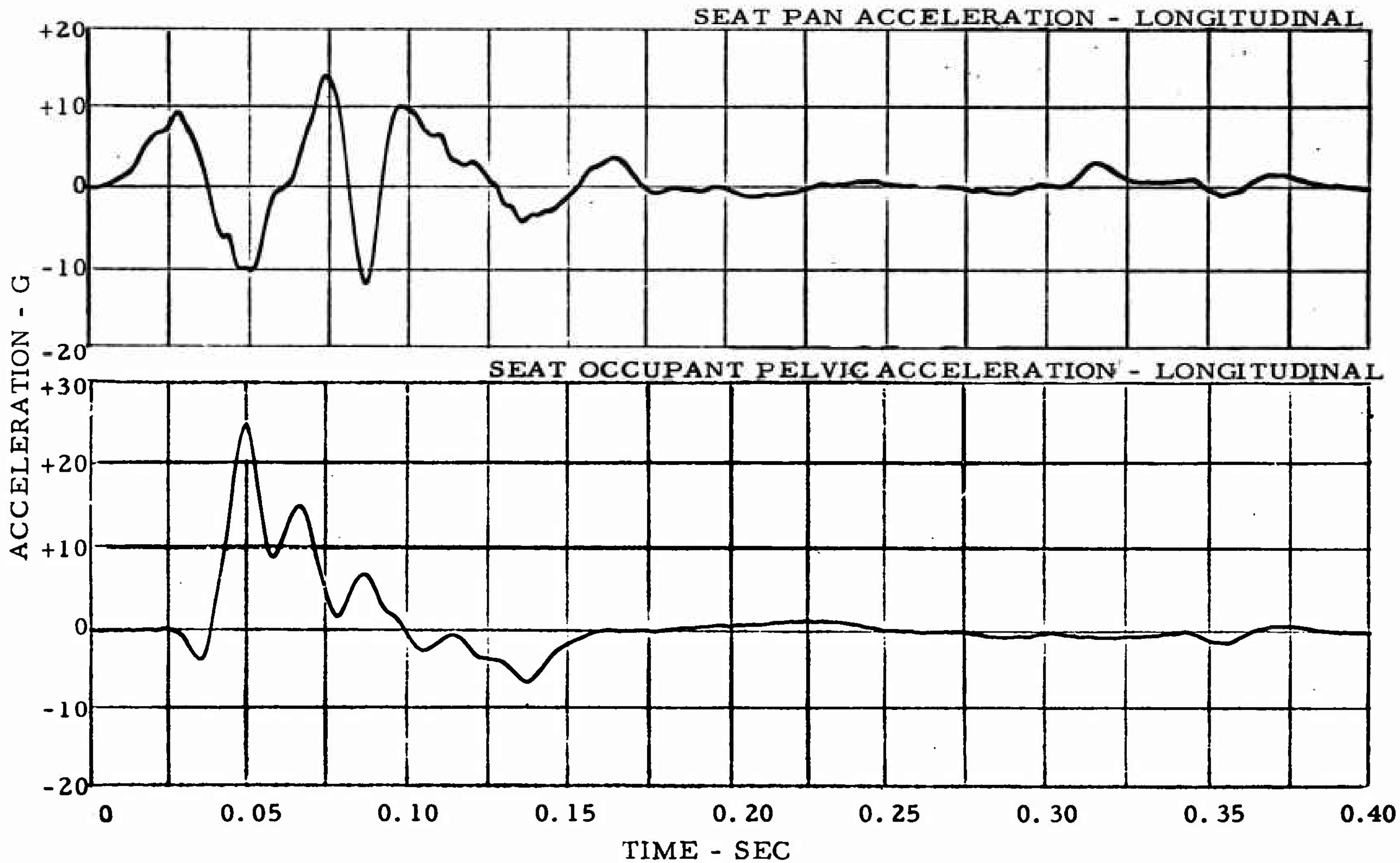

Figure 46. Acceleration-Time Histories - Test 2.

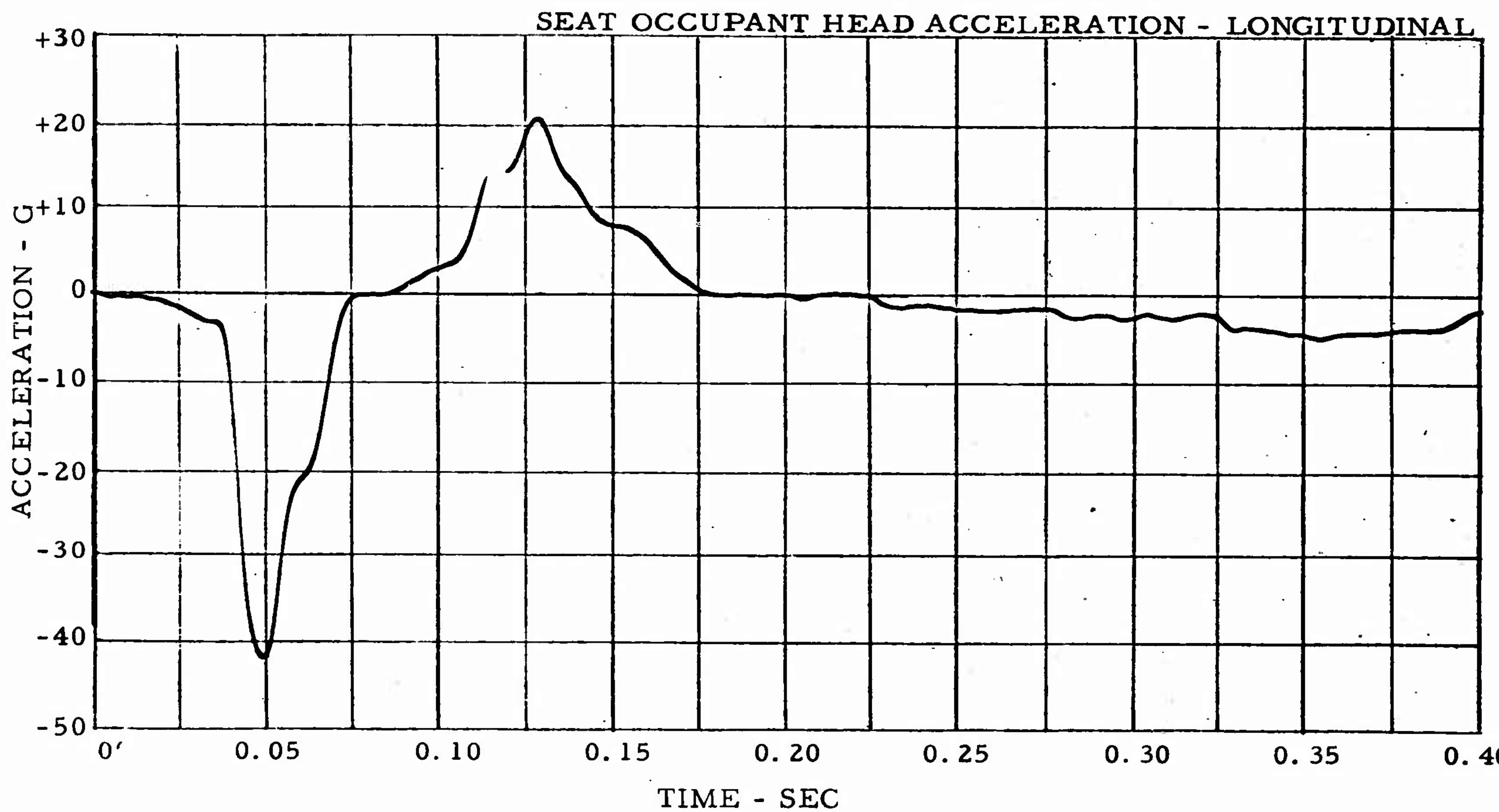

Figure 47. Acceleration-Time History - Test 2.

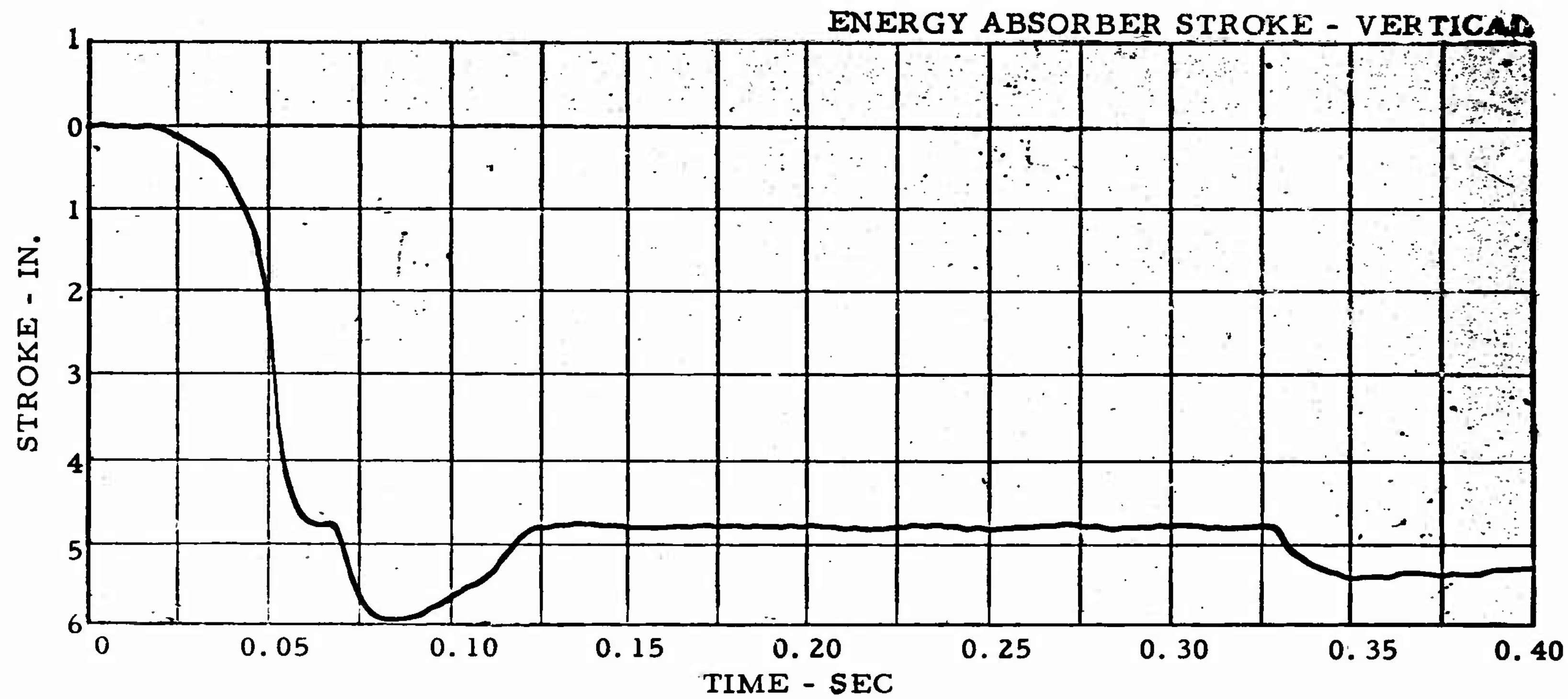

Figure 48. Stroke-Time History - Test 2.

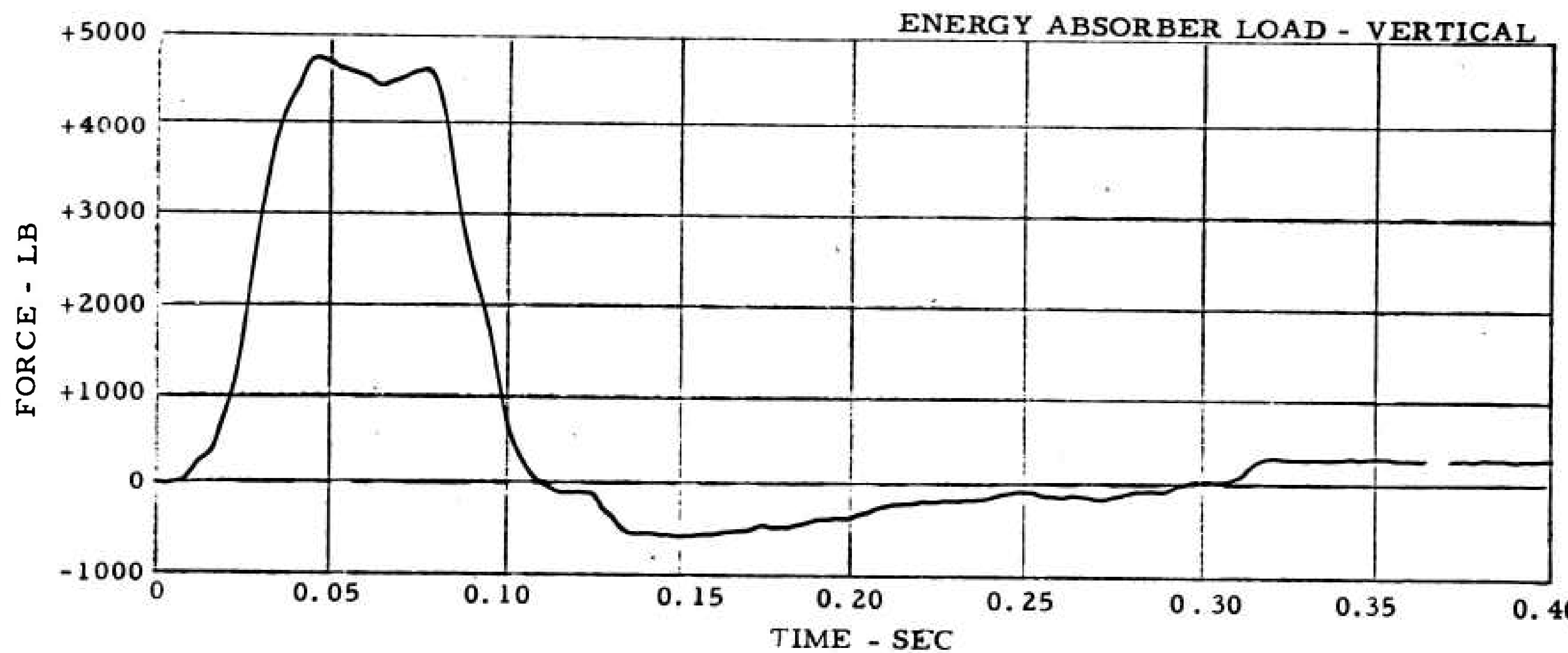

Figure 49. Force-Time History - Test 2

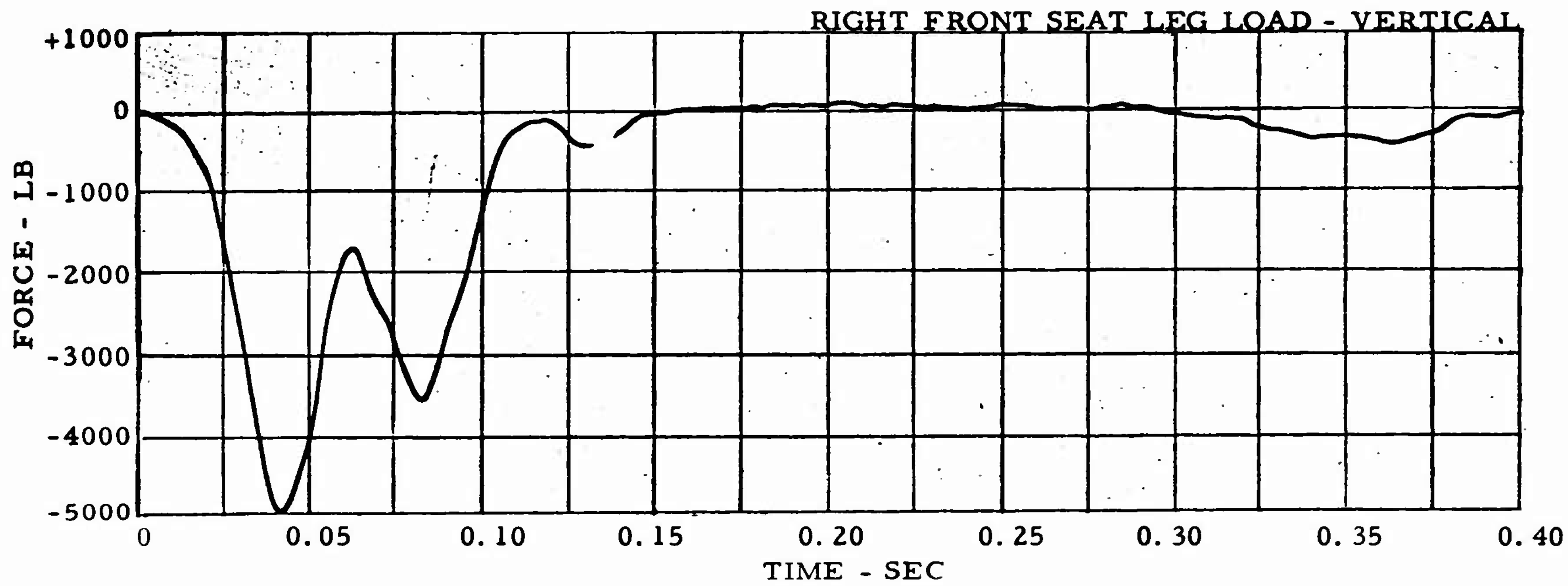

Figure 50. Force-Time History - Test 2.

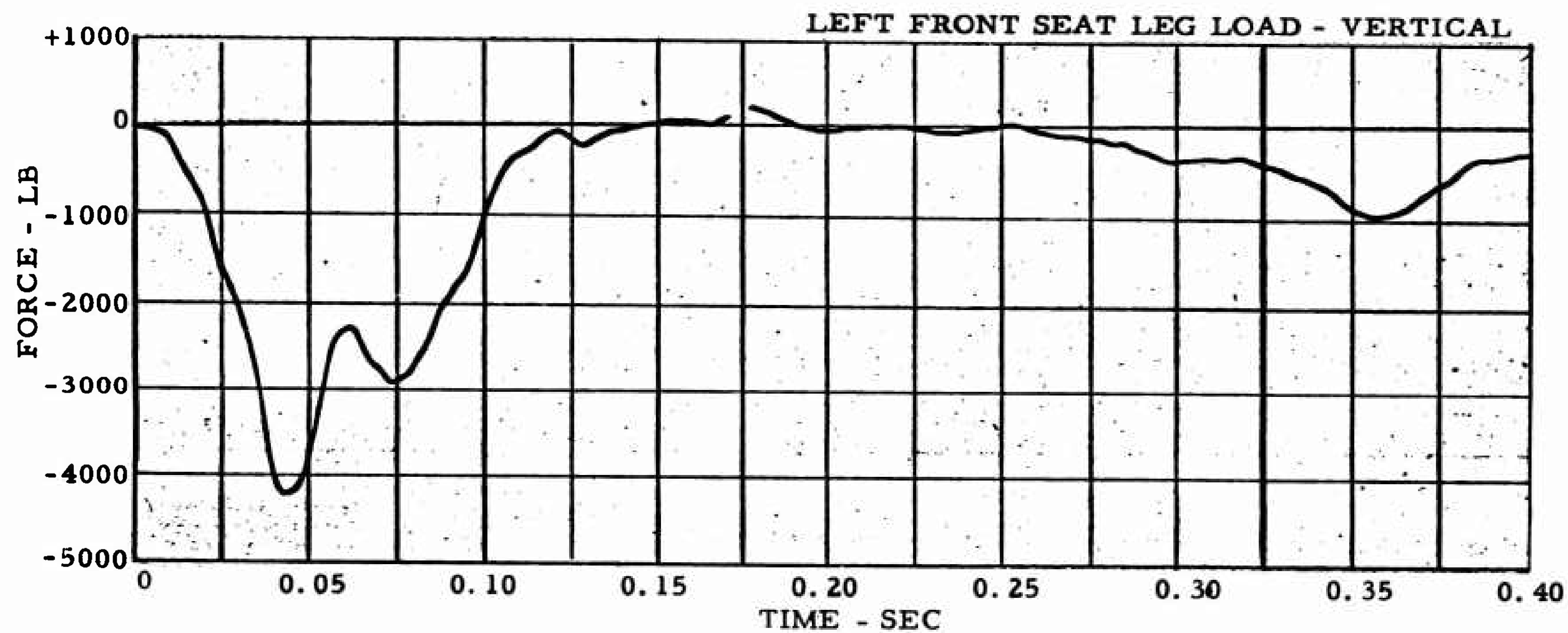

Figure 51. Force-Time History - Test 2.

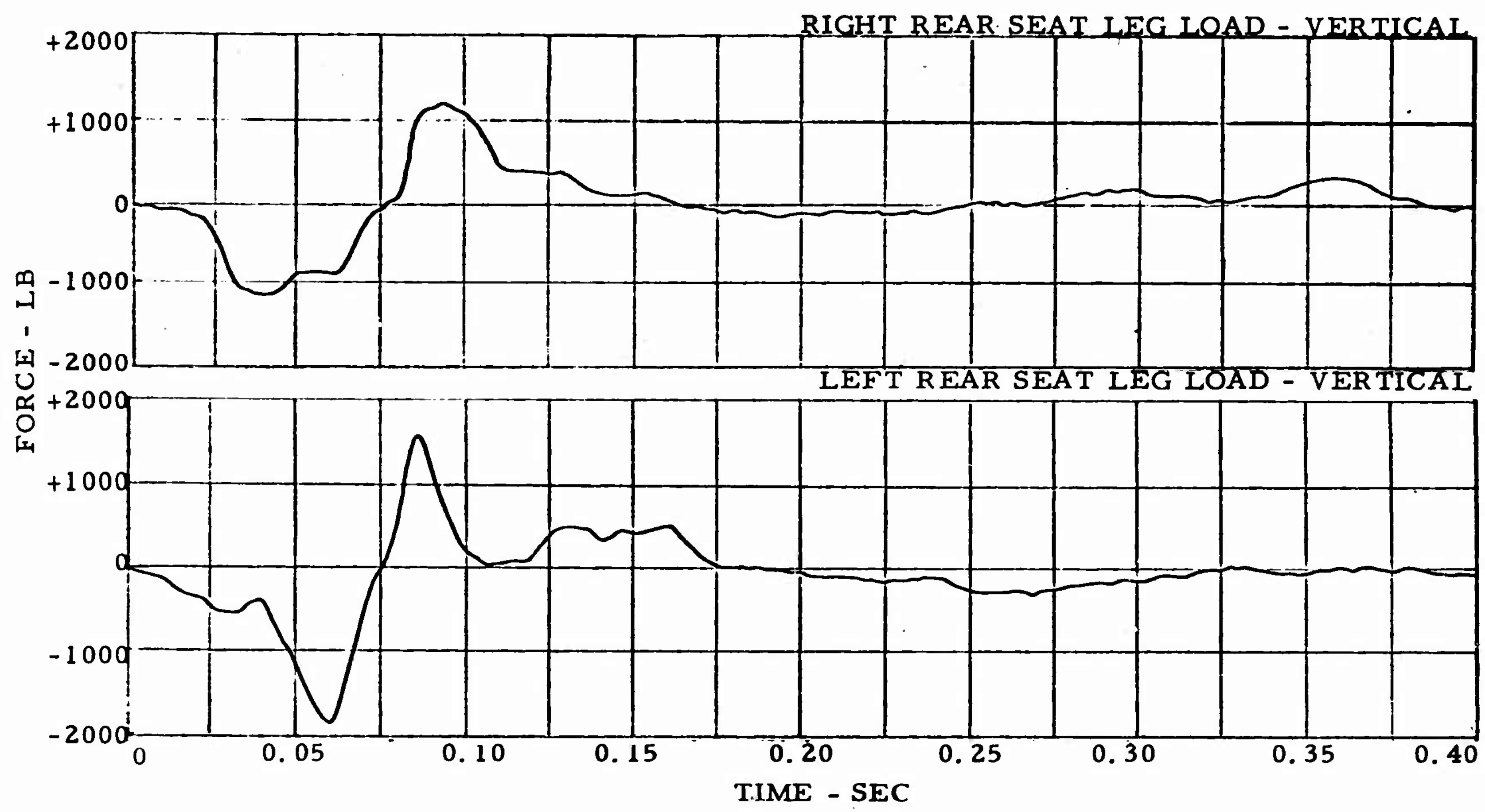

Figure 52. Force-Time Histories - Test 2.

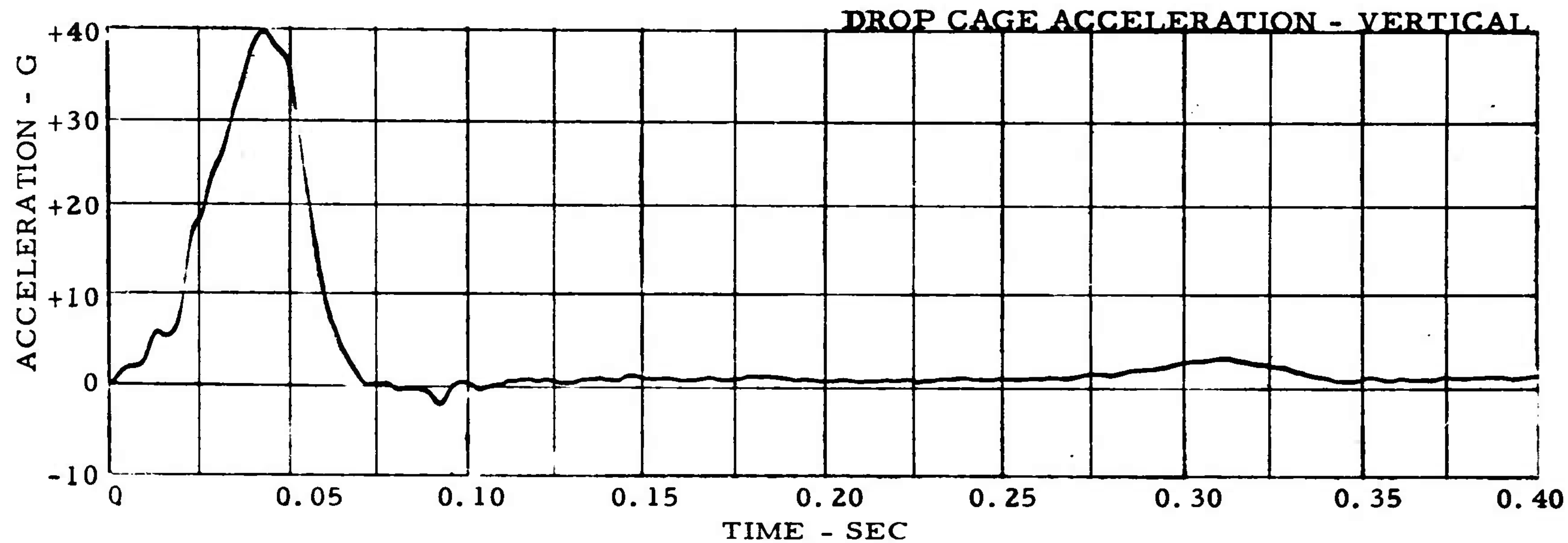

Figure 53. Acceleration-Time History - Test 3.

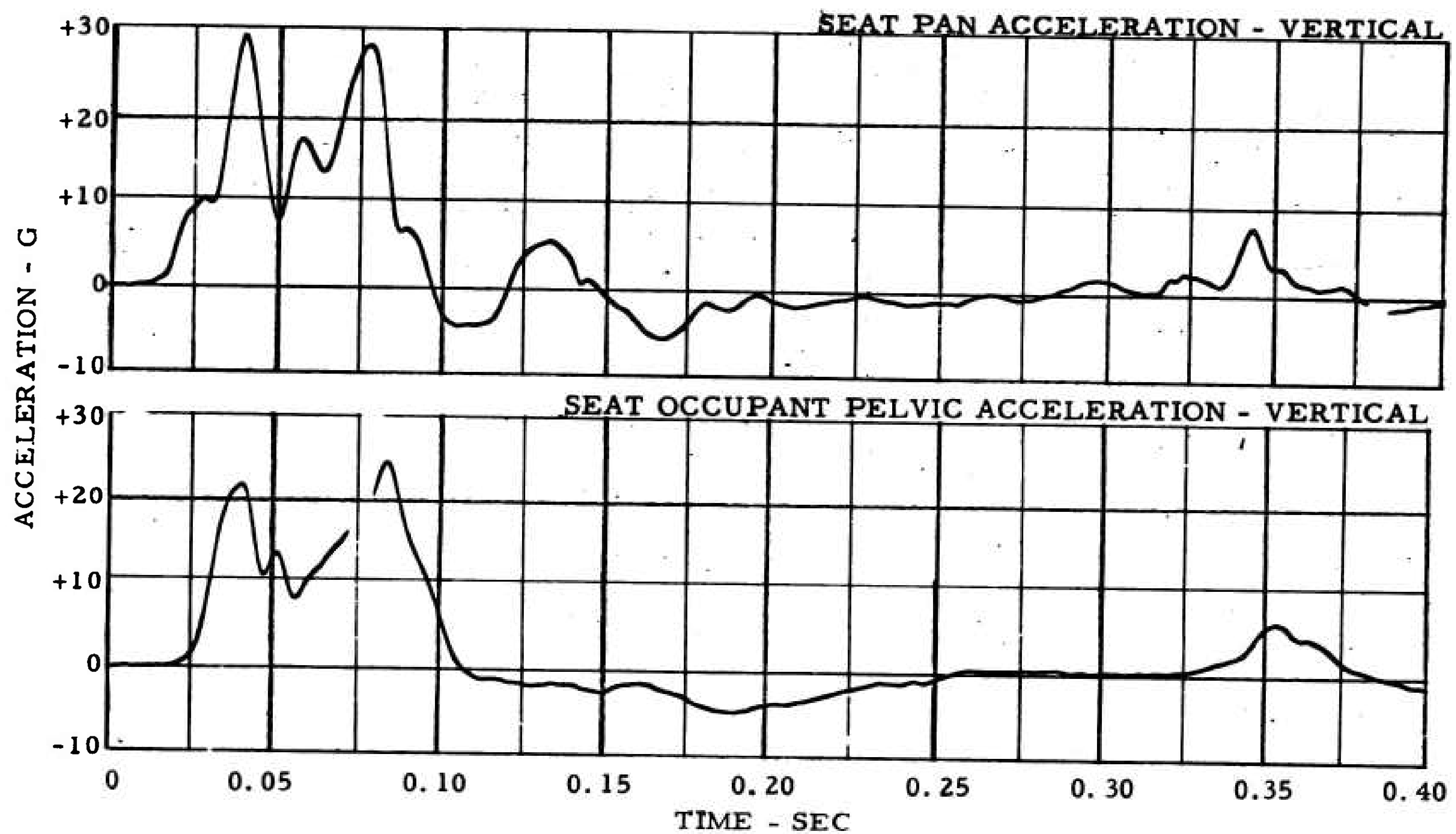

Figure 54. Acceleration-Time Histories - Test 3.

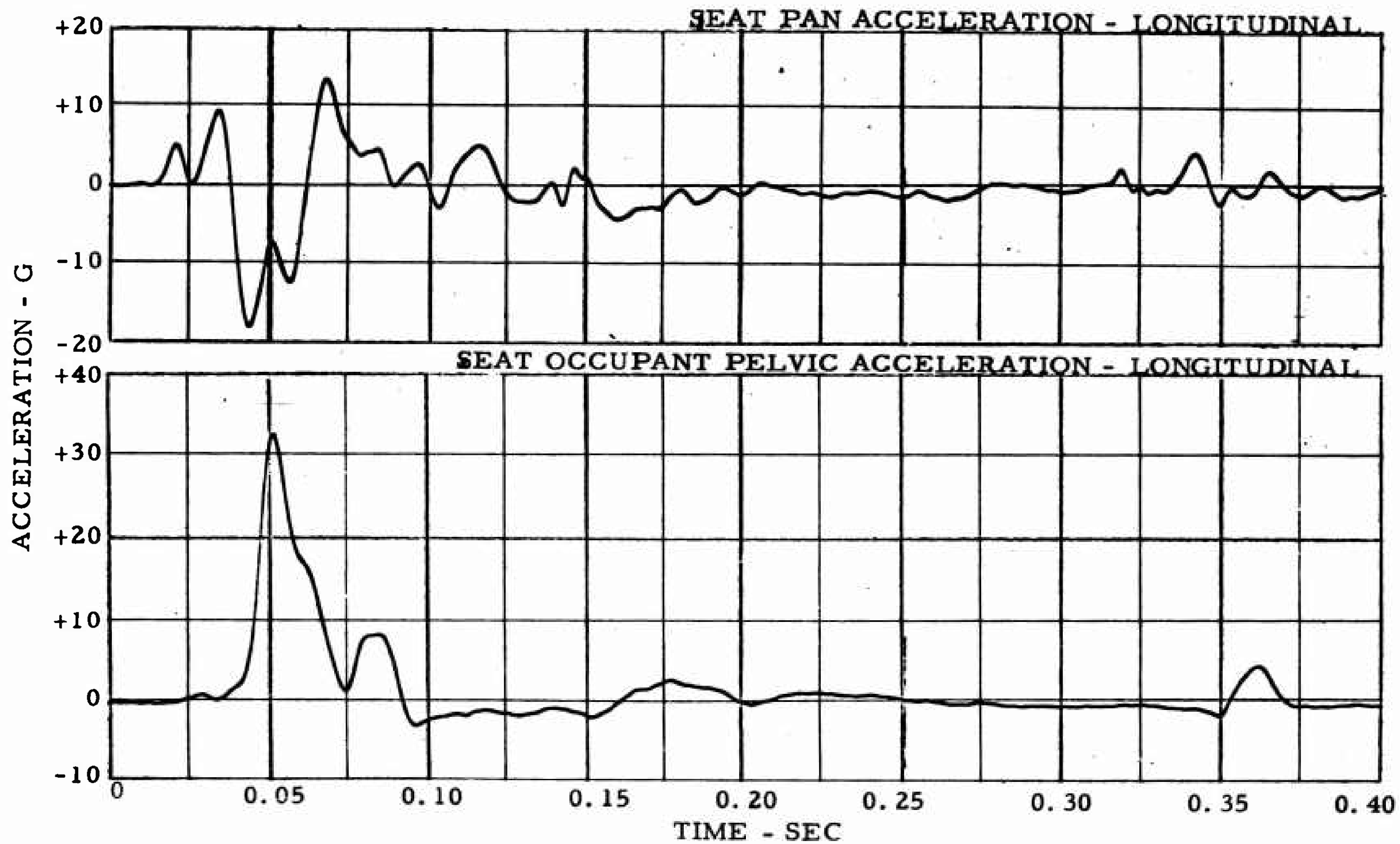

Figure 55. Acceleration-Time Histories - Test 3.

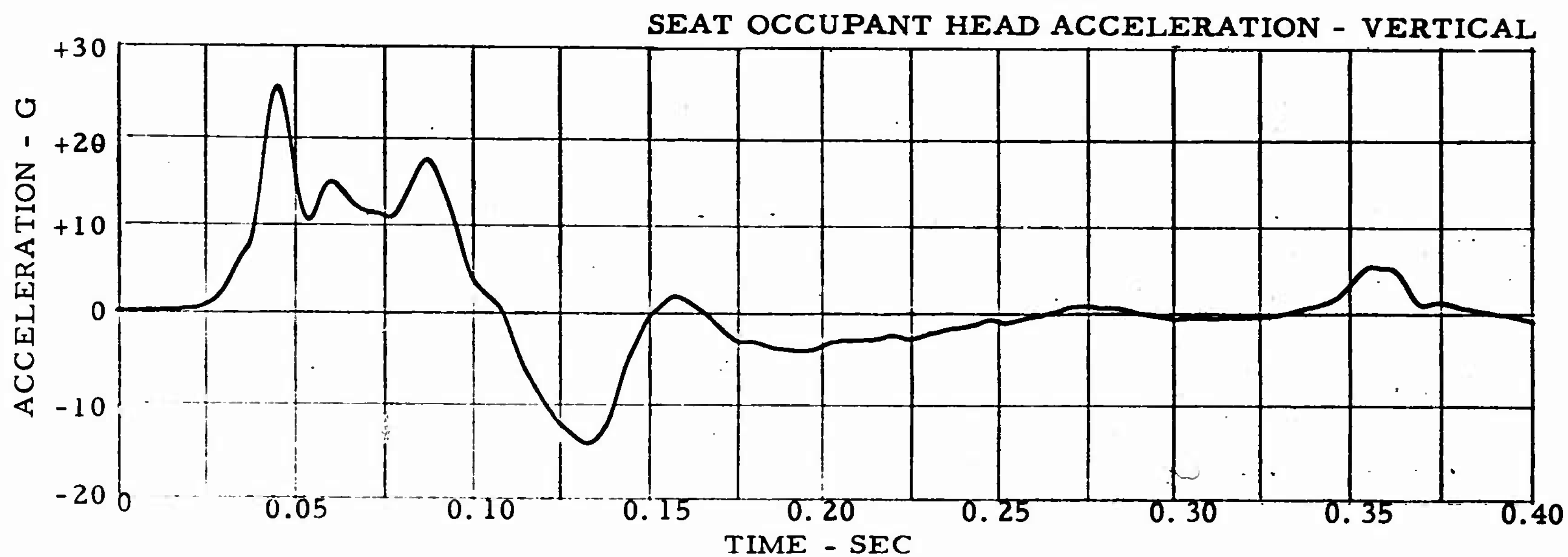

Figure 56. Acceleration-Time History - Test 3.

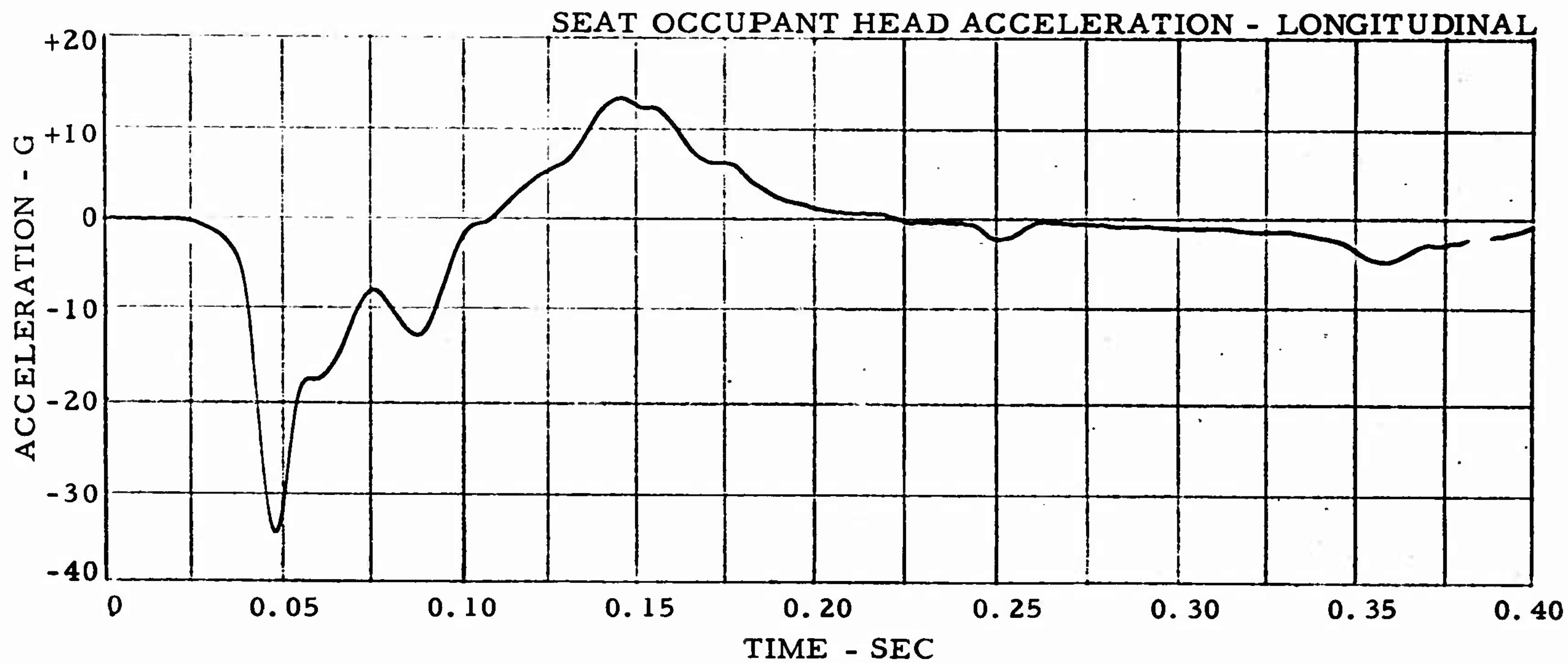

Figure 57. Acceleration-Time History - Test 3.

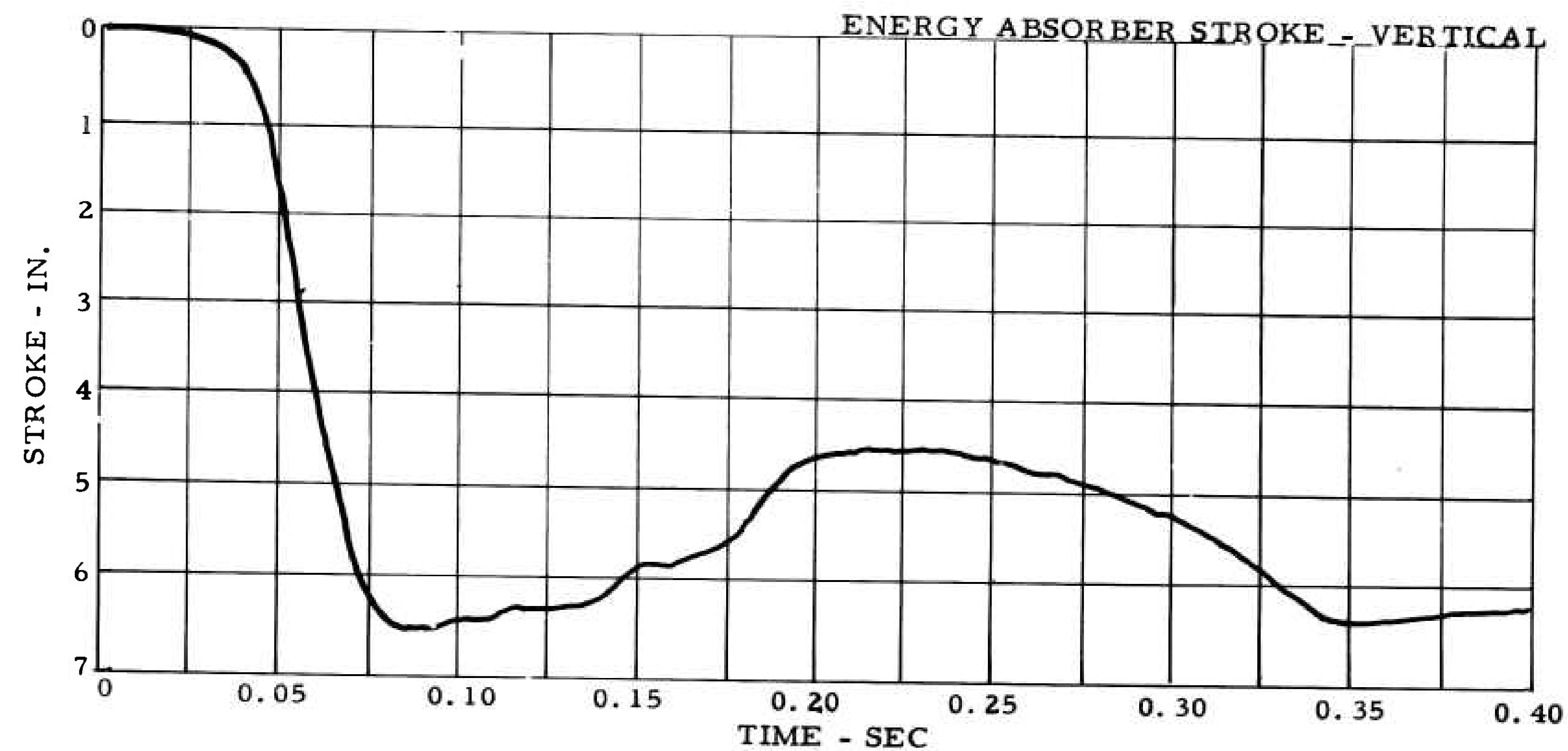

Figure 58. Stroke-Time History - Test 3.

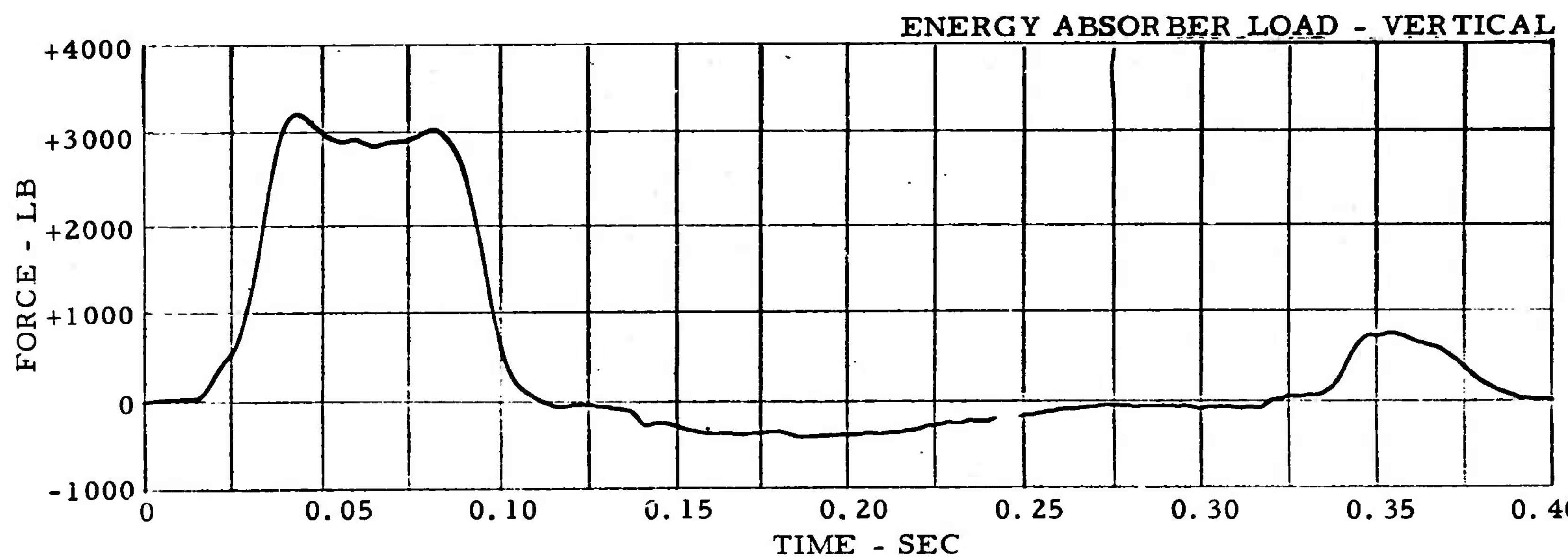

Figure 59. Force-Time History - Test 3.

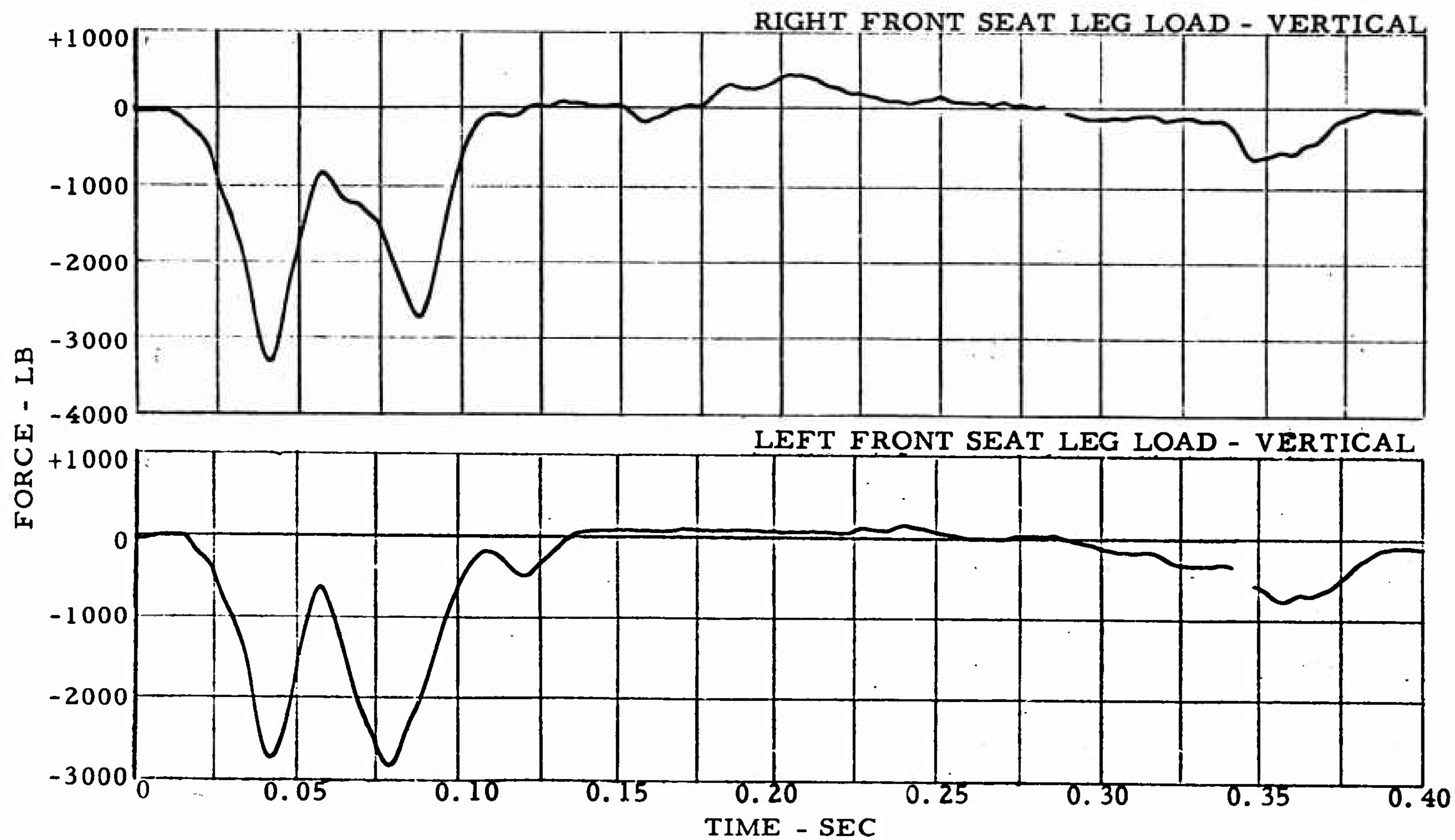

Figure 60. Force-Time Histories - Test 3.

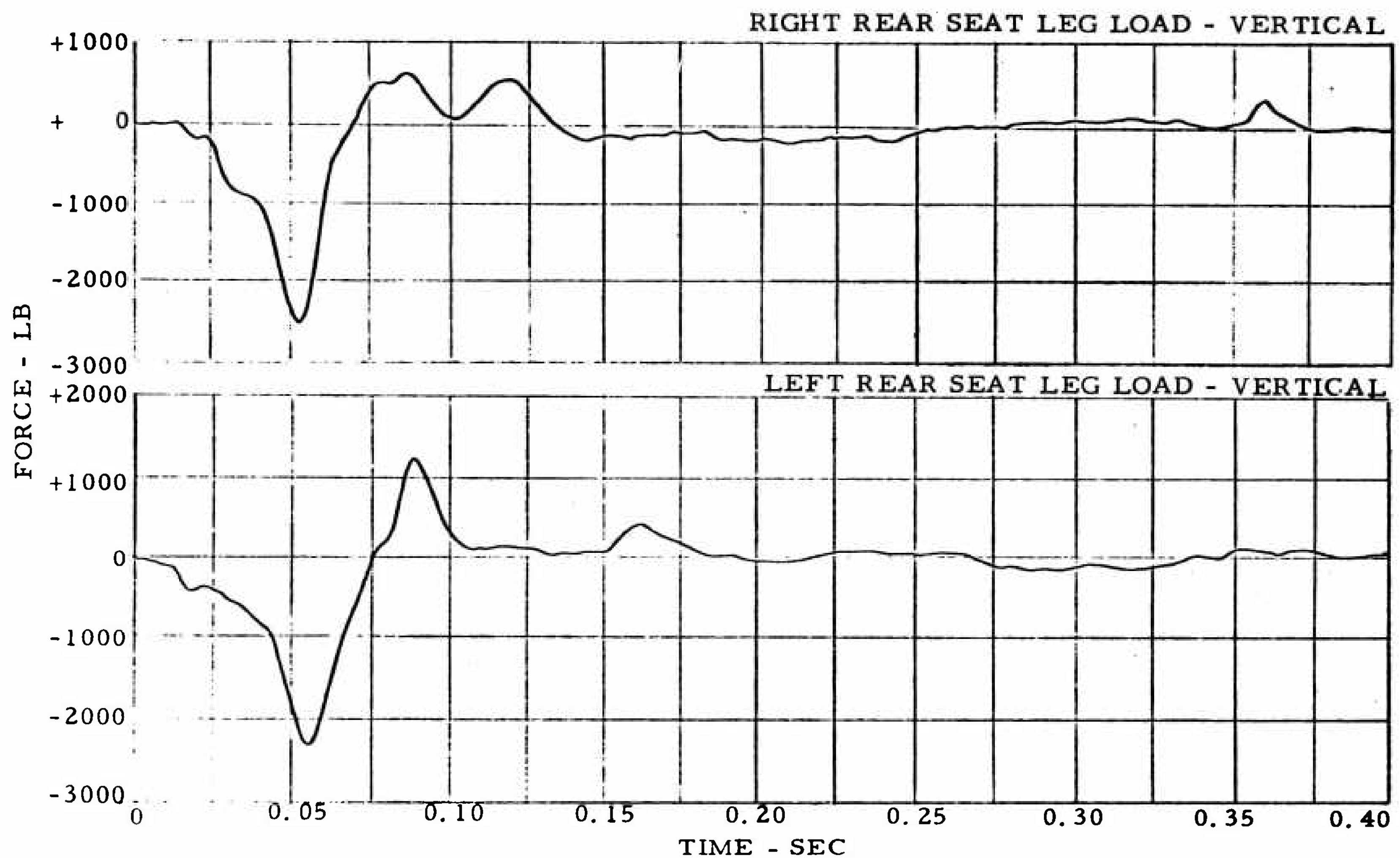

Figure 61. Force-Time Histories - Test 3.

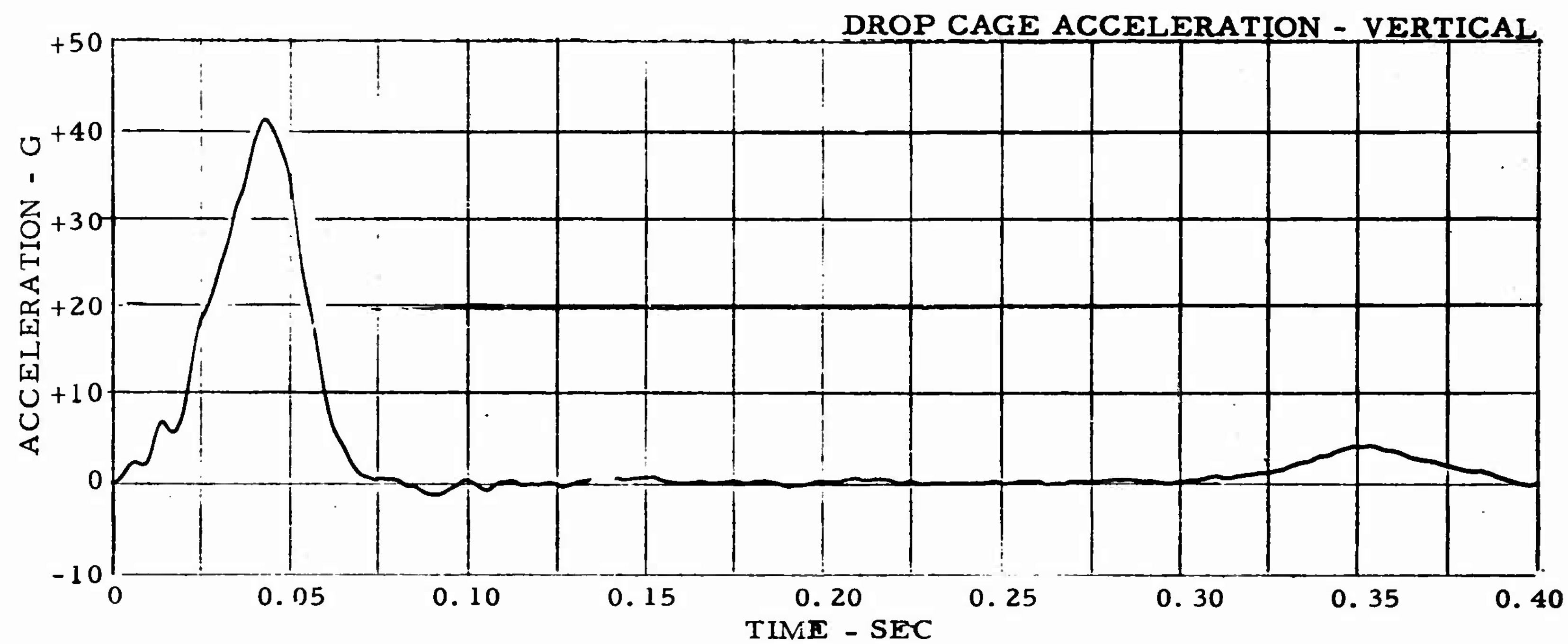

Figure 62. Acceleration-Time History - Test 4.

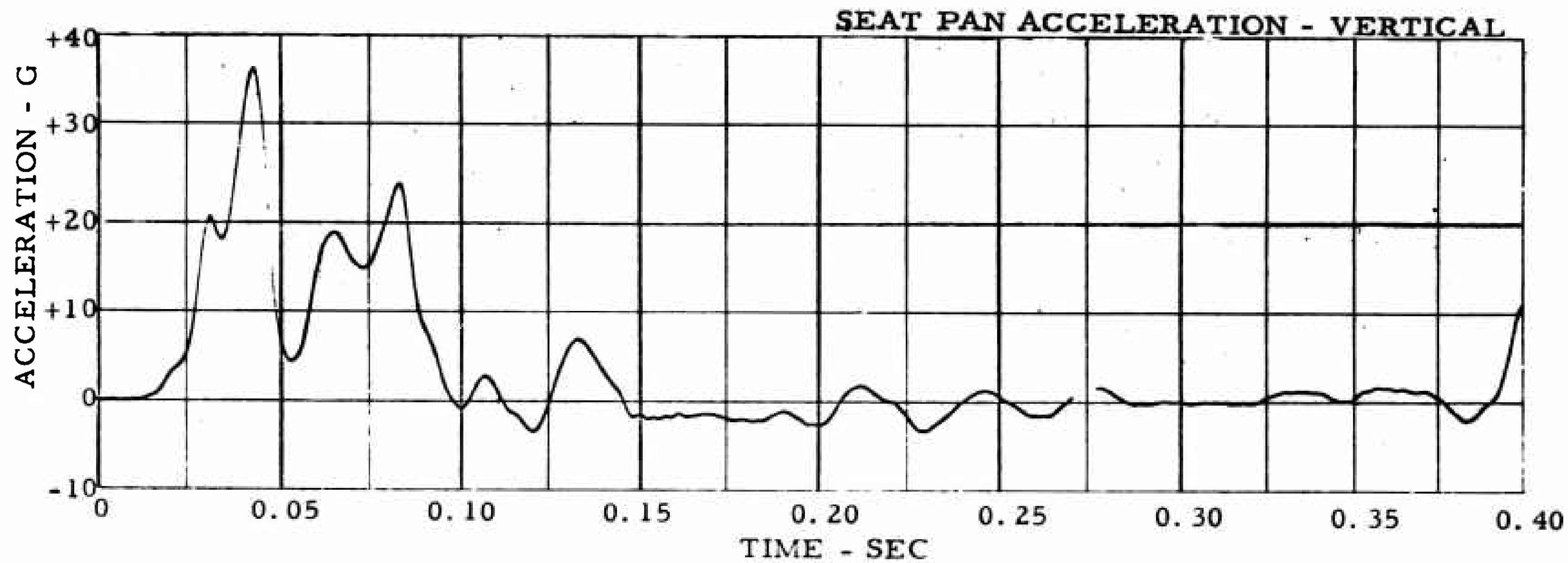

Figure 63. Acceleration-Time History - Test 4.

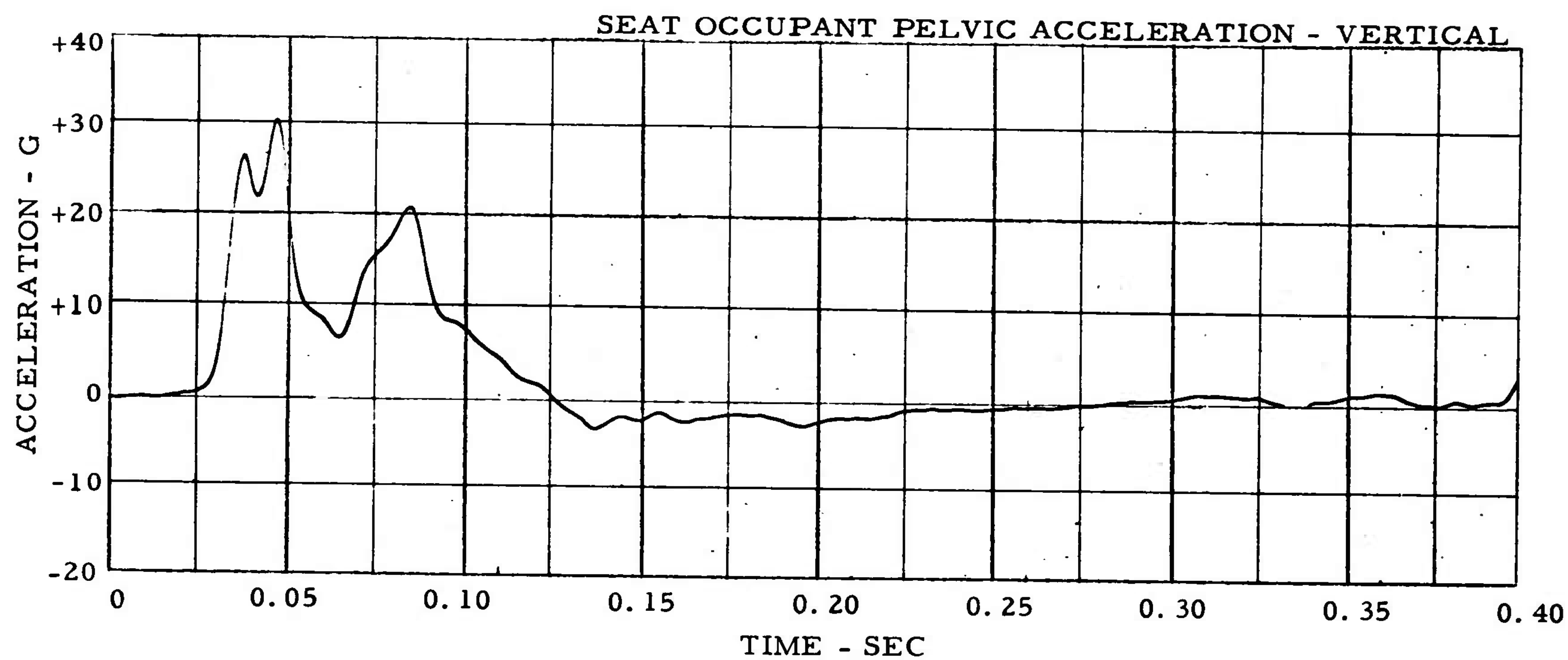

Figure 64. Acceleration-Time History - Test 4.

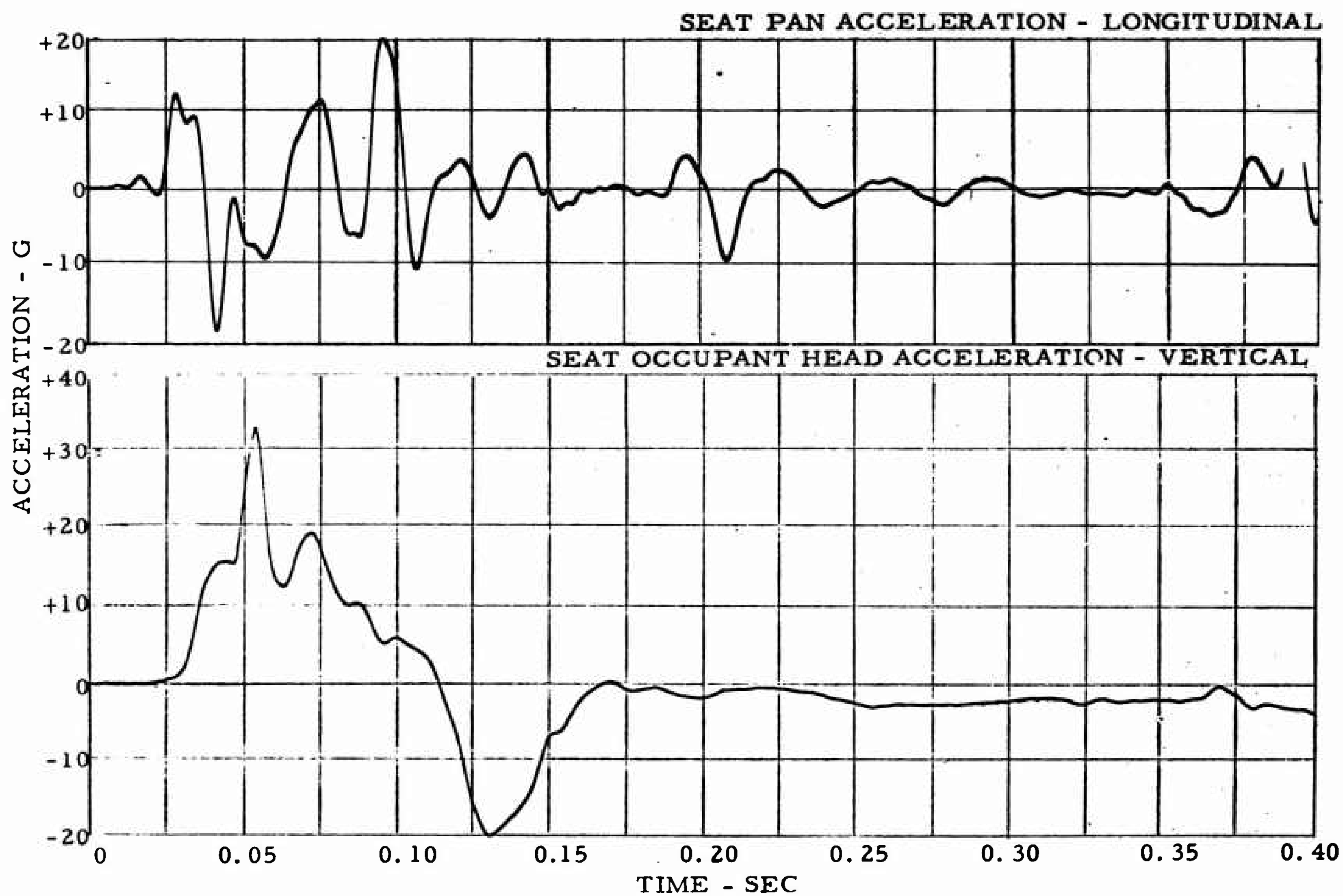

Figure 65. Acceleration-Time Histories - Test 4.

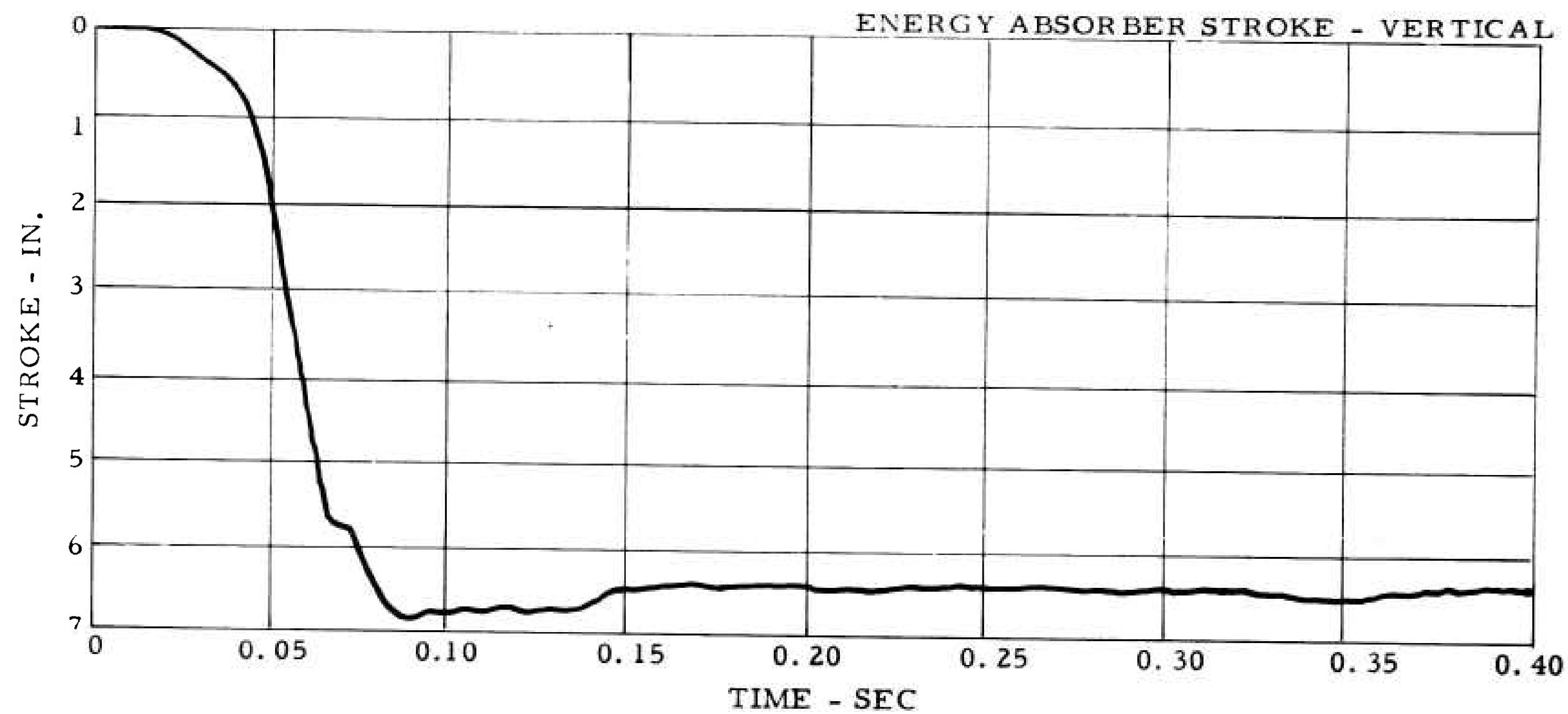

Figure 66. Stroke-Time History - Test 4.

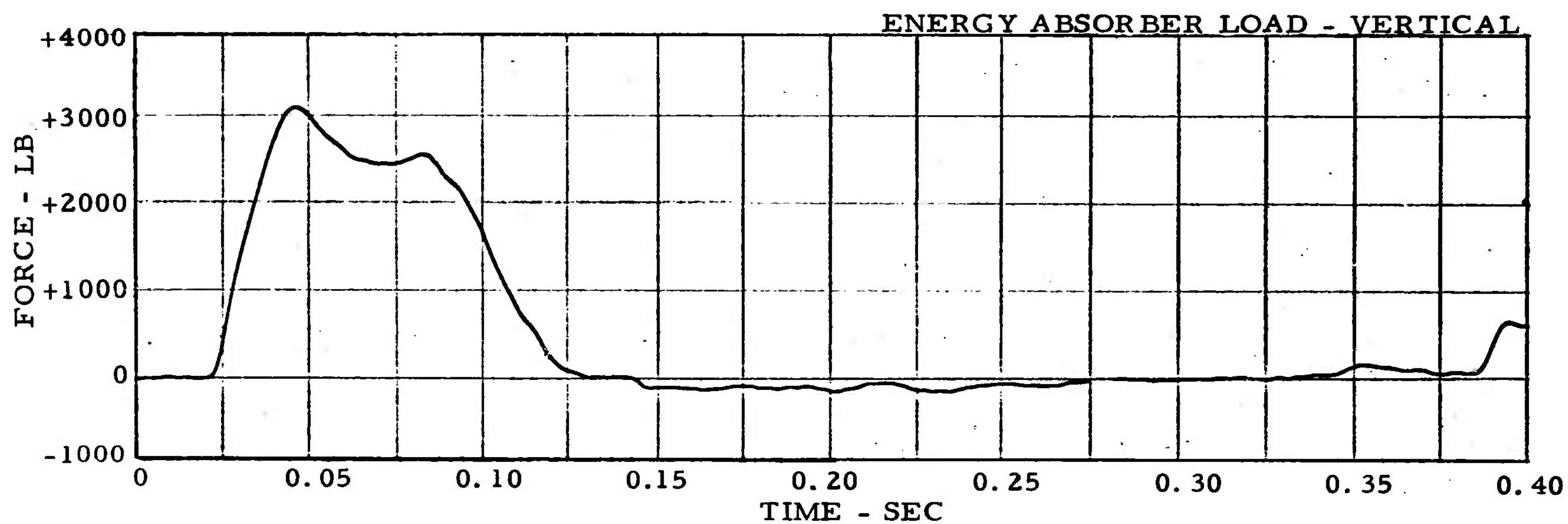

Figure 67. Force-Time History - Test 4.

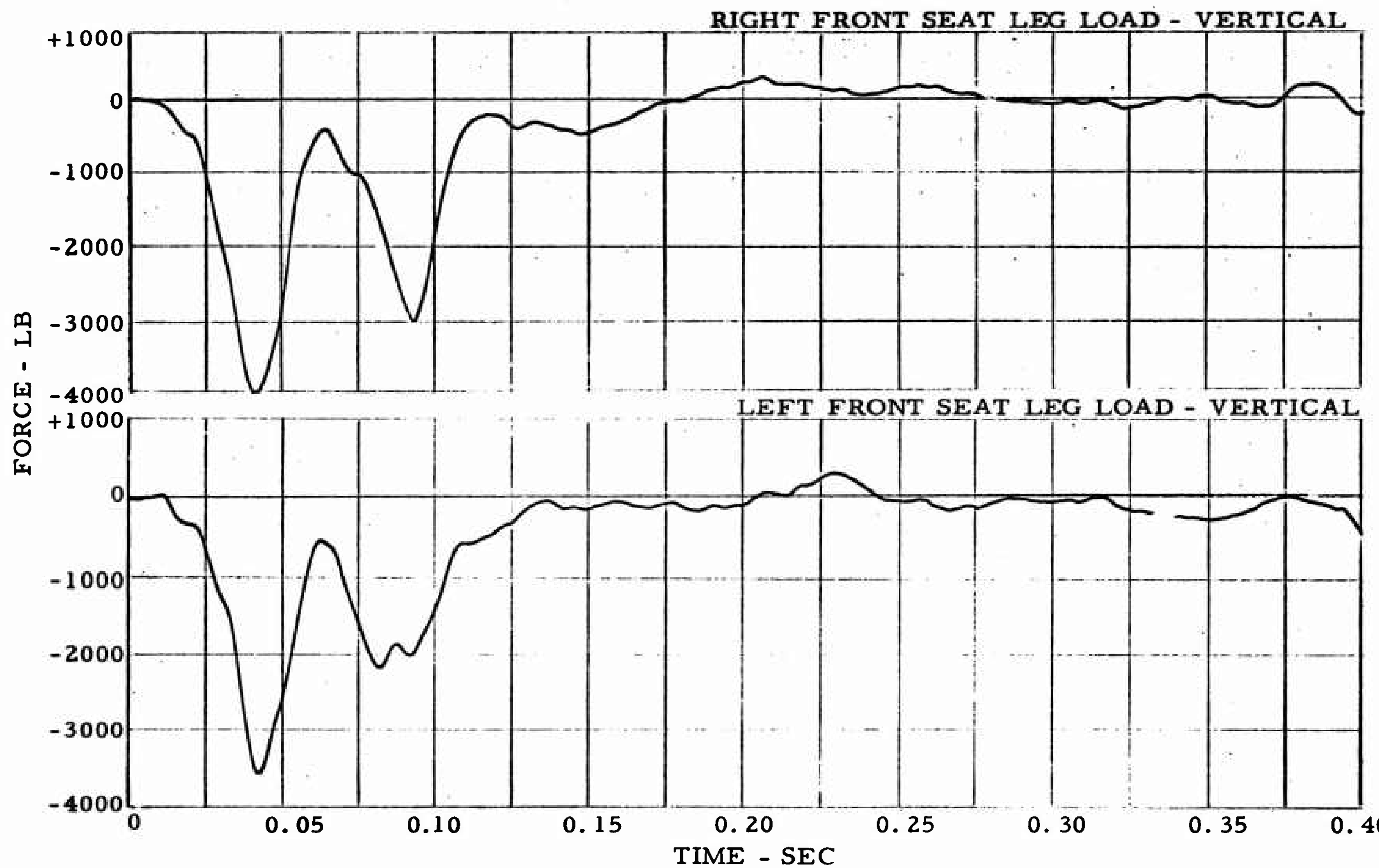

Figure 68. Force-Time Histories - Test 4.

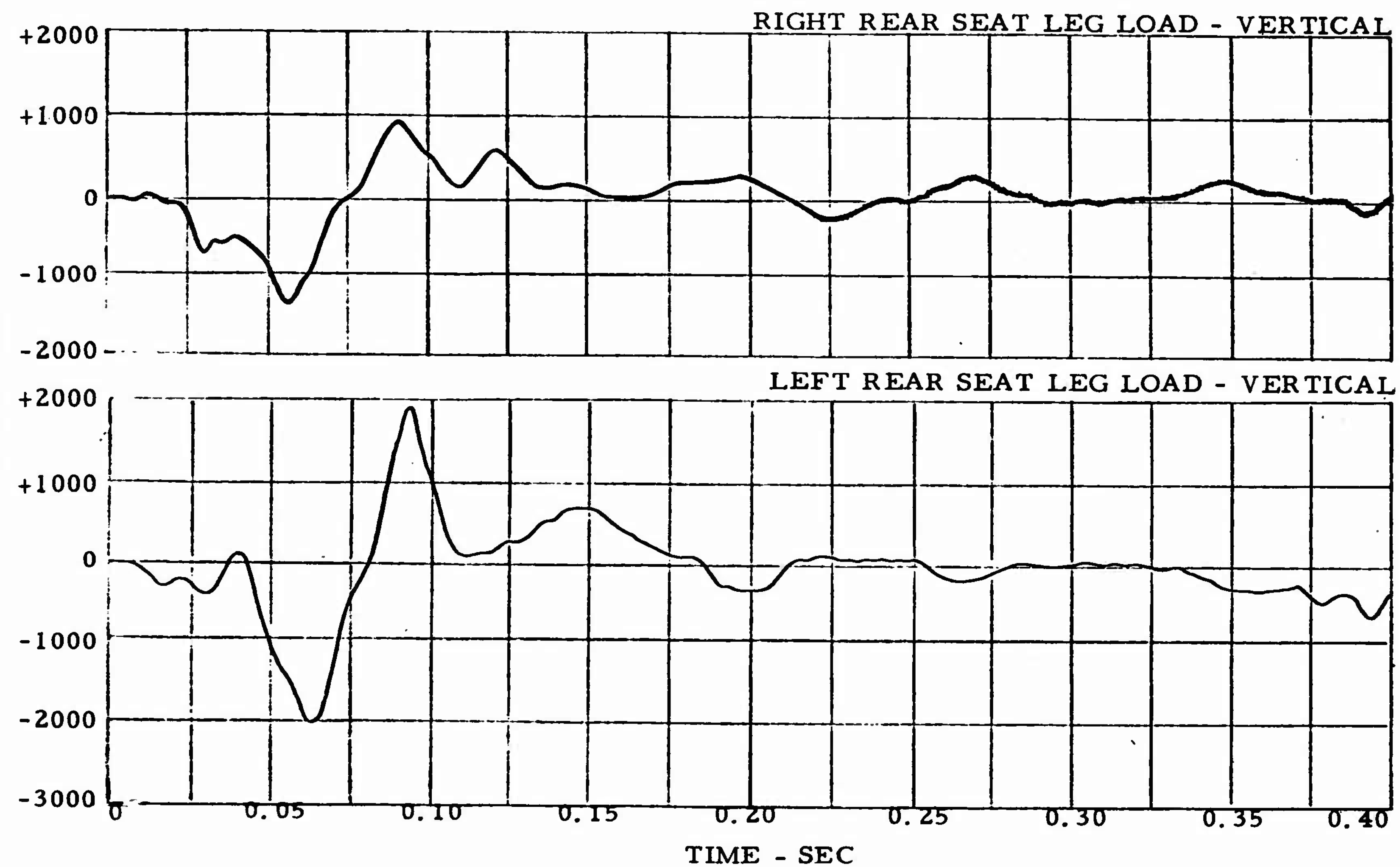

Figure 69. Force-Time Histories - Test 4.

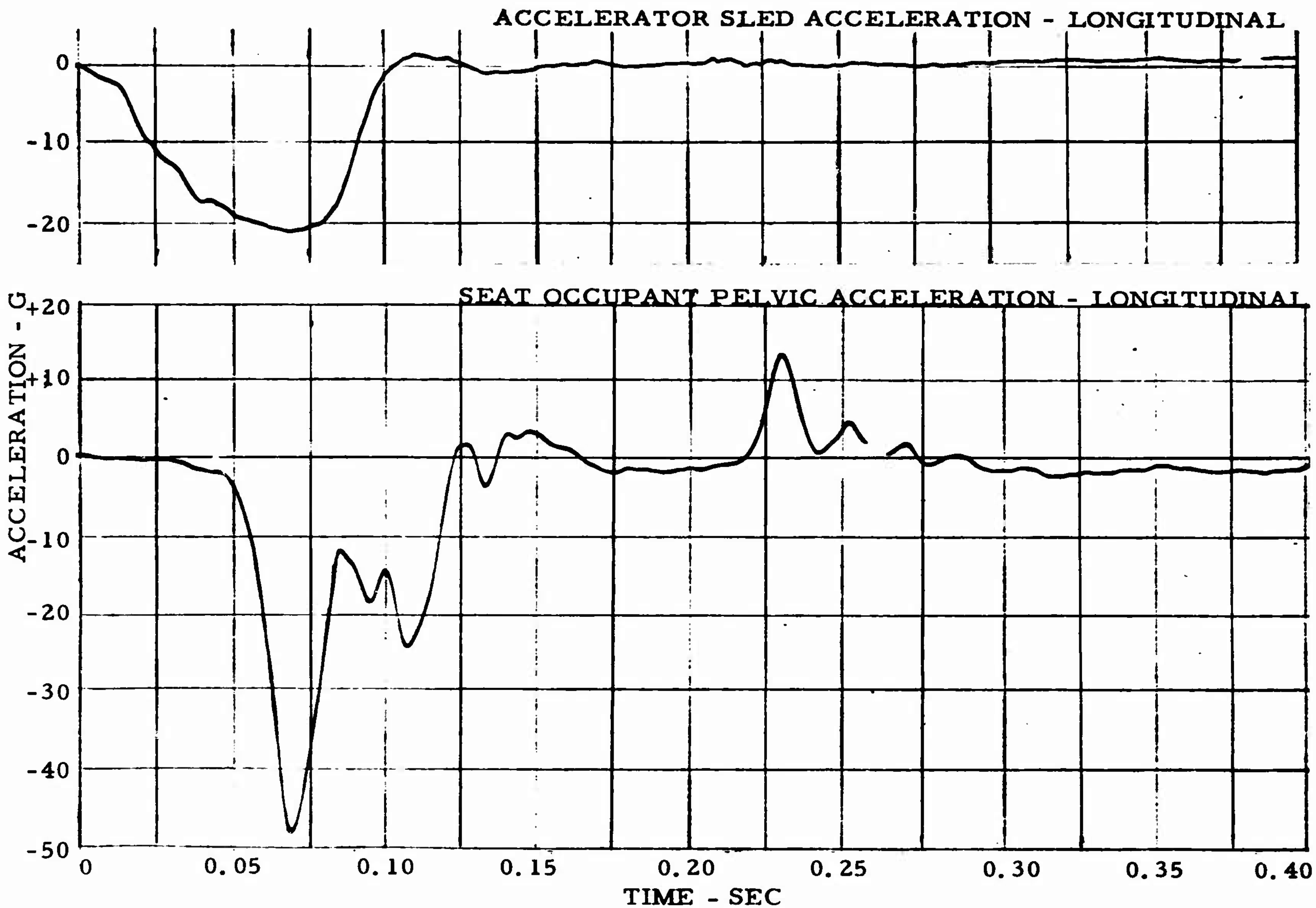

Figure 70. Acceleration-Time Histories - Test 6.

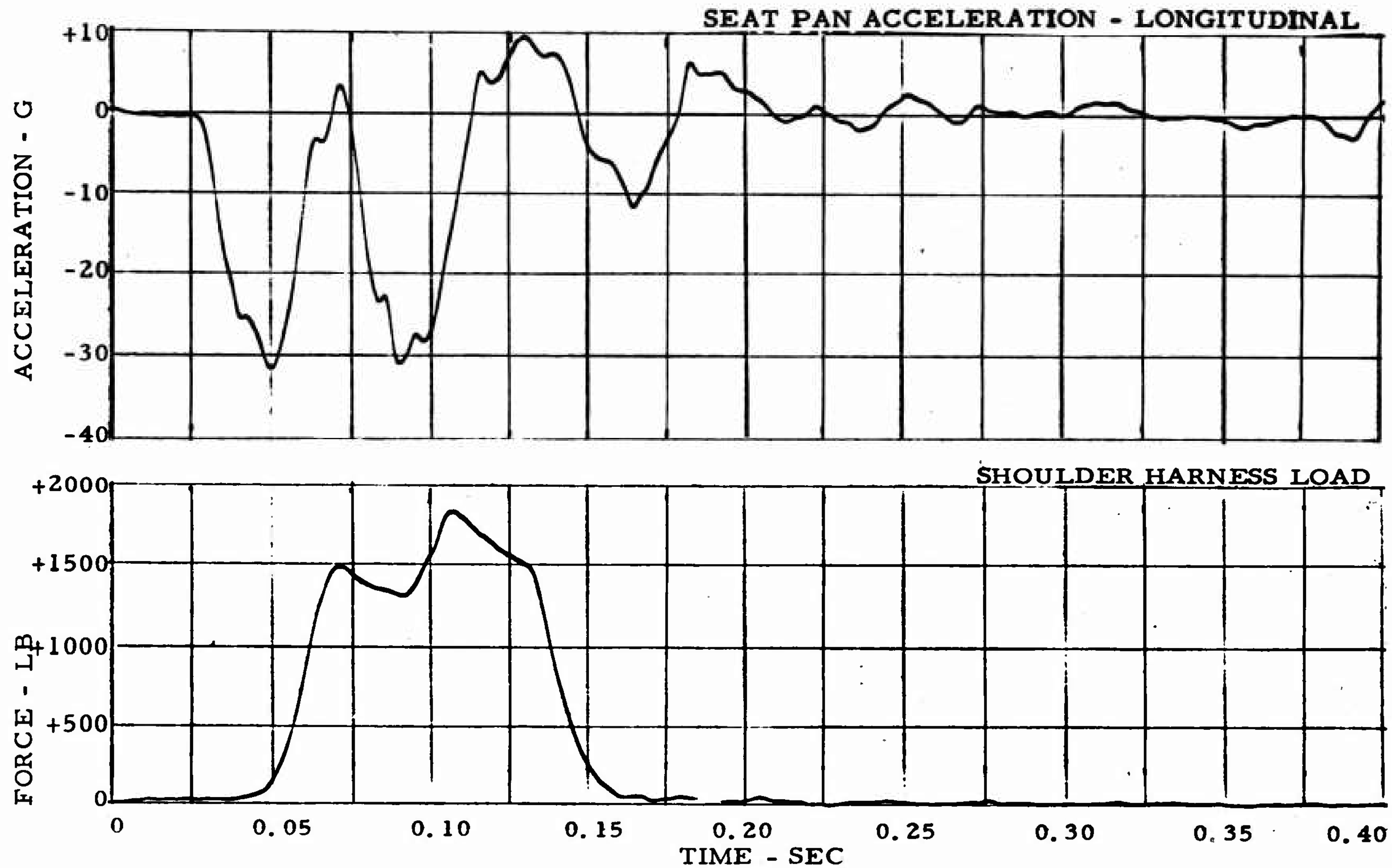

Figure 71. Acceleration/Force-Time Histories - Test 6.

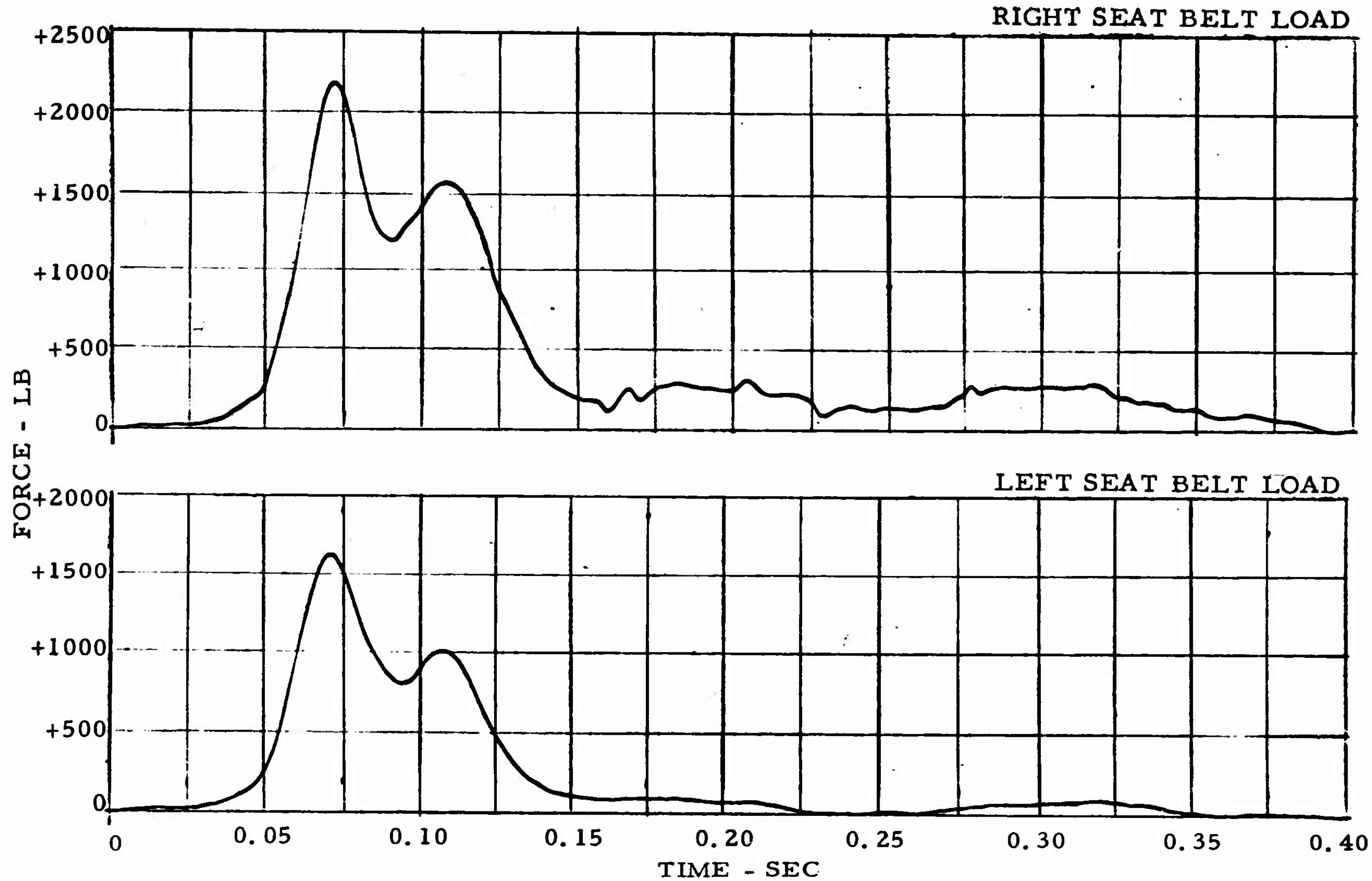

Figure 72. Force-Time Histories - Test 6.

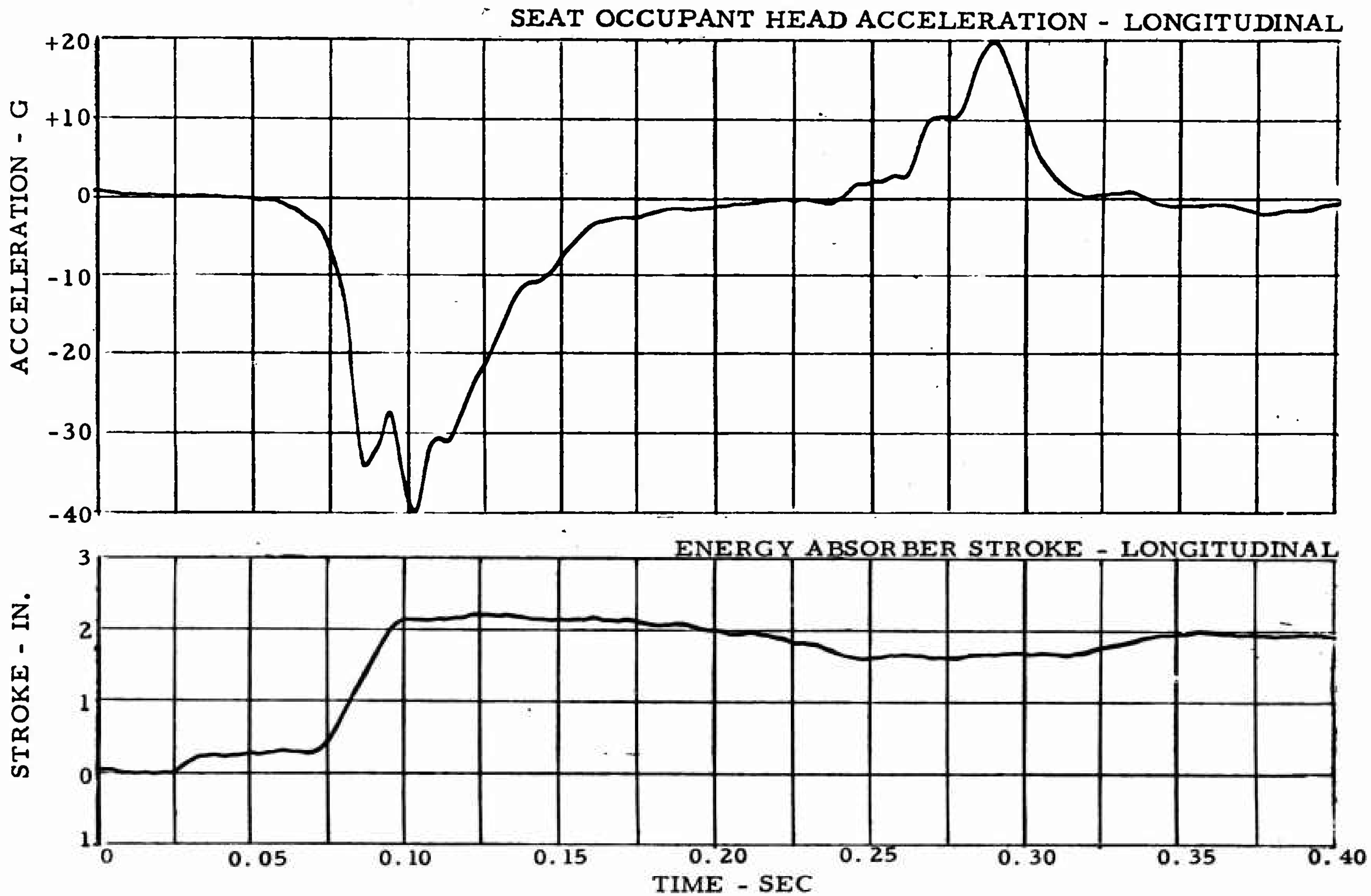

Figure 73. Acceleration/Stroke-Time Histories - Test 6.

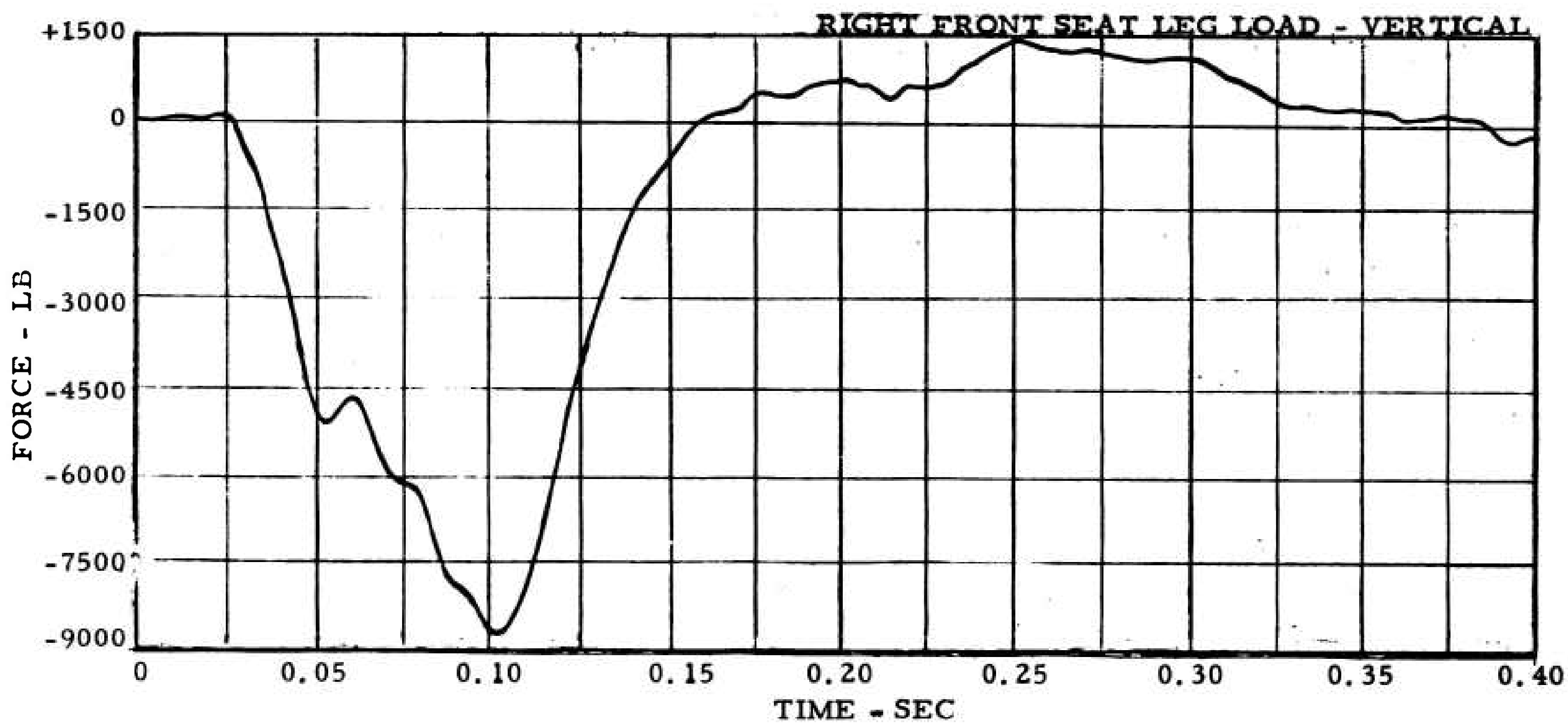

Figure 74. Force-Time History - Test 6.

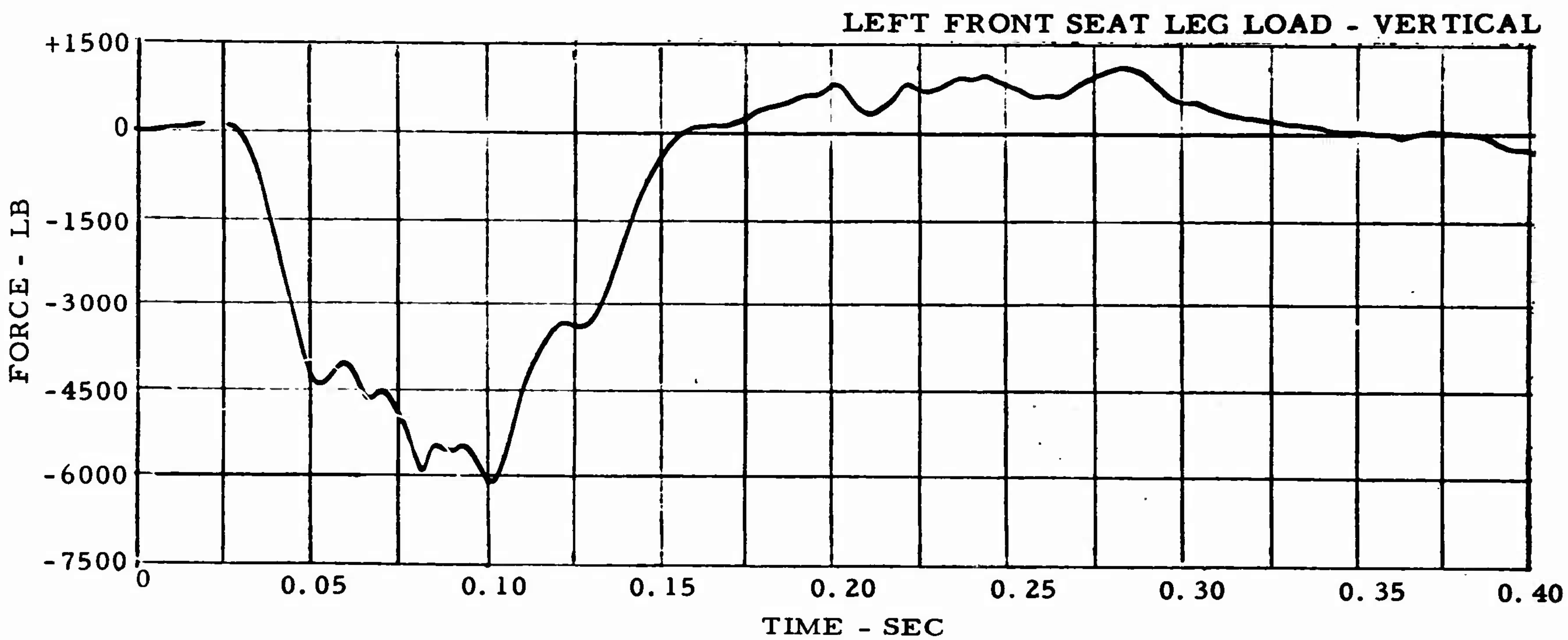

Figure 75. Force-Time History - Test 6.

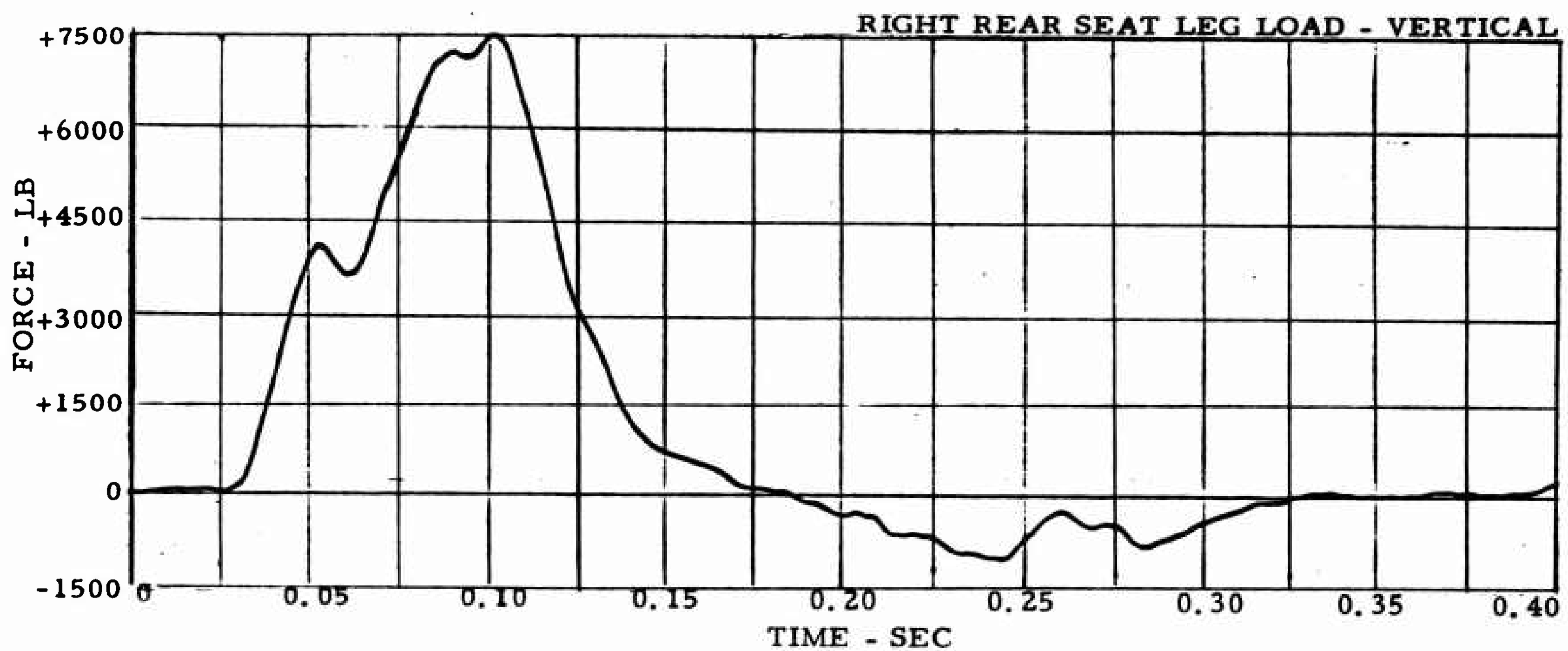

Figure 76. Force-Time History - Test 6.

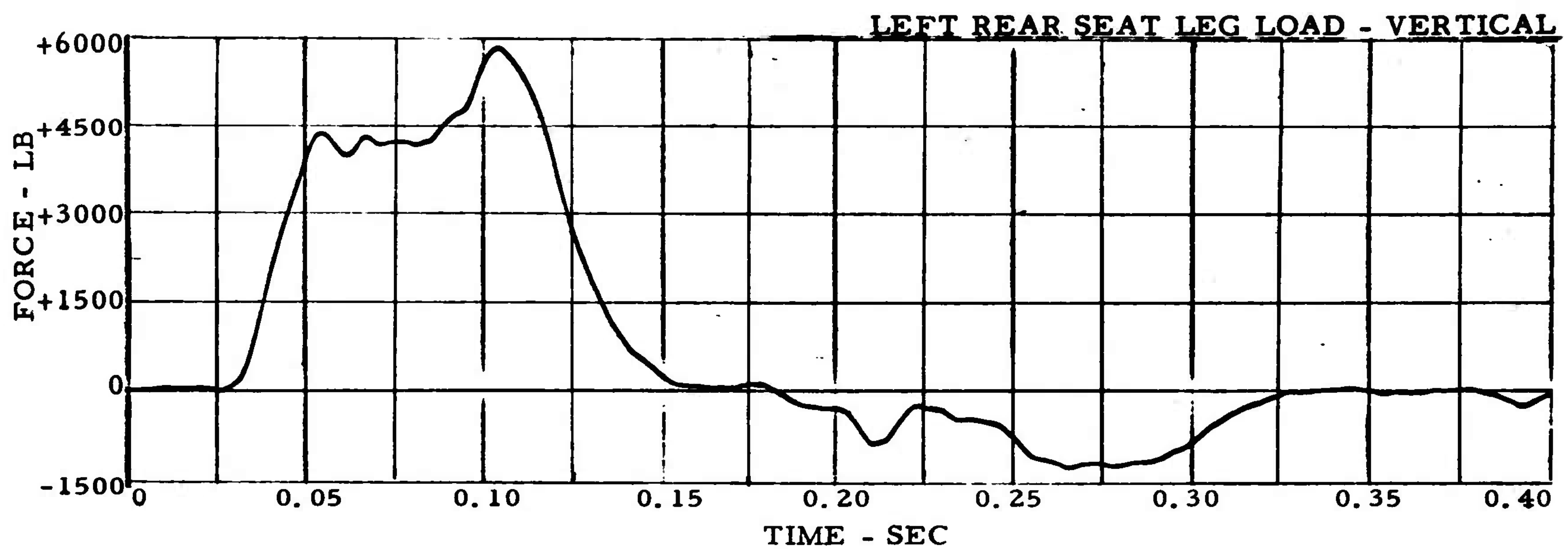

Figure 77. Force-Time History - Test 6.

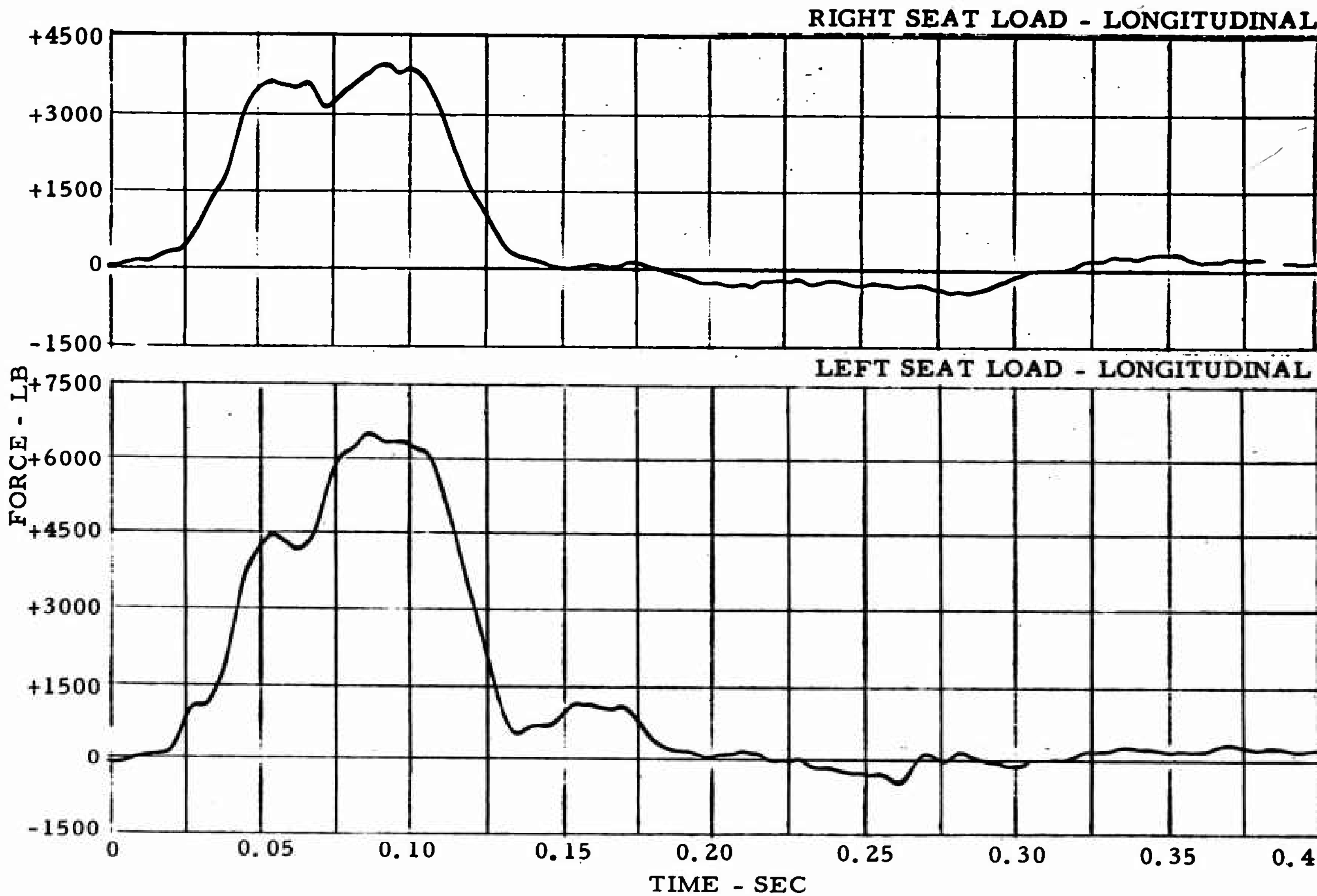

Figure 78. Force-Time Histories - Test 6.

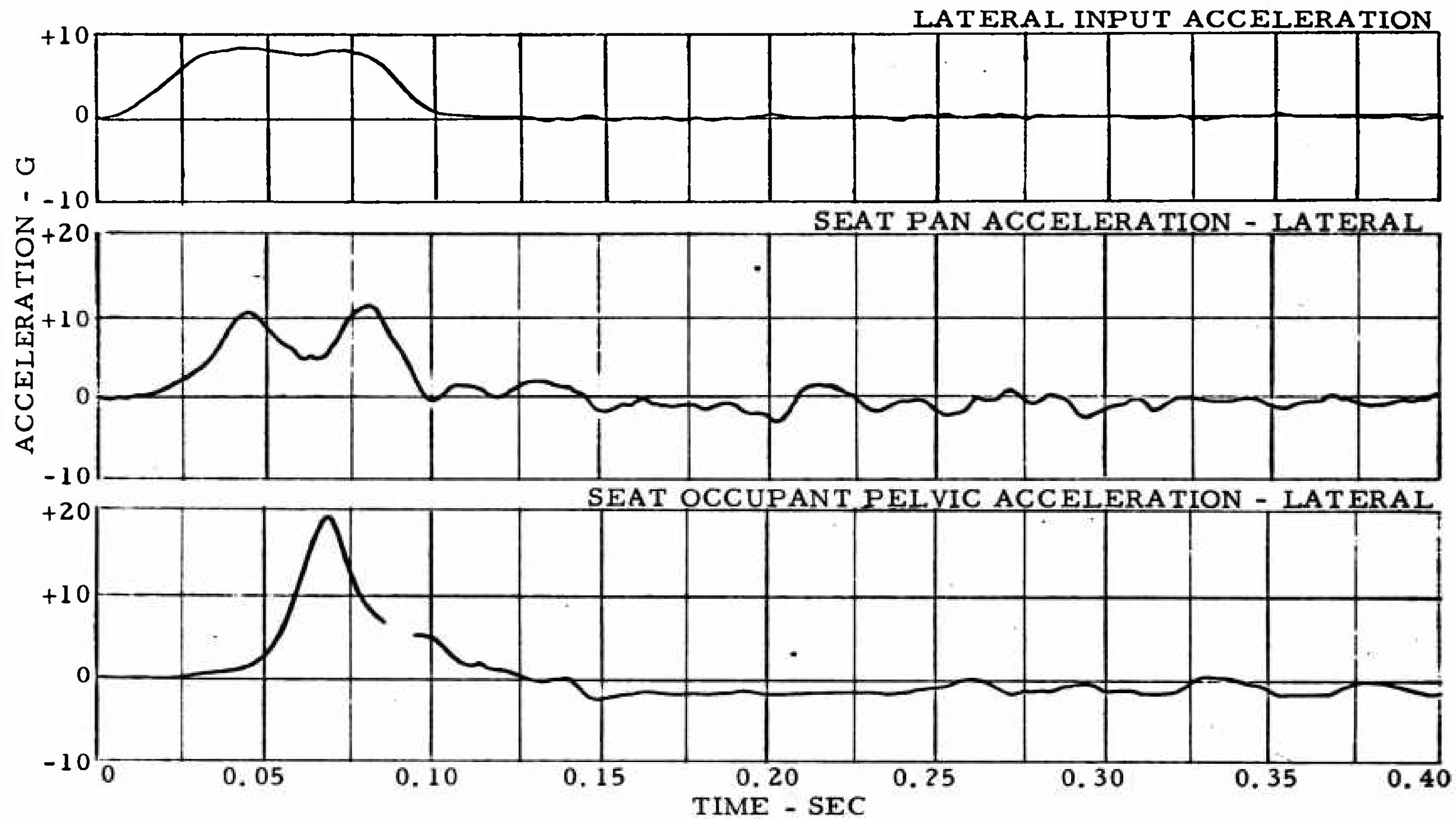

Figure 79. Acceleration-Time Histories - Test 8.

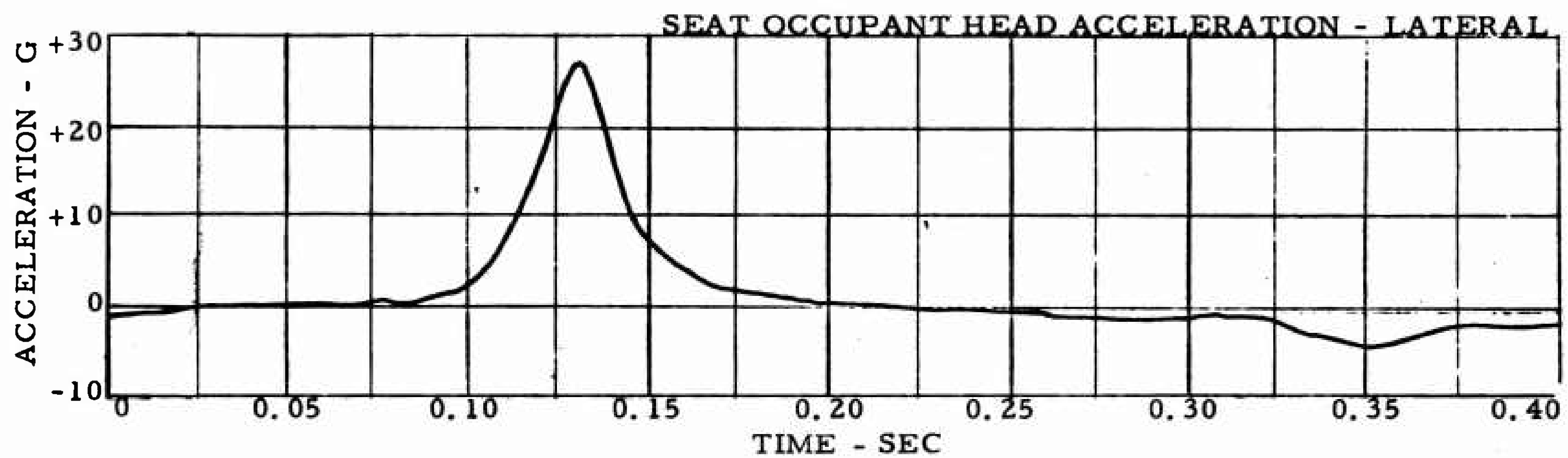

Figure 80. Acceleration-Time History - Test 8.

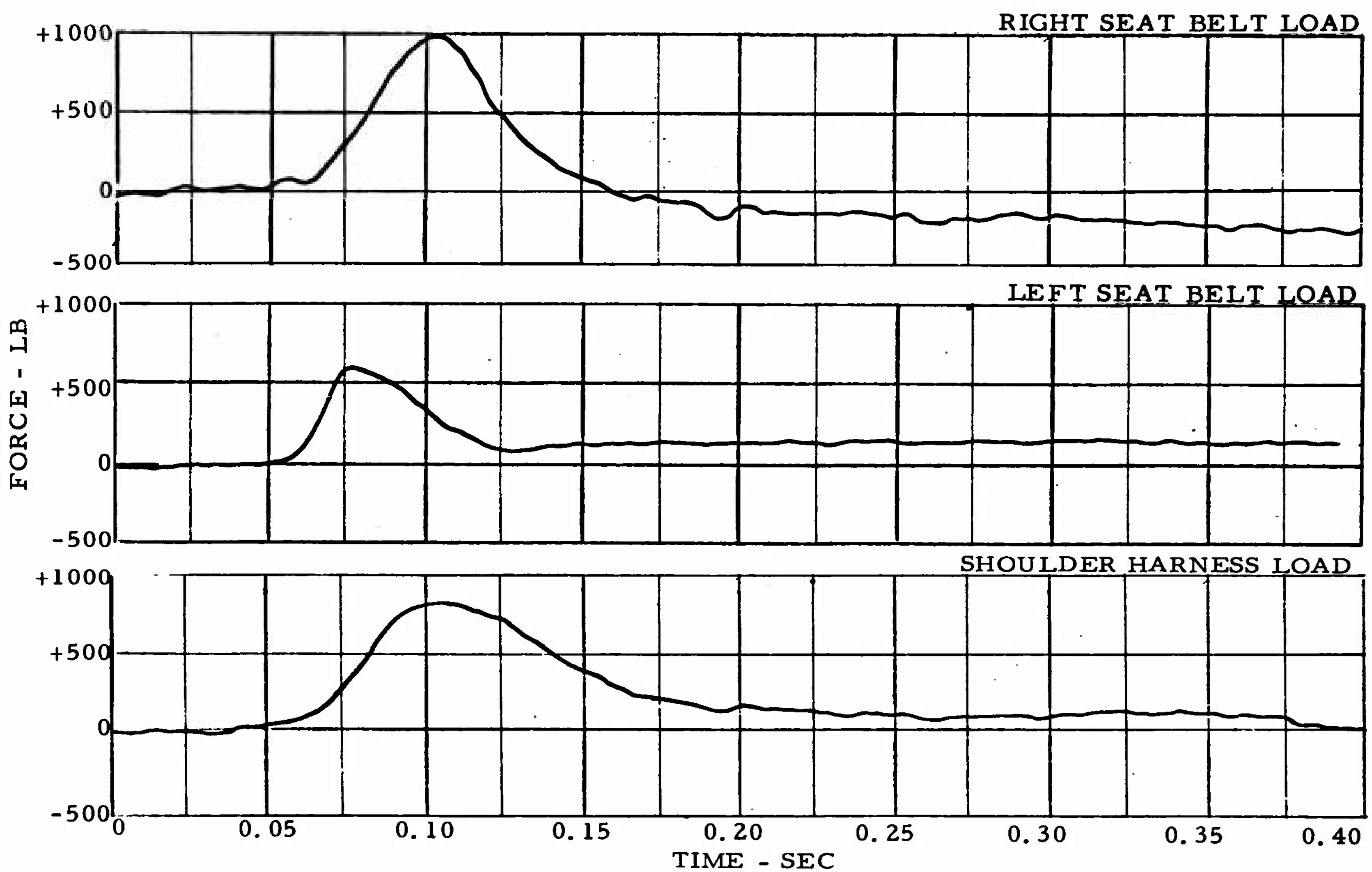

Figure 81. Force-Time Histories - Test 8.

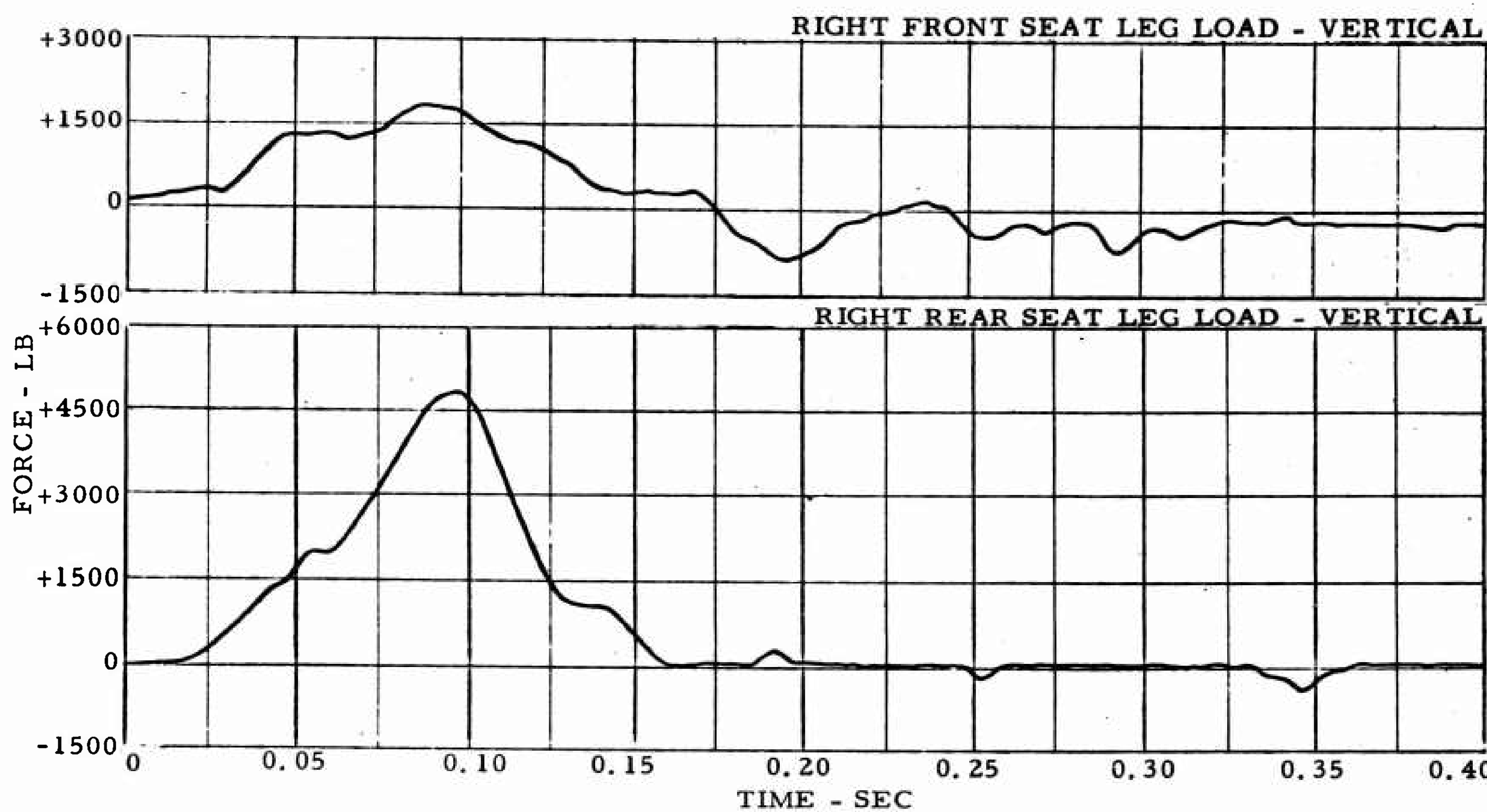

Figure 82. Force-Time Histories - Test 8.

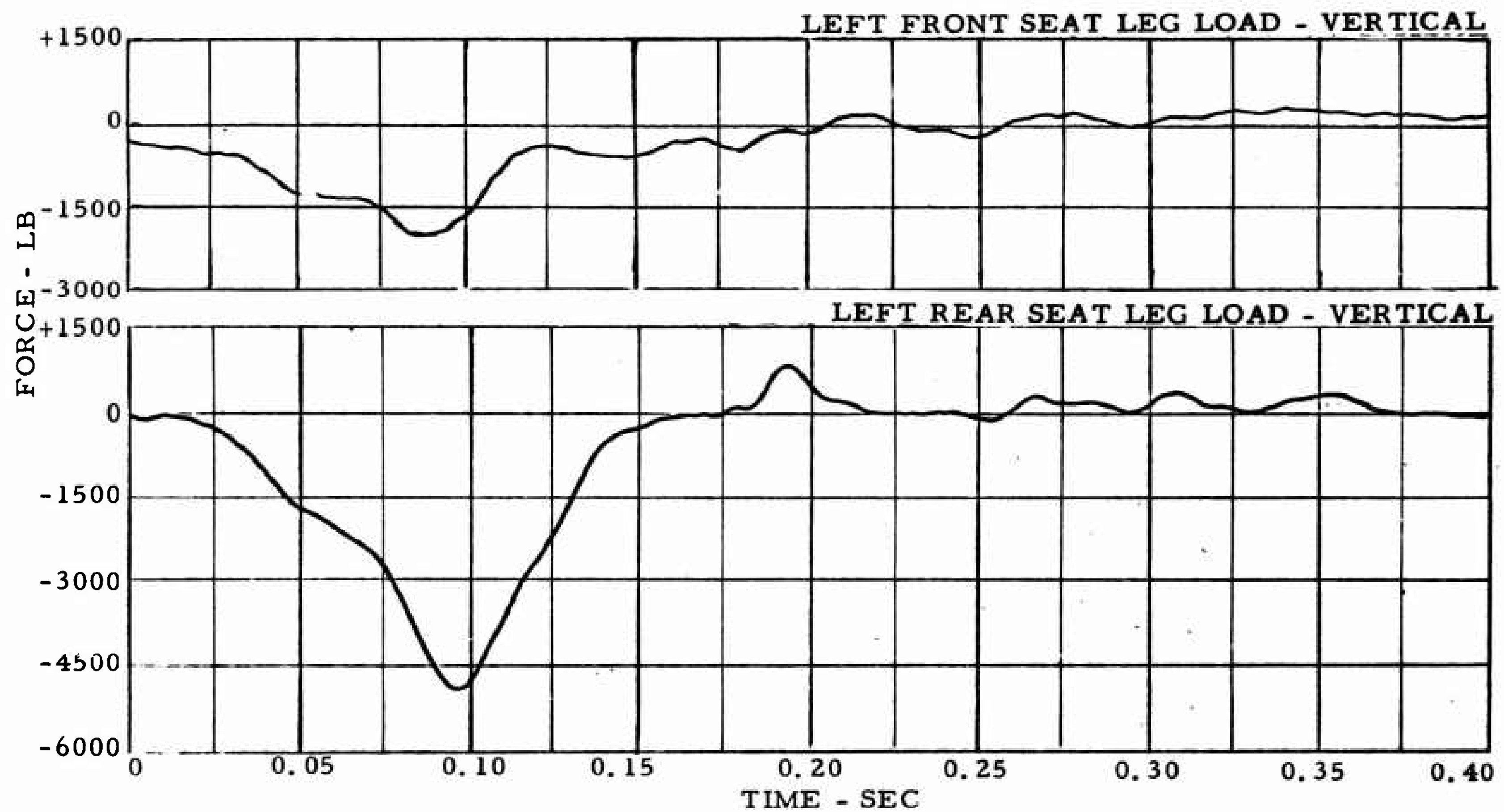

Figure 83. Force-Time Histories - Test 8.

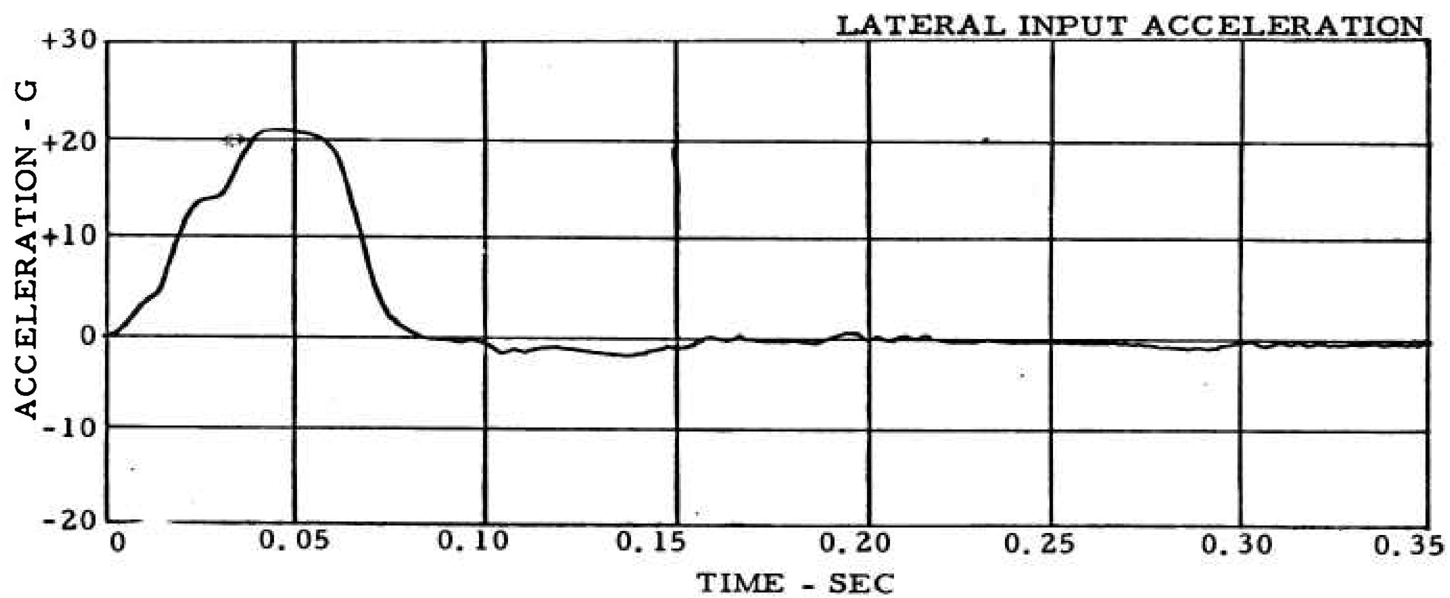

Figure 84. Acceleration-Time History - Test 8A.

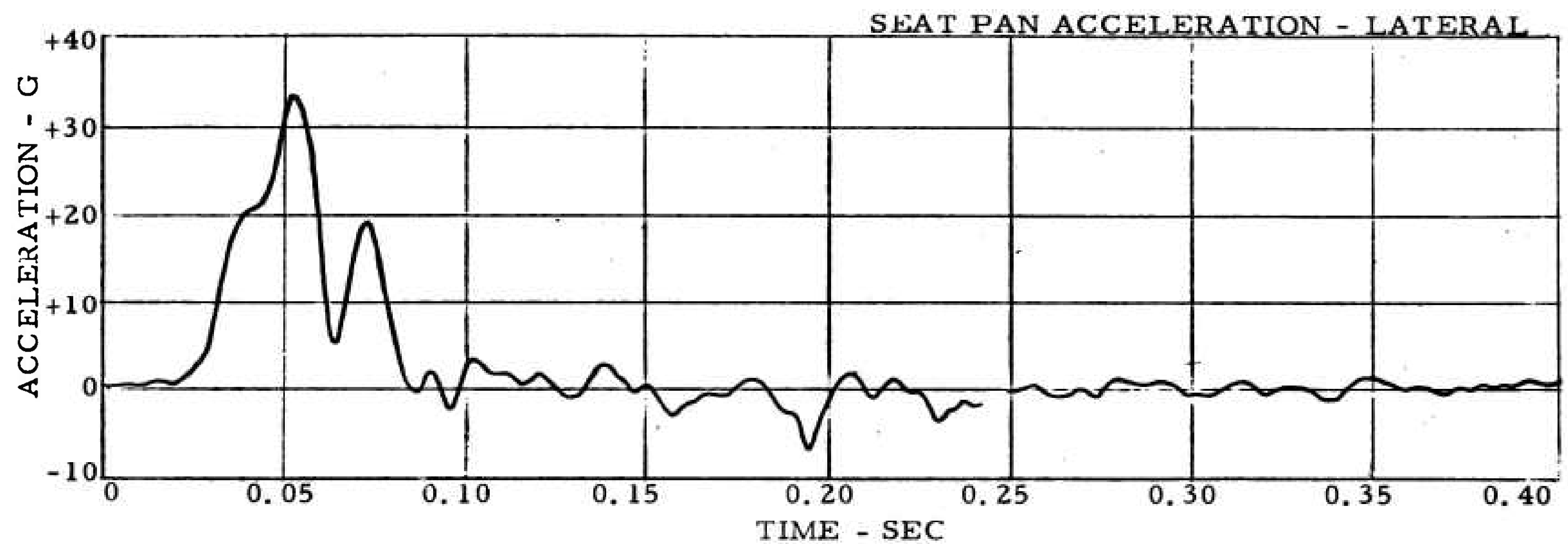

Figure 85. Acceleration-Time History - Test 8A.

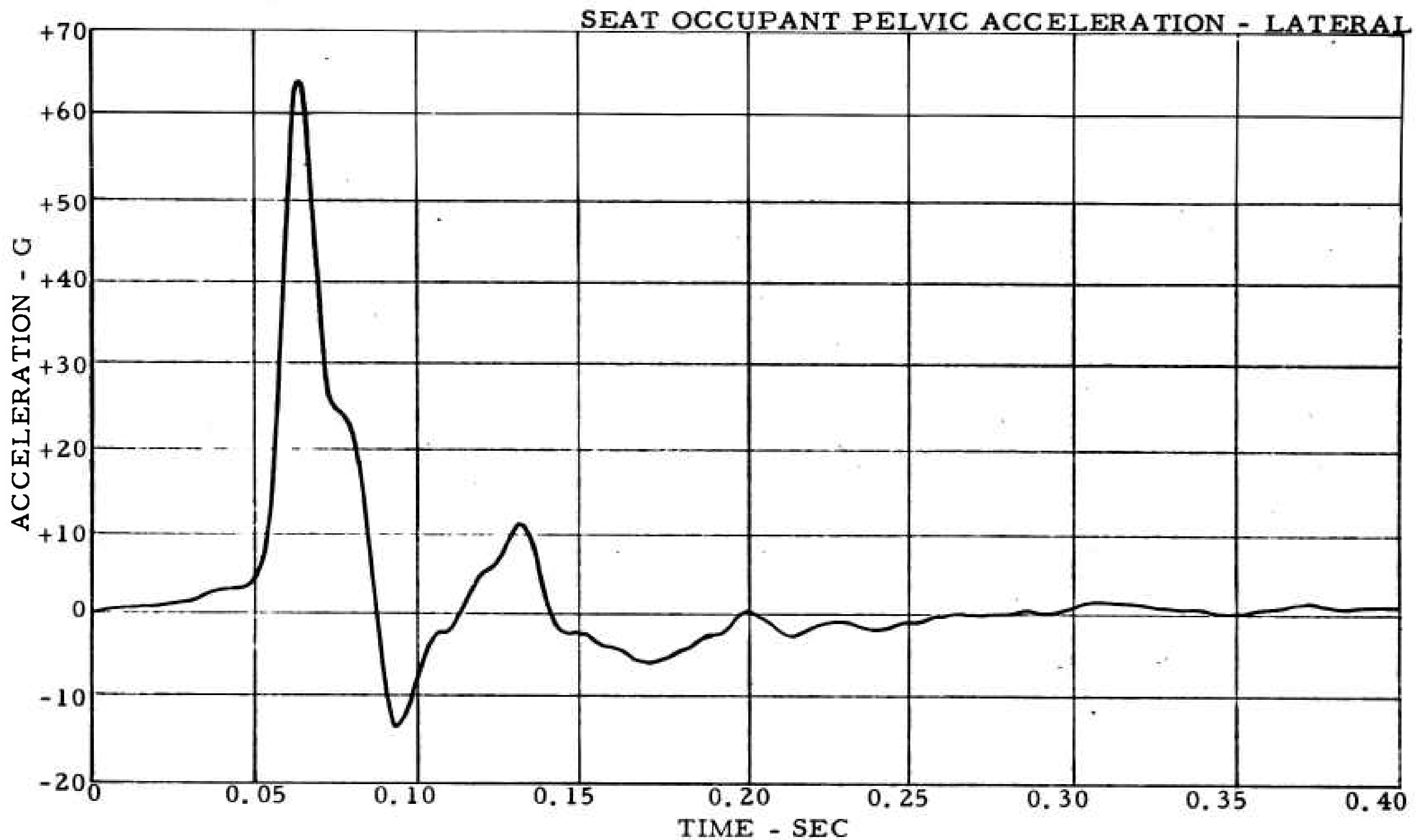

Figure 86. Acceleration-Time History - Test 8A.

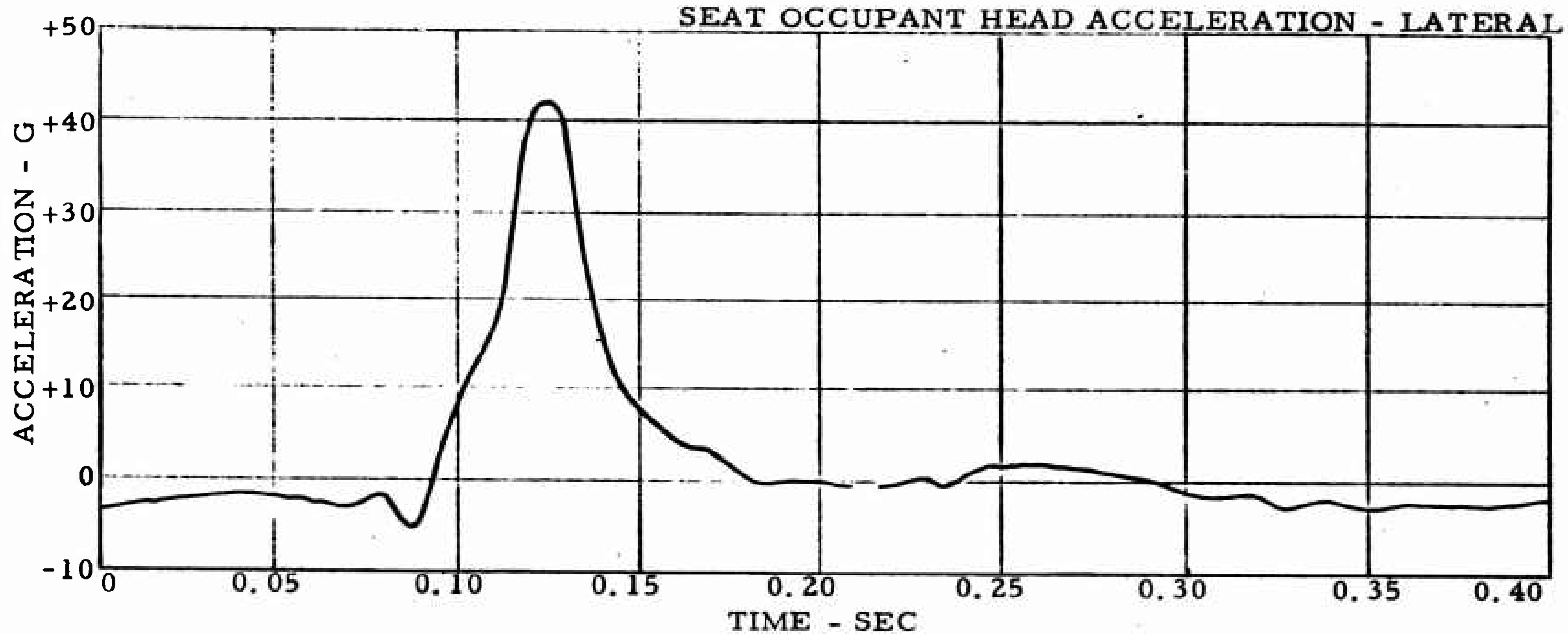

Figure 87. Acceleration-Time History - Test 8A.

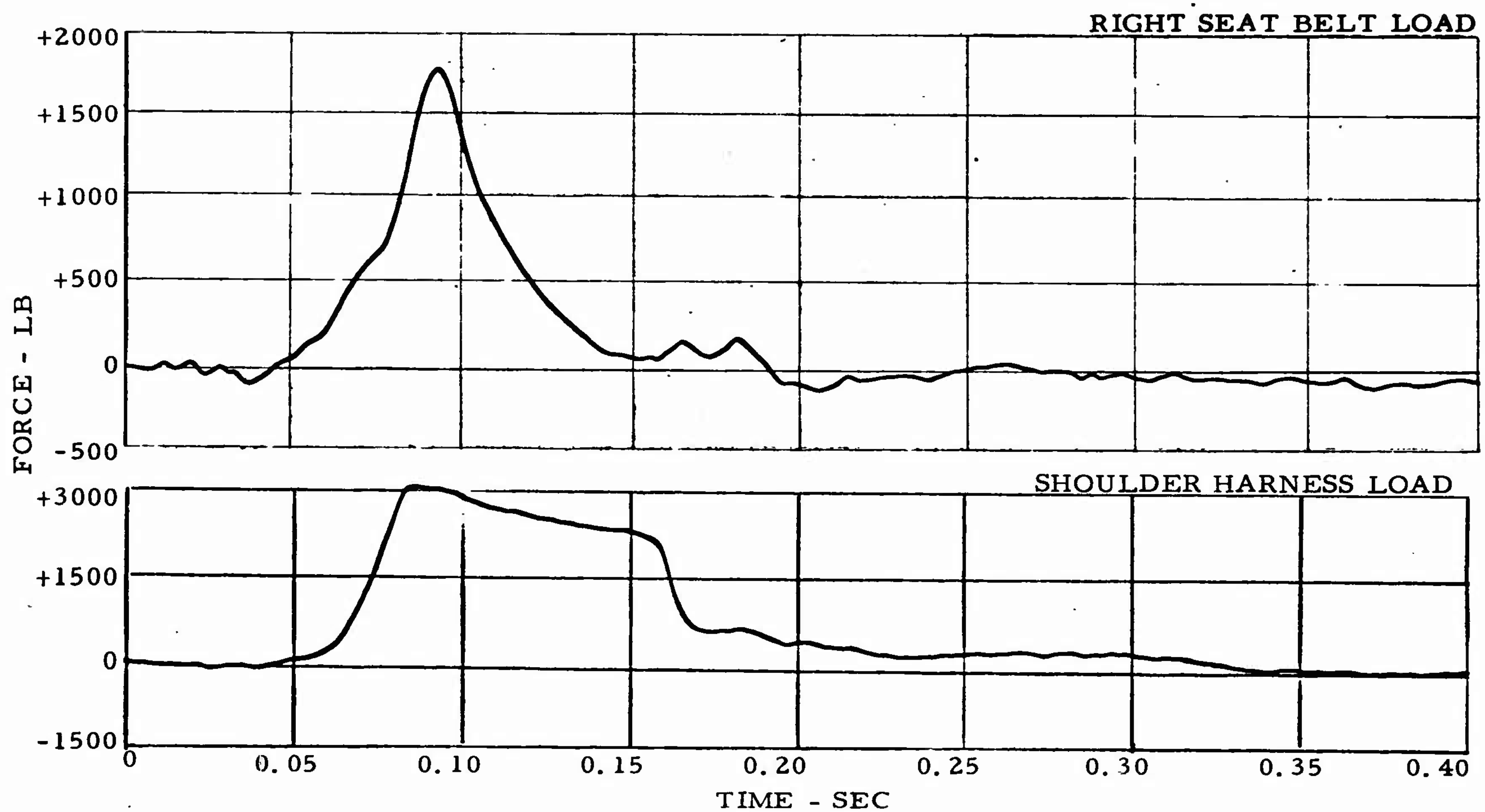

Figure 88. Force-Time Histories - Test 8A.

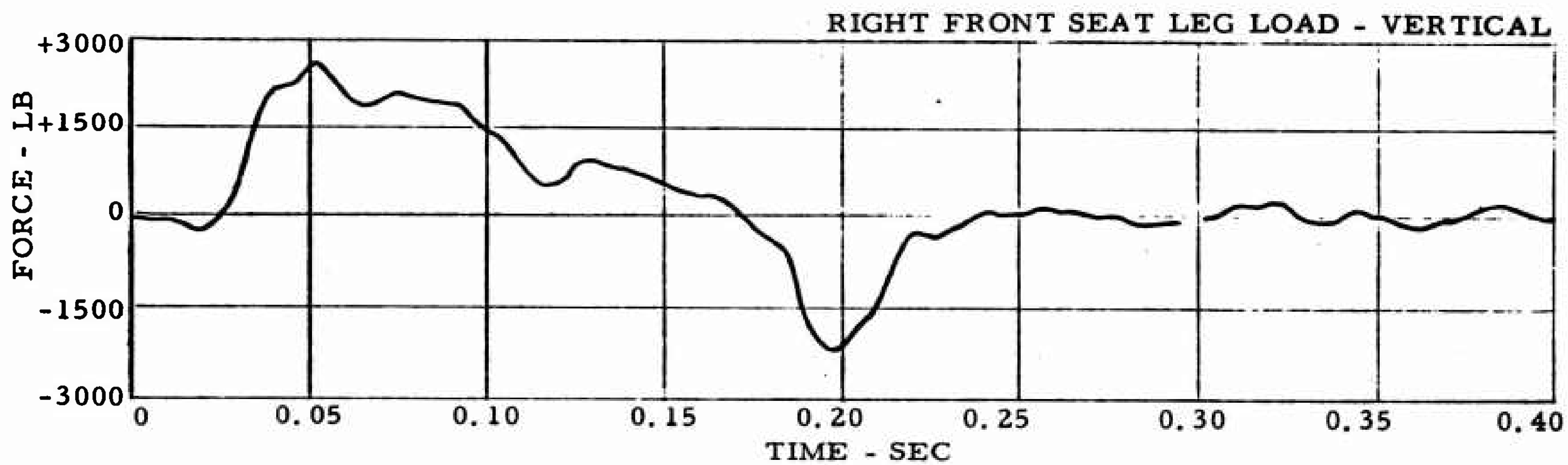

Figure 89. Force-Time History - Test 8A.

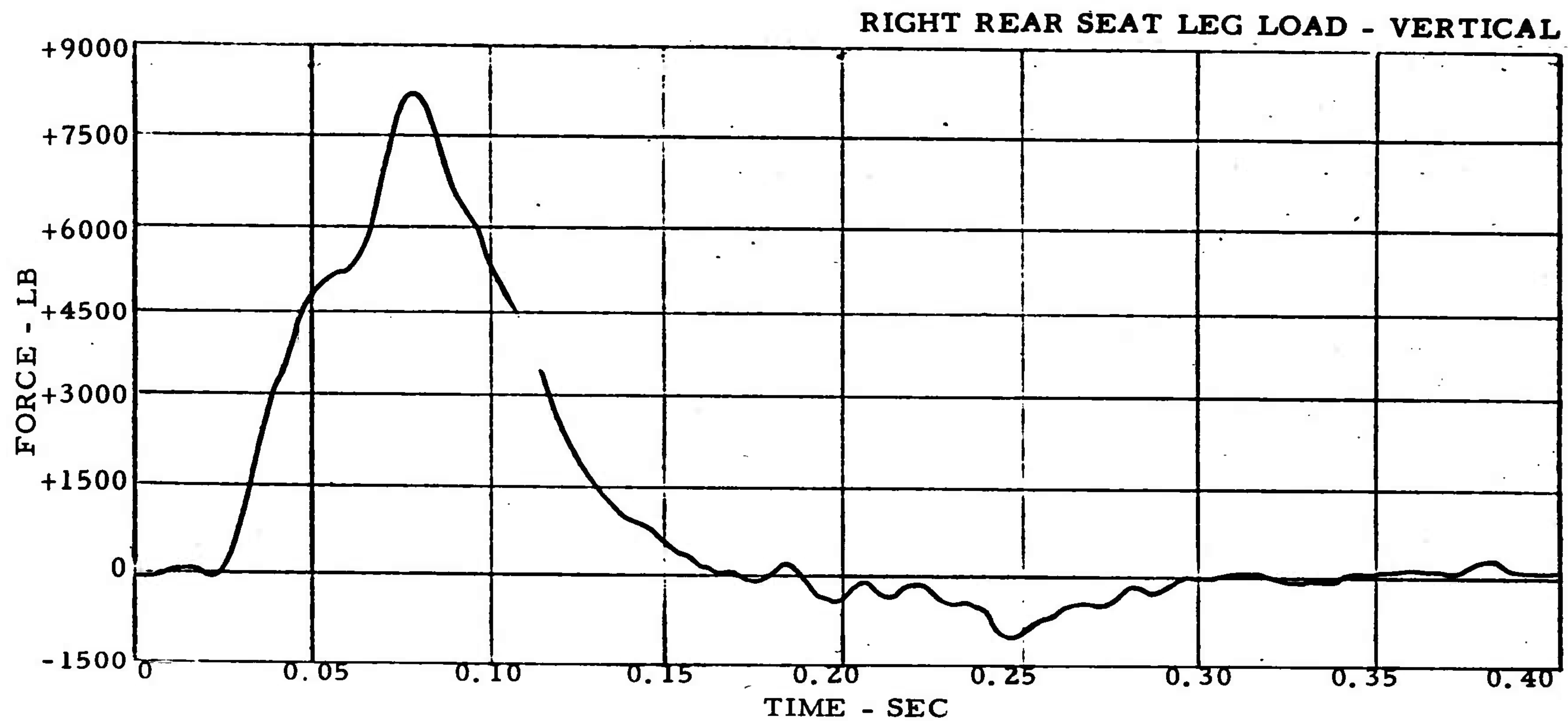

Figure 90. Force-Time History - Test 8A.

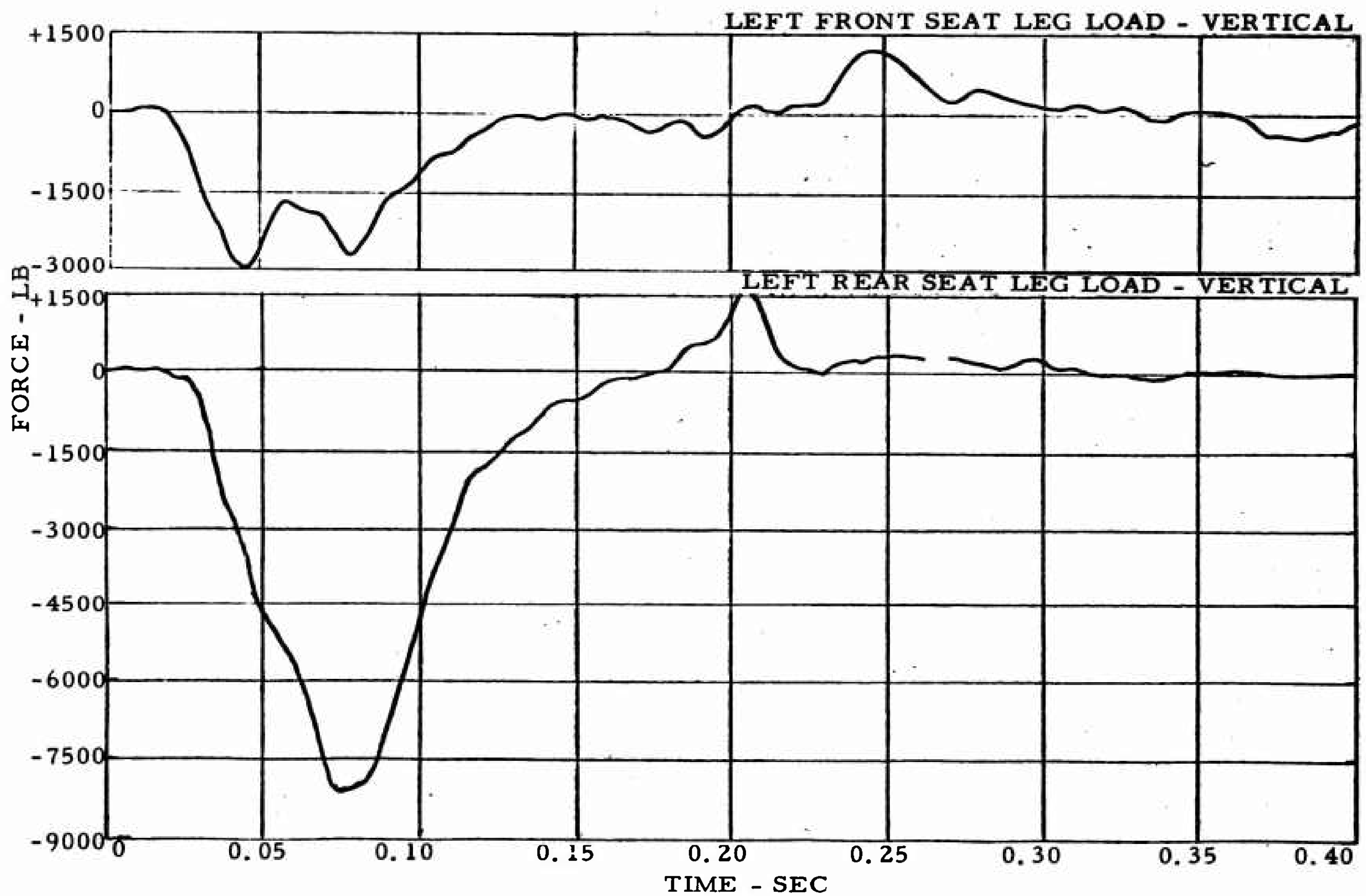

Figure 91. Force-Time Histories - Test 8A.

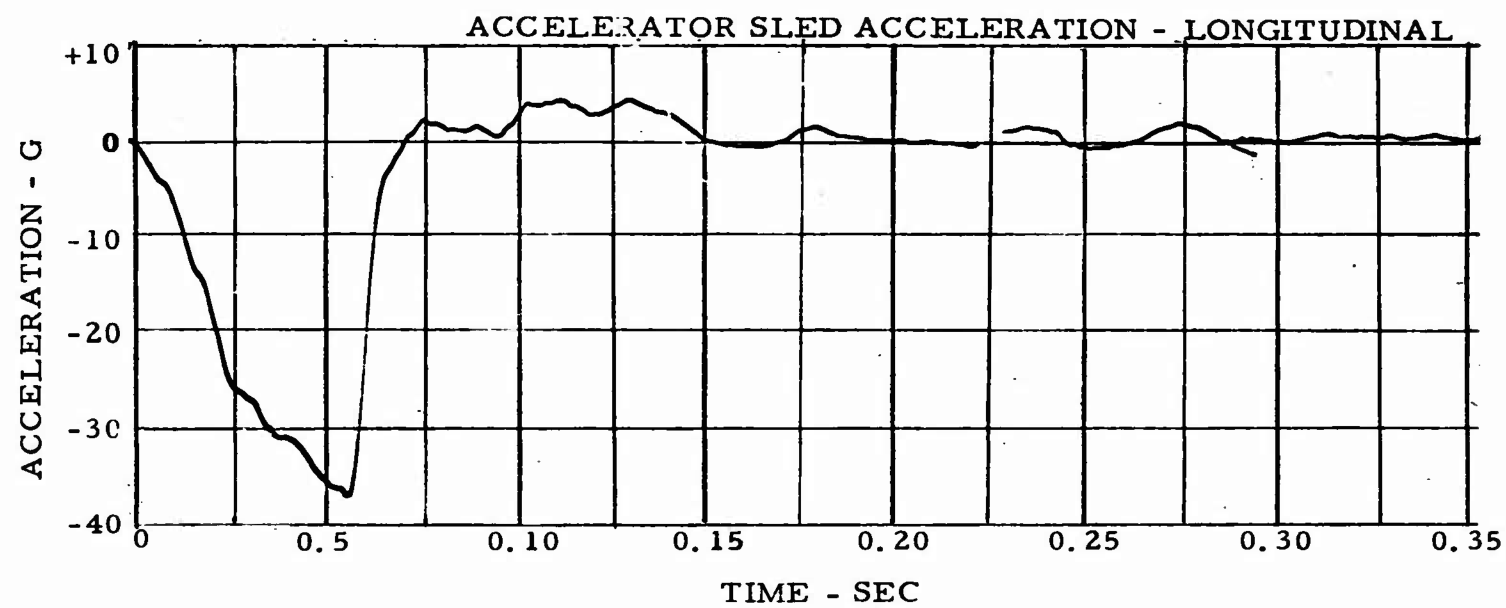

Figure 92. Acceleration-Time History - Test 9.

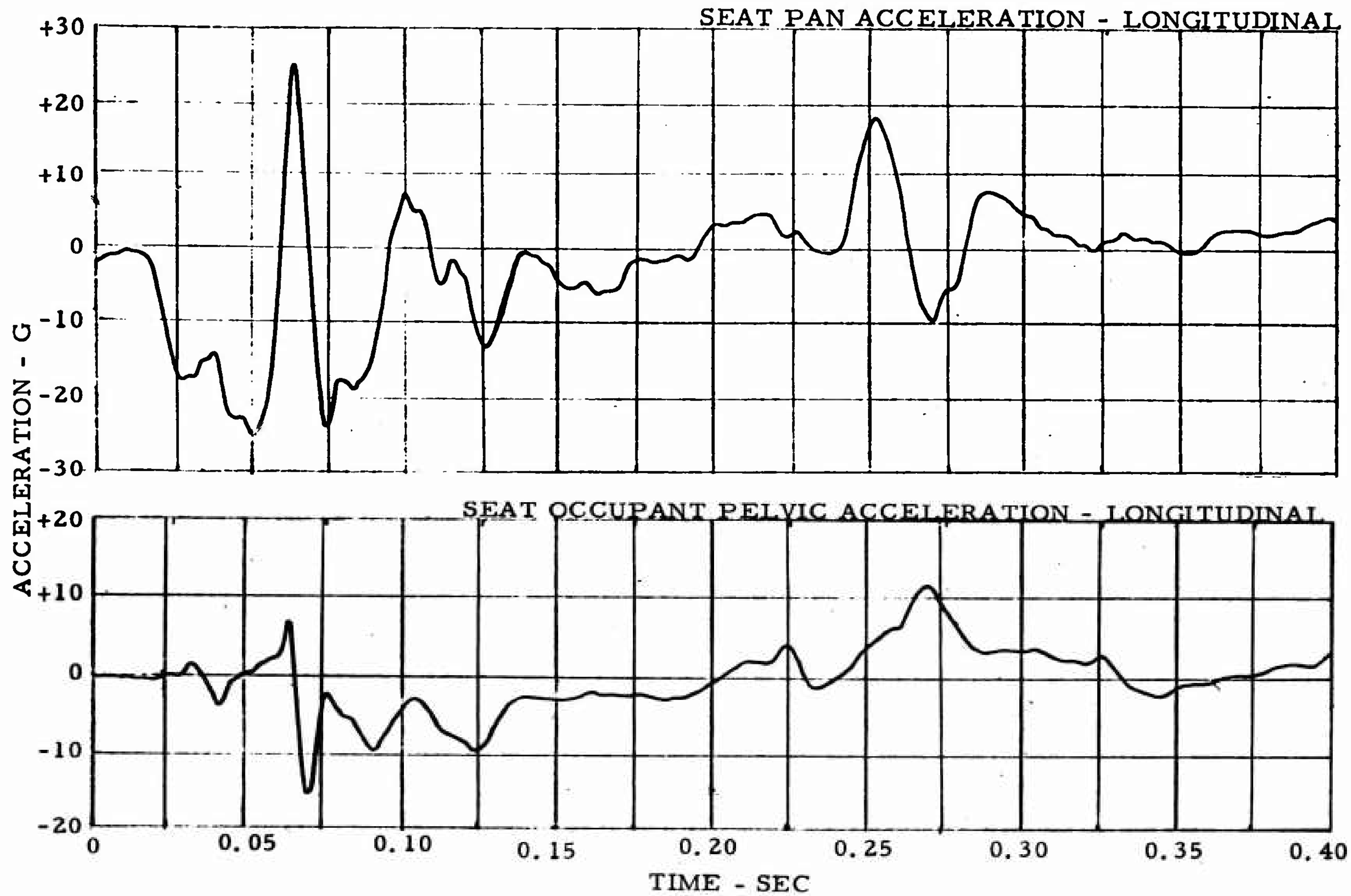

Figure 93. Acceleration-Time Histories - Test 9.

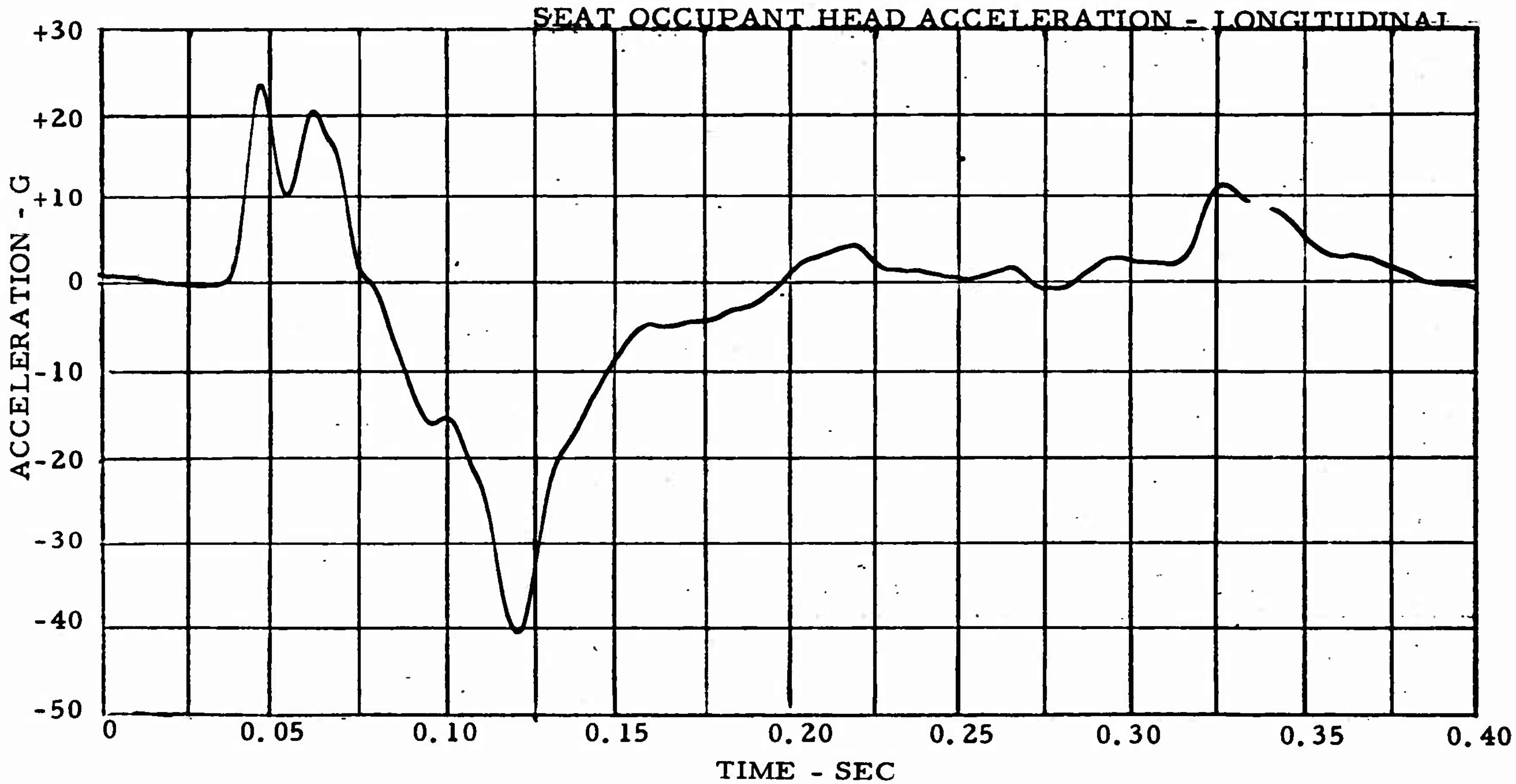

Figure 94. Acceleration-Time History - Test 9.

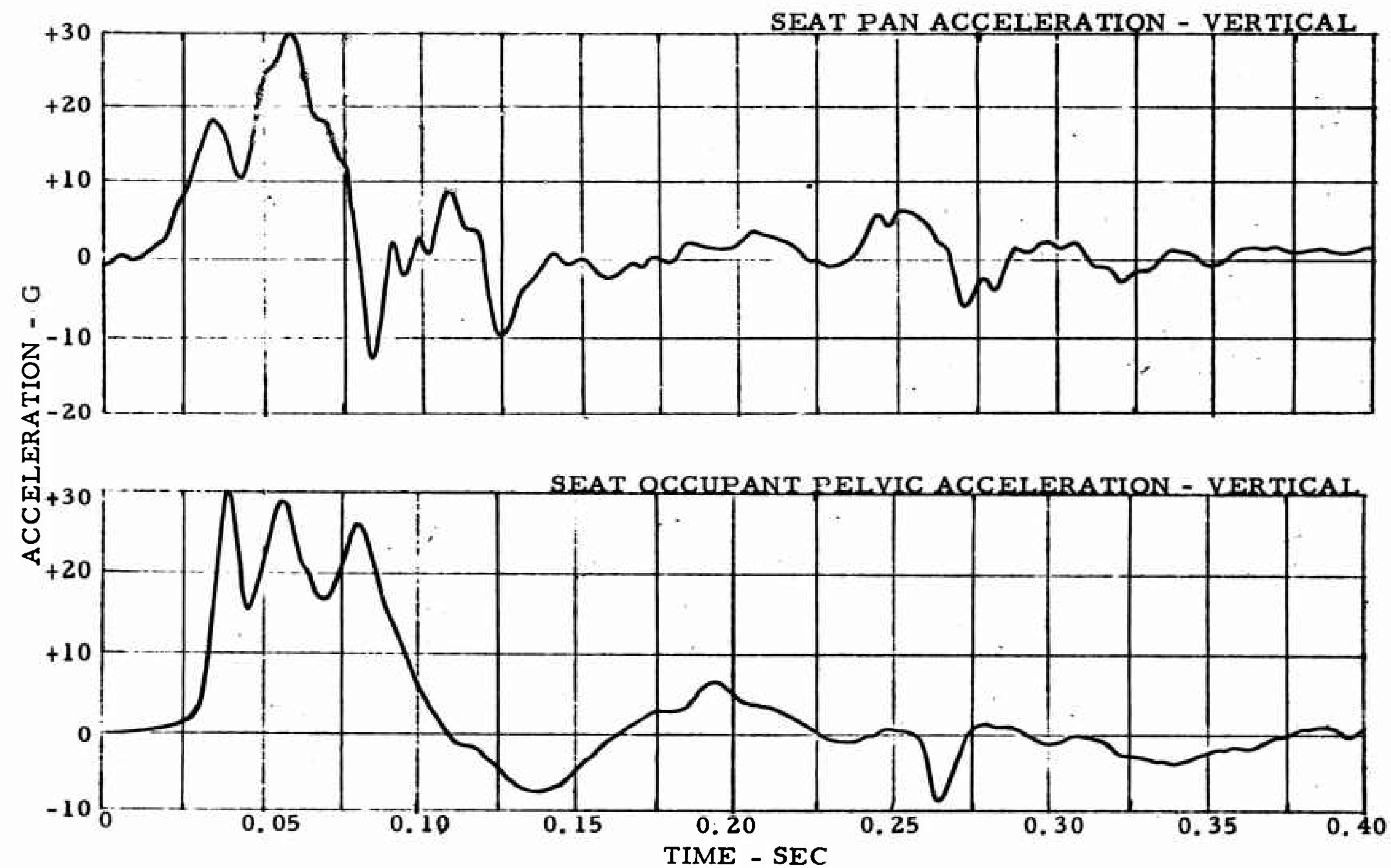

Figure 95. Acceleration - Time Histories - Test 9.

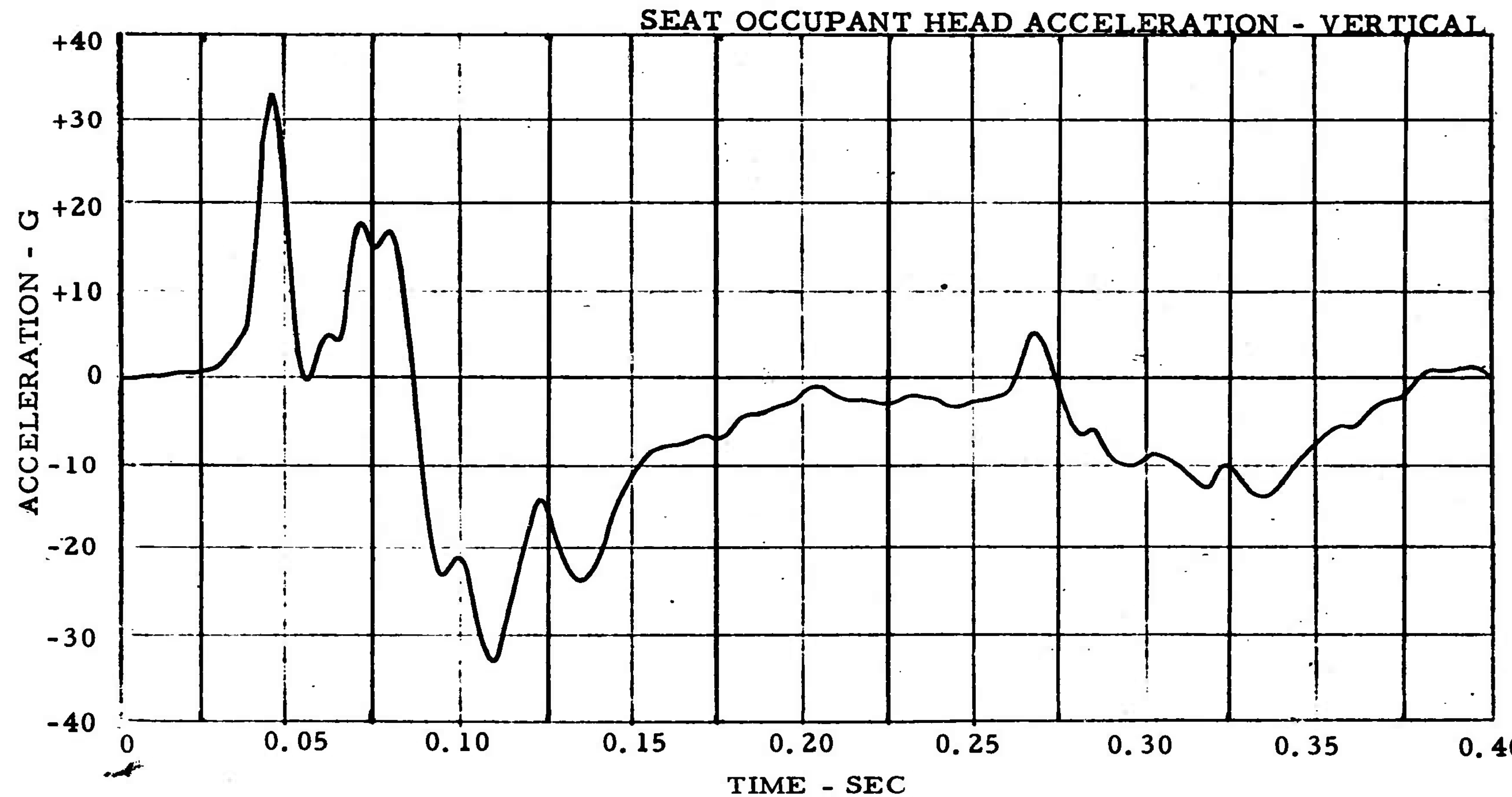

Figure 96. Acceleration-Time History - Test 9.

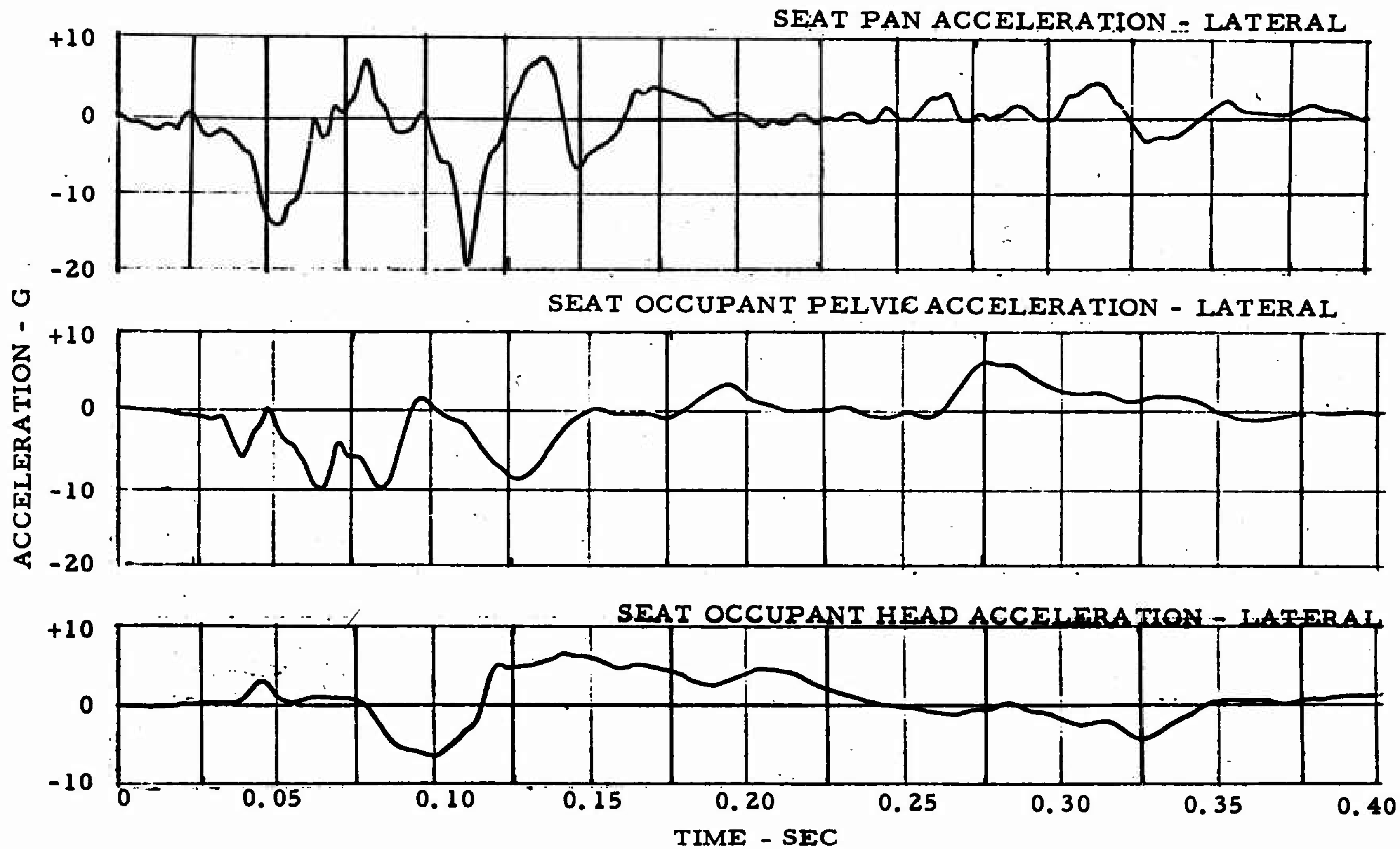

Figure 97. Acceleration-Time Histories - Test 9.

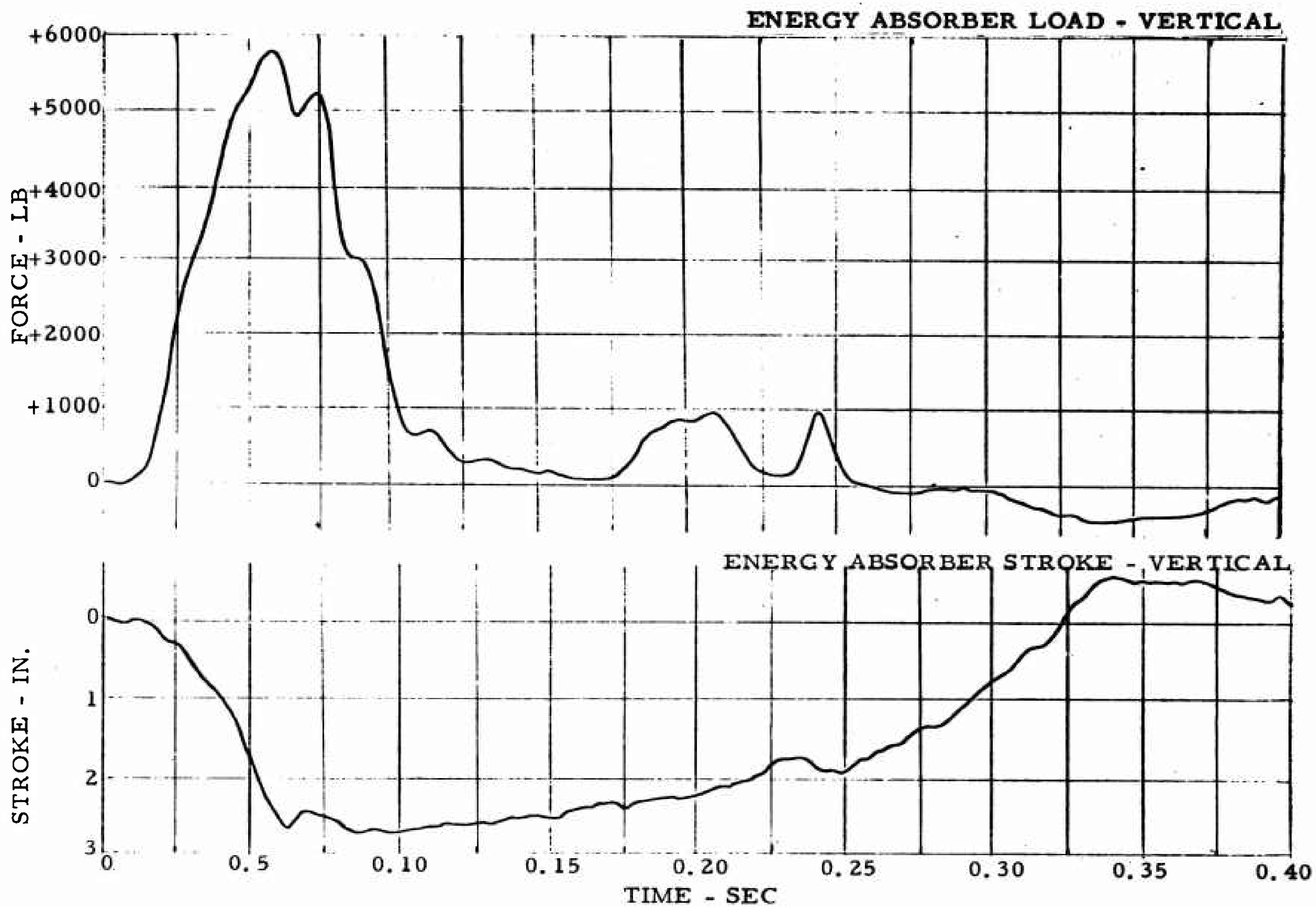

Figure 98. Force/Stroke-Time Histories - Test 9.

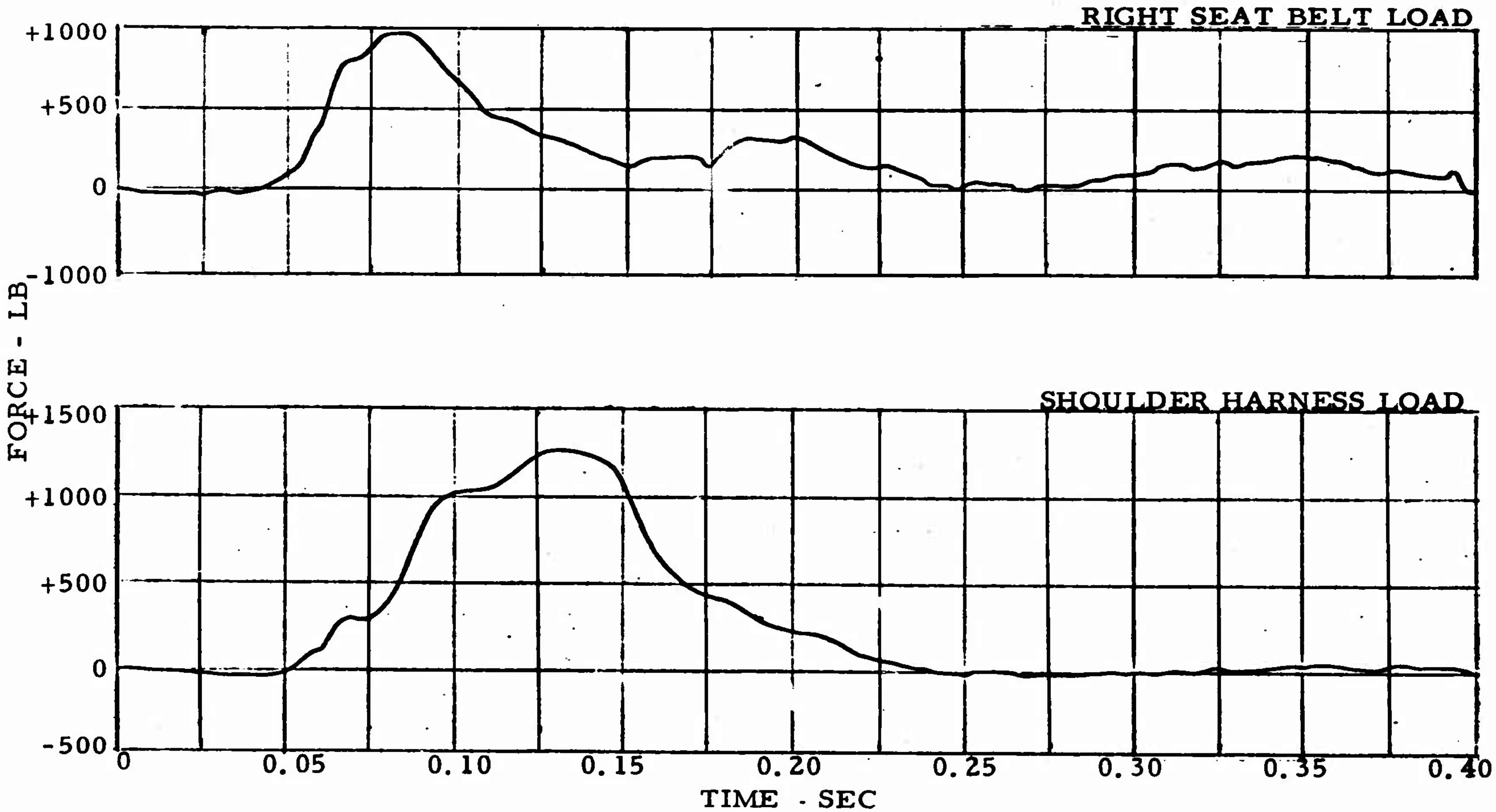

Figure 99. Force-Time Histories - Test 9.

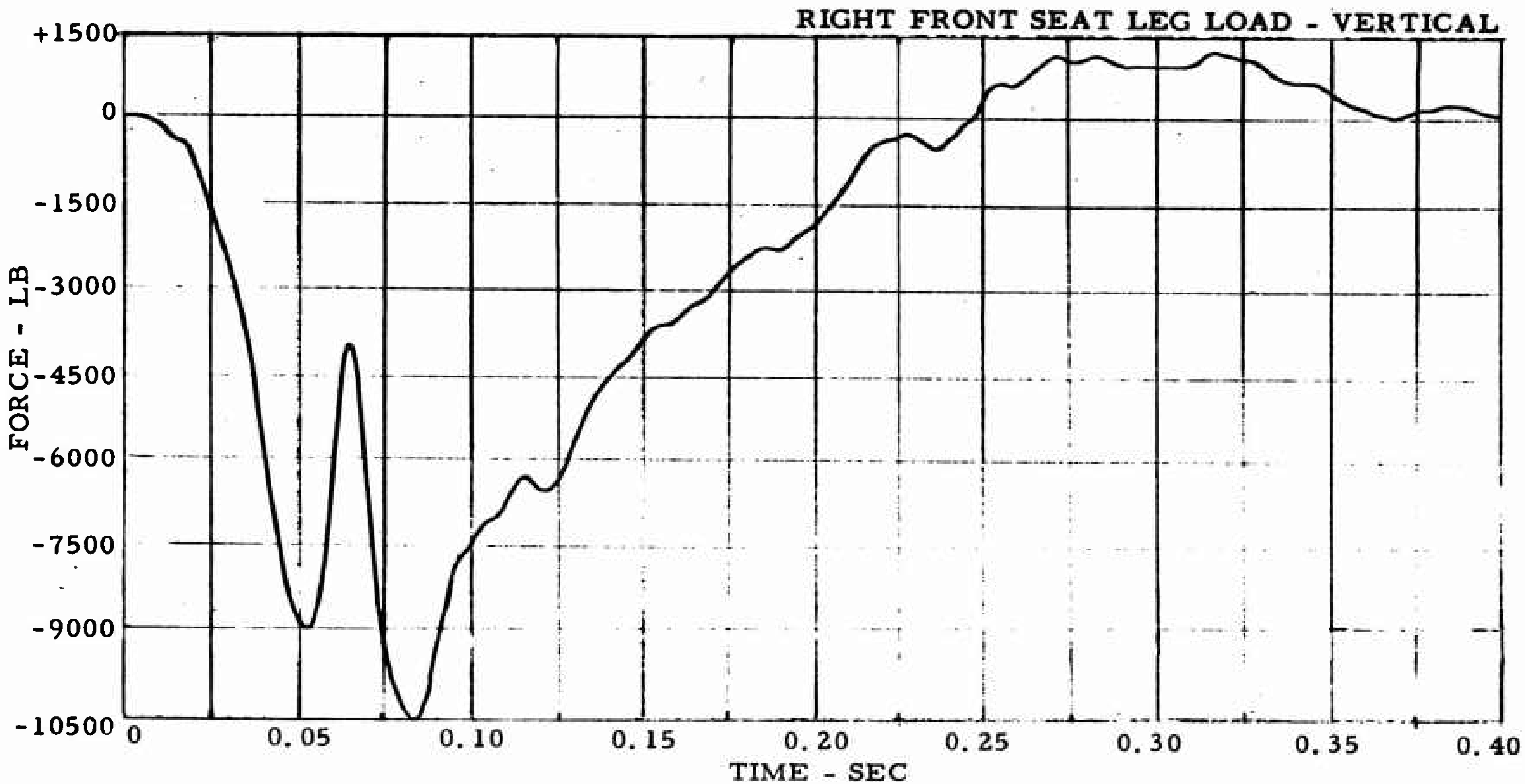

Figure 100. Force-Time History - Test 9.

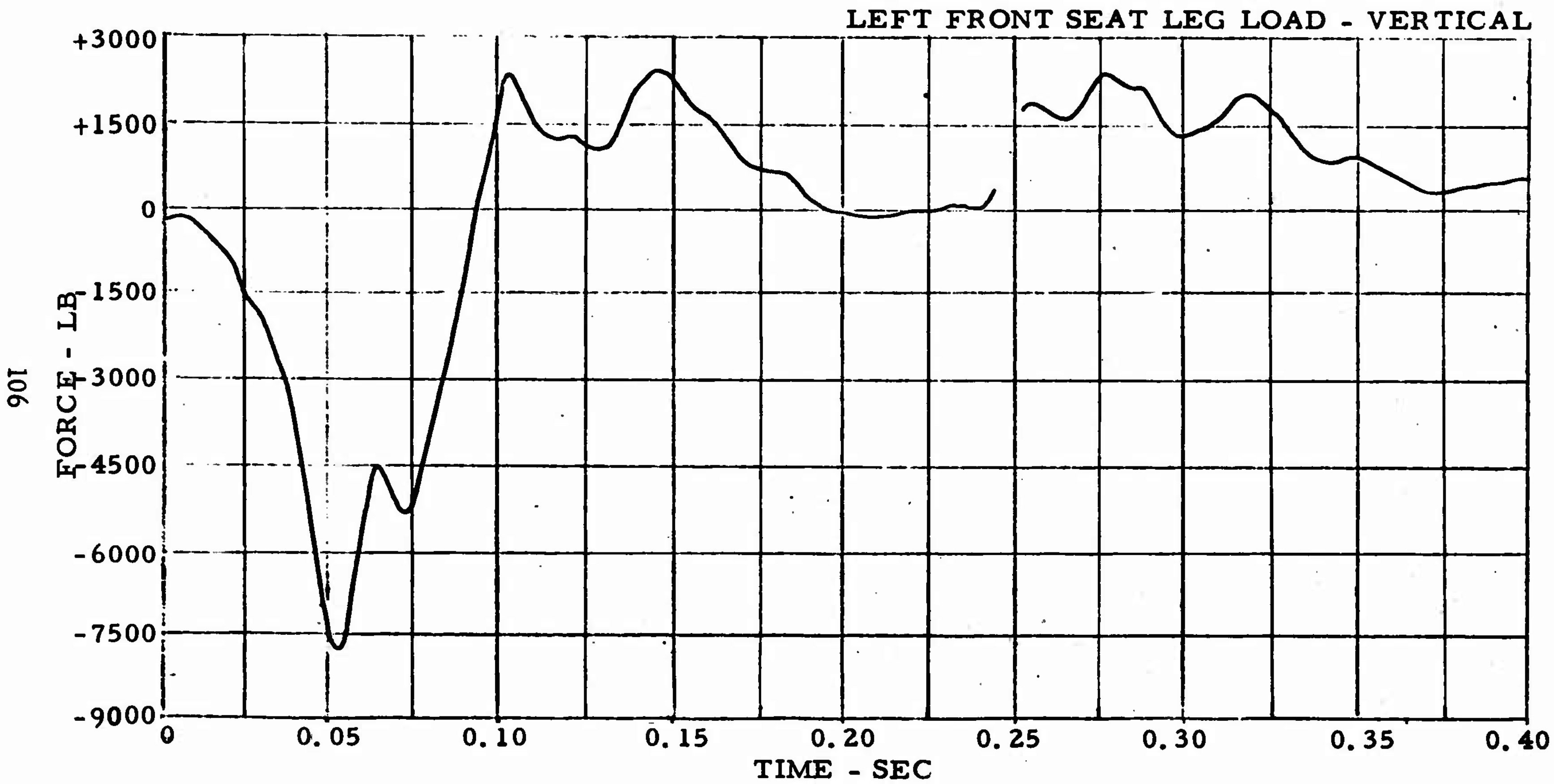

Figure 101. Force-Time History - Test 9.

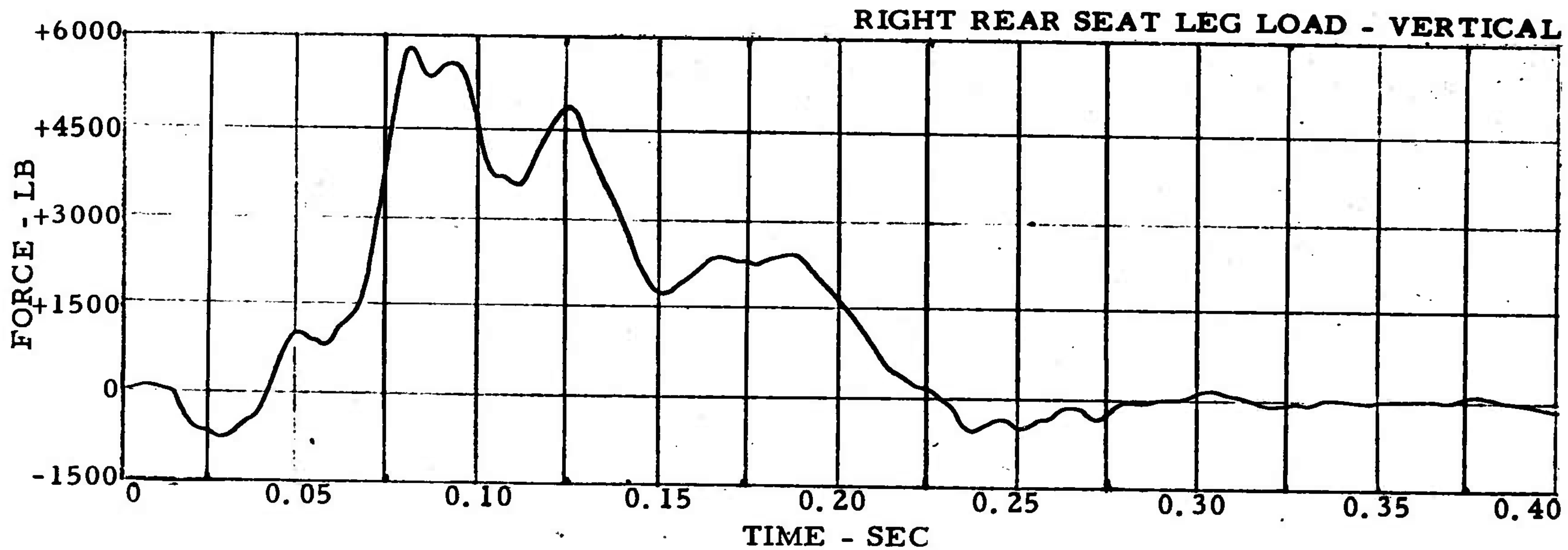

Figure 102. Force-Time History - Test 9.

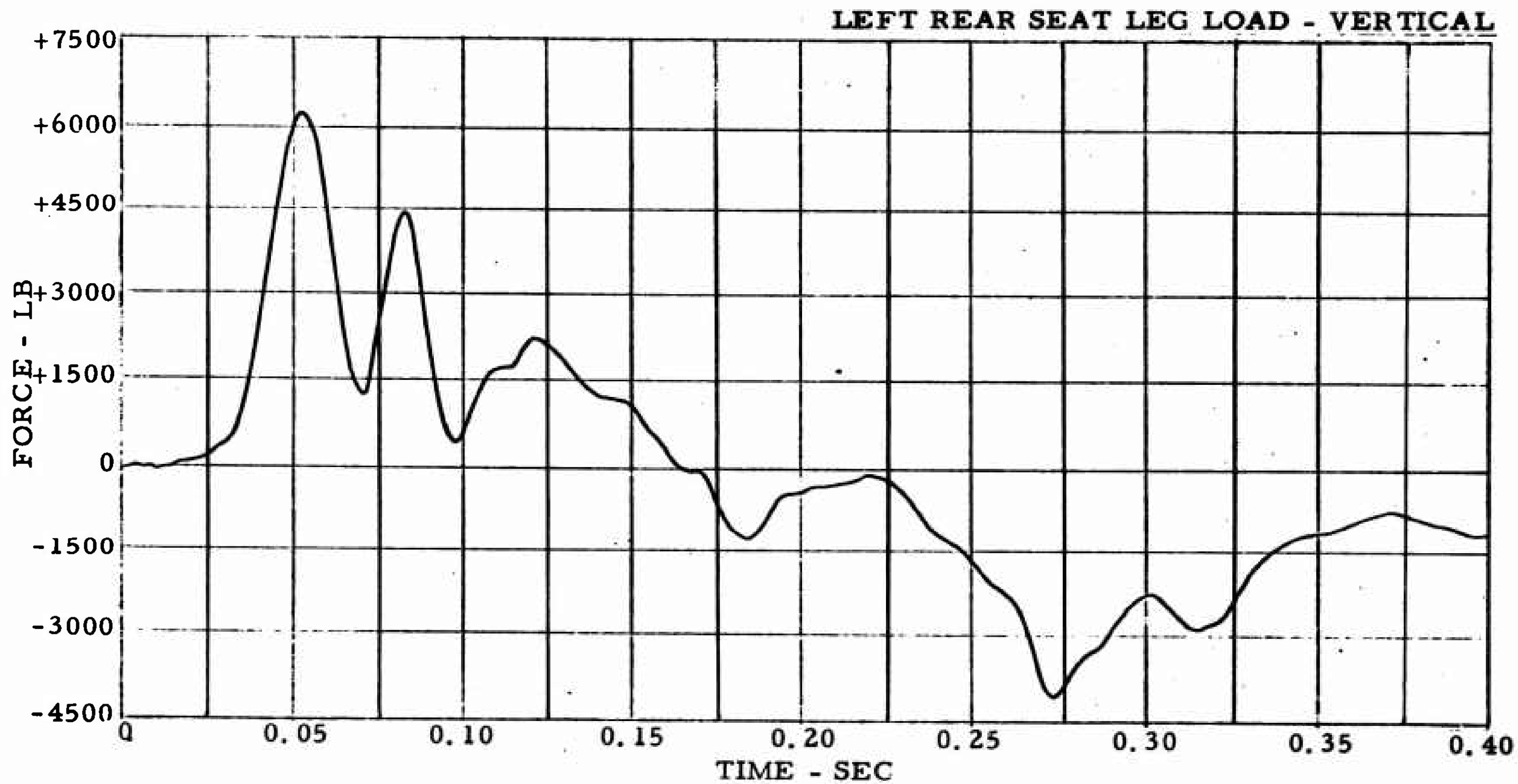

Figure 103. Force-Time History - Test 9.

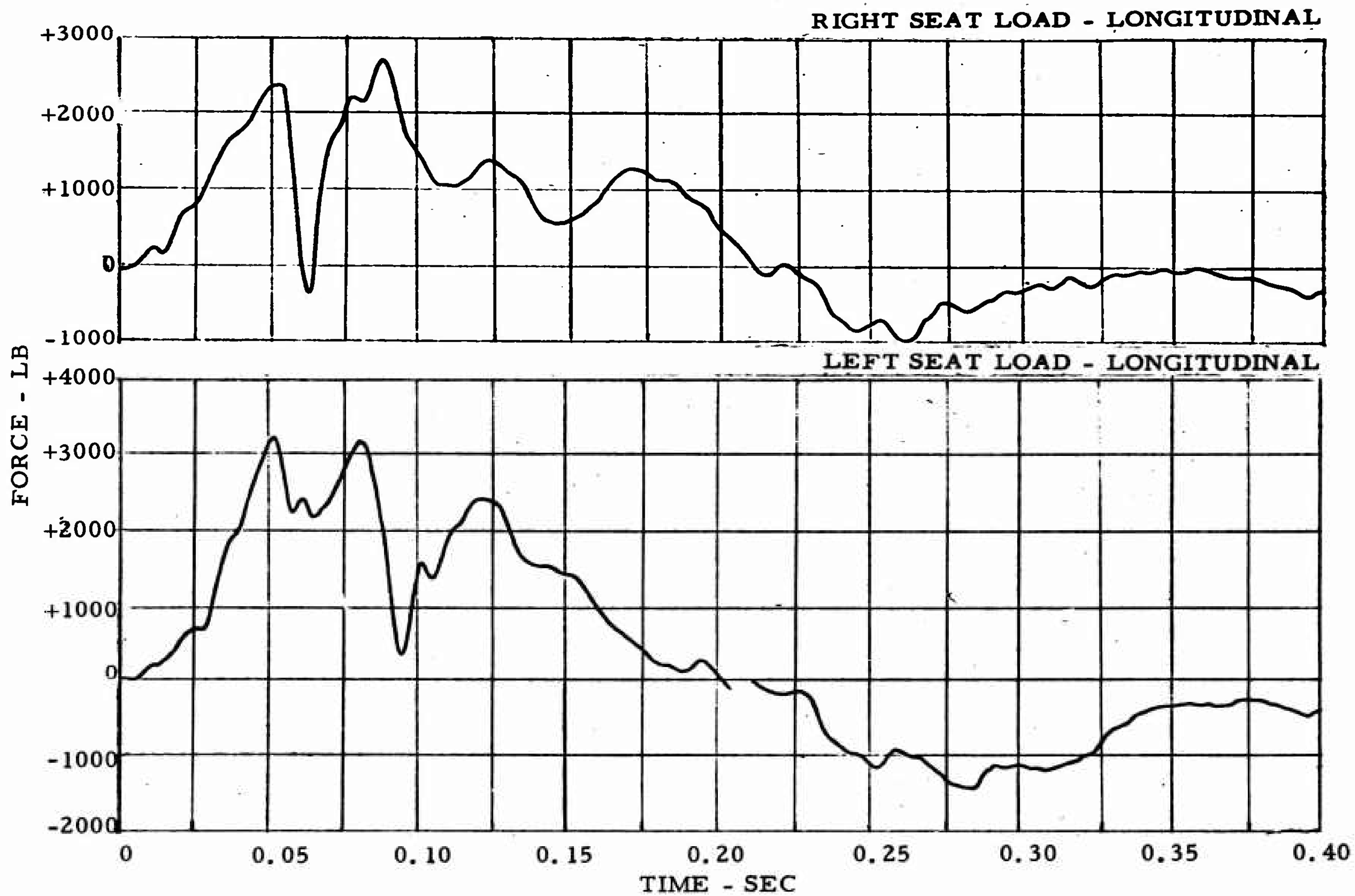

Figure 104. Force-Time Histories - Test 9.

Unclassified

Security Classification

DOCUMENT CONTROL DATA - R & D

(Security classification of title, body of abstract and indexing annotation must be entered when the overall report is classified)

1. ORIGINATING ACTIVITY (Corporate author) Dynamic Science (The "AvSER" Facility) 1800 West Deer Valley Road Phoenix, Arizona 85027	2a. REPORT SECURITY CLASSIFICATION Unclassfied 2b. GROUP

3. REPORT TITLE

An Evaluation of Armored Aircrew Crash Survival Seats

4. DESCRIPTIVE NOTES (Type of report and inclusive dates)

5. AUTHOR(S) (First name, middle initial, last name)

Clifford I. Gatlin
James ~~W.~~ Turnbow, PhD.

6. REPORT DATE	7a. TOTAL NO. OF PAGES	7b. NO. OF REFS
July 1968	124	None

8a. CONTRACT OR GRANT NO. Contract DAAJ02-68-C-0027 b. PROJECT NO. Task 1F121401A15003 c. d.	9a. ORIGINATOR'S REPORT NUMBER(S) USAAVLABS Technical Report 68-51 9b. OTHER REPORT NO(S) (Any other numbers that may be assigned this report) AvSer 68-4

10. DISTRIBUTION STATEMENT

Each transmittal of this document outside the Department of Defense must have prior approval of US Army Aviation Materiel Laboratories, Fort Eustis, Virginia 23604.

11. SUPPLEMENTARY NOTES	12. SPONSORING MILITARY ACTIVITY U.S. Army Aviation Materiel Laboratories Fort Eustis, Virginia

13. ABSTRACT

This report presents an evaluation of an armored seat design incorporating a new energy absorption concept. The seat was designed by Hayes International Corporation and was provided to AvSER by the U. S. Army Aviation Materiel Laboratories, Fort Eustis, Virginia (USAAVLABS).

The structure of the test seat is unique in that it is made up of two triangular frames interconnected by cross members at each apex and by diagonal braces in the plane of the aft members. Energy absorption in all axes is accomplished by bending steel rods around rollers in a controlled manner. The armor is not integral to the seat; thus, the seat can be used either with or without armor.

The tests indicate that additional design effort is warranted to make the seat function more properly within the design limitations.

DD FORM 1 NOV 65 1473 REPLACES DD FORM 1473, 1 JAN 64, WHICH IS OBSOLETE FOR ARMY USE.

Unclassified

Security Classification

14. KEY WORDS	LINK A		LINK B		LINK C	
	ROLE	WT	ROLE	WT	ROLE	WT
Dynamic Testing of Armored Aircrew Seat.						
Performance of bending rod energy absorber under dynamic loading						